# University of Alberta

Cholesterol Metabolism in the Niemann-Pick Type C Brain

by

Kyle Bradley Peake

A thesis submitted to the Faculty of Graduate Studies and Research
in partial fulfillment of the requirements for the degree of

Doctor of Philosophy
in
Experimental Medicine

Department of Medicine


Spring 2011
Edmonton, Alberta

**EXAMINING COMMITTEE**

Dr. Jean Vance, Department of Medicine, University of Alberta

Dr. Robert Campenot, Department of Cell Biology, University of Alberta

Dr. Kathryn Todd, Department of Psychiatry, University of Alberta

Dr. Satya Kar, Department of Psychiatry, University of Alberta

Dr. Joyce Repa, Department of Physiology, University of Texas Southwestern

## Dedication

*To my wife and family, who have supported me every step of the way*

## Abstract

Niemann-Pick Type C (NPC) disease is an autosomal recessive disorder that results in accumulation of unesterified cholesterol in late endosomes/lysosomes (LE/Ls), leading to progressive neurodegeneration and premature death. Microglia are resident immune cells of the central nervous system, which upon activation can secrete potentially neurotoxic molecules such as tumor necrosis factor-alpha (TNFα). Inappropriate activation of microglia has been implicated in NPC disease. Primary microglia cultures from the cerebral cortex of *Npc1*$^{-/-}$ mice have an altered cholesterol distribution characteristic of NPC-deficient cells. Immunocytochemical analysis revealed increased TNFα staining in *Npc1*$^{-/-}$ microglia. However, *Npc1*$^{-/-}$ and *Npc1*$^{+/+}$ microglia showed similar mRNA levels of pro-inflammatory cytokines and similar levels of TNFα secretion. To determine whether *Npc1*$^{-/-}$ microglia contribute to neuron death in NPC disease, microglia were co-cultured with cerebellar granule cells. Surprisingly, the extent of neuronal death was the same in neurons cultured with *Npc1*$^{+/+}$ or *Npc1*$^{-/-}$ microglia. Thus, *Npc1*$^{-/-}$ microglia have an altered phenotype compared to *Npc1*$^{+/+}$ microglia, but this does not lead to neuron death in an *in vitro* co-culture system.

Treatment options for NPC disease remain limited. A consequence of cholesterol sequestration in the LE/Ls, is that cholesterol movement to the endoplasmic reticulum, where cholesterol metabolism is regulated, is impaired. Cyclodextrin (CD), a compound that binds cholesterol, has

recently been found to delay the onset of neurological symptoms and prolong life of *Npc1*$^{-/-}$ mice. Since the brain consists of both neurons and glia, it remains unclear if CD acts directly on neurons and/or other cells in the brain. Neurons cultured from the cerebellum and astrocytes cultured from the cortex of *Npc1*$^{-/-}$ mice were treated with a low dose (0.1mM) of CD. This treatment decreased cholesterol sequestration and decreased the rate of cholesterol synthesis in *Npc1*$^{-/-}$ neurons and astrocytes. CD also decreased mRNAs encoding proteins involved in cholesterol synthesis in *Npc1*$^{-/-}$ neurons and increased genes involved in cholesterol efflux in *Npc1*$^{-/-}$ astrocytes. Moreover, CD increased cholesterol esterification in *Npc1*$^{-/-}$ astrocytes. These results suggest that cholesterol trapped in LE/Ls in *Npc1*$^{-/-}$ neurons and astrocytes was released by CD treatment and reached the ER, thereby regulating cholesterol homeostasis.

**Acknowledgement**

I would like to extend my sincerest gratitude to Dr. Jean Vance, for giving me this opportunity to work in such a wonderful and accomplished environment, and for helping me grow into a scientist.

I would like to show my deepest appreciation to Dr. Hideki Hayashi and Dr. Barbara Karten for their mentorship and guidance.

I would also like to thank Dr. Dennis Vance, Dr. Bob Campenot, Dr. Satya Kar, and Dr. Kathryn Todd for their valuable discussions and insights into my projects.

Lastly, I would like to thank Mr. Russ Watts and Mr. Randy Nelson for their incredible technical expertise, assistance, and friendship.

**TABLE OF CONTENTS**

## LIST OF TABLES

## LIST OF FIGURES



***Microglia Experiments***

***Cyclodextrin Experiments***

## ABBREVIATIONS

ABCA1, ATP-binding cassette transporter A1; ABCG1, ATP-binding cassette transporter G1; ACAT, acyl-CoA:cholesterol acyltransferase; AD, Alzheimer disease; ALLO, allopregnanolone; BBB, blood-brain barrier; BSA, bovine serum albumin; CD, cyclodextrin; CE, cholesterol ester; CGCs, cerebellar granule cells; CNS, central nervous system; DMEM, Dulbecco's modified Eagle medium; DNAse I, deoxyribonuclease I; ER, endoplasmic reticulum; FBS, fetal bovine serum; GAPDH, glyceraldehyde-3-phosphate dehydrogenase; GLTase, glutaminase; GSLs, glycosphingolipids; HDLs, high-density lipoproteins; HMGCR, 3-hydroxy-3-methylglutaryl coenzyme A reductase; HPCD, 2-hydroxypropyl-β-cyclodextrin; Iba1, ionized calcium binding adaptor molecule 1; IL1β, interleukin-1β; IL10, interleukin-10; iNOS, inducible nitric oxide synthase; LDLR, low-density lipoprotein receptor; LDLs, low-density lipoproteins; LE/L, late endosome/lysosome; LPS, lipopolysaccharide; LXR, liver X receptor; M-CSFR, macrophage colony-stimulating factor receptor; MβCD, methyl-β-cyclodextrin; MAP2, microtubule-associated protein 2; NADPHox, nicotinamide adenine dinucleotide phosphate-oxidase; NPC, Niemann-Pick Type C; PBS, phosphate-buffered saline; PCSK9, proprotein convertase subtilisin/kexin type 9; qPCR, quantitative real-time polymerase chain reaction; Scap, SREBP cleavage activating protein; SREBP2, sterol regulatory element-binding protein 2; TACE, tumor necrosis factor-α converting enzyme; TGFβ, transforming growth factor-β; TNFα, tumor necrosis factor-α; TNFR1, tumor necrosis factor receptor 1; U18666A, 3-β-[2-(diethylamino)ethoxy]androst-5-en-17-one

## 1. BACKGROUND AND INTRODUCTION[¶]

Cholesterol is a key component of mammalian cell membranes, playing essential roles in membrane integrity, fluidity, and organization. For instance, membrane domains highly enriched in cholesterol and sphingolipids are believed to play important roles in cellular processes such as signal transduction and membrane trafficking [1, 2]. Cholesterol is also the precursor for a variety of important molecules including oxysterols, bile acids, and steroid hormones. Due to the biological importance of cholesterol, dysregulation of cholesterol metabolism can have a number of detrimental effects. Elevated levels of plasma cholesterol packaged in low-density lipoproteins (LDLs) are correlated with an increased risk of atherosclerosis [3]. Furthermore, in the brain, alterations in cholesterol metabolism have been implicated in a number of neurodegenerative disorders including Alzheimer disease (AD), Huntington disease, and Niemann-Pick Type C (NPC) disease. Thus, cholesterol concentrations must be tightly maintained in order to preserve proper cell function.

### *1.A CHOLESTEROL METABOLISM*

Cholesterol is synthesized from acetate through a complex pathway catalyzed by more than 25 different enzymes [4]. Nearly all mammalian

---

[¶] *A portion of this chapter has been published. Peake and Vance 2010. FEBS Letters. 584: 2731-2739.*

cells are capable of synthesizing cholesterol [5]. Additionally, cells can obtain cholesterol through the uptake of exogenous lipoproteins, particularly LDLs. LDLs are brought into the cell via receptor-mediated or bulk-phase endocytosis [6, 7], and are delivered to the late endosome/lysosome (LE/L), where cholesterol esters (CE) within the LDL particle are hydrolyzed by lysosomal acid lipase [6, 8, 9]. Unesterified cholesterol exits the LE/L, through an NPC1/NPC2-dependent mechanism, and is distributed primarily to the plasma membrane as well as the endoplasmic reticulum (ER), which serves as a cholesterol sensor [6, 10]. Excess cholesterol can be esterified by acyl-CoA:cholesterol acyltransferase (ACAT), allowing cholesterol to be stored in a relatively inert form [6, 11]. Moreover, excess cholesterol can be transferred out of cells by members of the ATP-binding cassette transporter family such as ATP-binding cassette transporters A1 (ABCA1) and G1 (ABCG1). It has been proposed that ABCA1 is involved in transferring cholesterol and phospholipids to lipid-poor apolipoprotein AI [12], while ABCG1 transfers additional lipids to the partially lipidated particle [13], forming mature high-density lipoproteins (HDLs). These HDLs are then brought through the circulation to the liver, where cholesterol is converted into bile acids and excreted from the body [14, 15]. Recent experiments, however, suggest both *Abca1*$^{+/+}$ and *Abca1*$^{-/-}$ mice are capable of excreting similar amounts of cholesterol [16]. The mechanism through which this is occurring remains to be determined.

*1.A(i) Regulation of Cholesterol Metabolism*

Due to the importance of cholesterol, cells have developed a number of intricate mechanisms through which to control cholesterol homeostasis. The ER is a key site that serves as a cholesterol sensor, allowing cells to regulate cholesterol metabolism according to cellular demand. Sterol regulatory element-binding protein 2 (SREBP2) is a transcription factor that is central in regulating cholesterol homeostasis [10]. The regulation of SREBP is tightly controlled by sterols. In the presence of sterols, full length SREBP is restricted to the ER [10]. Upon sterol depletion, the N-terminal fragment of SREBP is cleaved and enters the nucleus where it can increase the synthesis of genes involved in cholesterol synthesis and uptake [17]. These include genes encoding 3-hydroxy-3-methylglutaryl coenzyme A reductase (HMGCR), the rate-limiting enzyme in cholesterol biosynthesis [18], and the LDL-receptor (LDLR) [10]. SREBP is oriented in a hairpin fashion, with both the N-terminal active domain and the C-terminal regulatory domain extending into the cytosol, while a transmembrane loop crosses into the ER lumen [19]. The C-terminal regulatory domain binds to SREBP cleavage-activating protein (Scap) [20, 21], a protein involved in shuttling SREBP from the ER to the Golgi apparatus [22], where SREBP can be cleaved by two sequential proteases that release the active N-terminal fragment [17]. In the presence of sterols, Scap binds to either Insig-1 or Insig-2, both of which retain the SREBP/Scap complex in the ER, and thus prevent

SREBP processing [23, 24]. This occurs since binding of cholesterol to Scap or binding of oxysterols (oxygenated derivatives of cholesterol) to Insig both induce a conformational change in Scap [25-28]. The conformational change prevents Scap from binding CopII vesicles which transport the SREBP/Scap complex to the Golgi apparatus [28-30].

SREBP2 processing is not the only way through which cells are able to regulate cholesterol metabolism. For instance, sterols can promote ubiquitination and degradation of HMGCR through an Insig-dependent mechanism [31-34]. Moreover, PCSK9 (proprotein convertase subtilisin/kexin type 9) is capable of binding to the LDLR and promoting degradation of the LDLR via the lysosome [35-37]. The liver X receptor (LXR) is a nuclear hormone receptor, which functions as a heterodimer with the retinoid X receptor in order to regulate genes involved in cholesterol homeostasis [38-41]. Binding of oxysterols to LXR leads to the activation of genes such as ABCA1 and ABCG1, both of which are involved in promoting the flux of cholesterol out of cells [12, 38, 41-43]. Thus, there are several different ways through which cells can control cholesterol metabolism in order to maintain the appropriate concentrations of cholesterol within the cell.

*1.A(ii) Cholesterol Metabolism in the Brain*

Cholesterol metabolism in the brain is unique, particularly since plasma lipoproteins are unable to cross the blood-brain barrier (BBB).

Consequently, essentially all of the cholesterol in the brain must be synthesized endogenously [44]. The brain contains ~25% of the body's cholesterol, but comprises only ~5% of the body mass. The majority (70-80%) of cholesterol in the brain is present in myelin and as such, the rate of cholesterol synthesis in the brain is highest during active myelination, and declines once myelination is complete [45]. Despite being physically separated from plasma lipoproteins, the central nervous system (CNS) contains its own lipoproteins [46, 47], as well as proteins involved in lipoprotein assembly (ABCA1, ABCG1) [48-51] and uptake (LDLR and members of the LDLR superfamily) [46, 52, 53]. The predominant lipoproteins of the CNS are HDL-sized particles containing apolipoprotein E, which is mainly synthesized in the astrocytes [46, 54-56]. In the adult brain, cholesterol synthesis is thought to occur primarily in astrocytes [57], which can supply cholesterol to neurons in the form of apolipoprotein E-containing lipoproteins (reviewed in [58]). These astrocyte-derived lipoproteins have been shown to promote axon growth [59, 60] and synaptogenesis [61]. Controversy still exists whether neurons also synthesize cholesterol in the adult brain. It is clear that neurons have the ability to synthesize cholesterol, as primary cultures of neurons can be grown in the absence of any exogenous lipids [62, 63] (Fig. 3.19*A* and 3.21*A*), and incorporate [$^3$H]acetate into newly synthesized cholesterol (Fig. 3.25*A*). Furthermore, HMGCR and Dhcr7, the final enzyme in cholesterol biosynthesis, have been detected in adult mouse cortical and

hippocampal neurons by *in situ* hybridization [64]. Likewise, analysis of *in situ* data from the Allan Mouse Brain Atlas shows mRNAs encoding a number of genes involved in cholesterol synthesis and homeostasis are detectable in hippocampal neurons [65]. However, other studies have found that retinal ganglion cells down-regulate squalene synthase, the enzyme that catalyzes the first committed step in cholesterol biosynthesis, when they are co-cultured with astrocytes [66]. In support of this, Funfschilling *et al*. found very little squalene synthase in cerebellar granule cells (CGCs) of adult mice and disruption of the squalene synthase gene in CGCs of adult mice caused no detectable neurodegeneration [67]. Thus, while neurons appear to have the ability to synthesize cholesterol endogenously, in adult brains neurons may decrease cholesterol synthesis and instead rely primarily upon uptake of astrocyte-derived cholesterol.

Just as the BBB restricts movement of cholesterol into the CNS, it also prevents movement of excess cholesterol out of the CNS. Cholesterol synthesis continues at a slow rate in the mature brain [68, 69], and cholesterol is constantly being turned over. Since cells are unable to degrade the cholesterol backbone, the brain must have a mechanism to move excess cholesterol out of the CNS in order to maintain the appropriate concentrations of cholesterol within brain cells. One way this occurs is through the conversion of cholesterol into the oxysterol 24(S)-hydroxycholesterol [70-72], a reaction catalyzed by the cytochrome P450-containing enzyme cholesterol 24-hydroxylase [73]. This enzyme is

expressed in a subset of neurons that include Purkinje cells of the cerebellum and pyramidal cells of the cortex, but is essentially absent in astrocytes [73]. Unlike cholesterol, which is unable to penetrate the BBB, 24(S)-hydroxycholesterol appears able to cross the BBB, entering the circulation where it can be delivered to the liver and excreted from the body as bile [70-72]. When *Cyp46a1* (the gene encoding cholesterol 24-hydroxylase in mice) is disrupted the brain shows a 40% decrease in cholesterol synthesis, while the steady-state concentration of cholesterol remains the same [74]. Not only does this imply that a small number of neurons are responsible for the flux of at least 40% of cholesterol out of the brain, it also demonstrates that another significant pathway must exist to excrete cholesterol from the CNS. It remains to be determined what this other pathway is. Experiments by Repa *et al*., however, suggest this may be occurring through an LXR-dependent pathway, since administration of an LXR agonist to *Npc1*$^{-/-}$ mice led to increased flux of cholesterol out of the CNS and increases in ABCA1 and ABCG1 mRNA, but caused no changes in cholesterol synthesis or *Cyp46a1* [75].

### *1.B NIEMANN-PICK TYPE C DISEASE*

NPC disease is a fatal, autosomal recessive disorder that affects approximately 1 in 150,000 live births [76]. The majority of cases result from mutations in the *NPC1* gene (95%) while the remainder (5%) are caused by mutations in the *NPC2* gene. Loss of function of either of these proteins results in an accumulation of cholesterol and other lipids,

including sphingomyelin, sphingosine and gangliosides (GM2 and GM3) within the LE/L. In mice and humans, this impairment leads to progressive neurodegeneration, hepatosplenomegaly, lung disease and, ultimately, premature death. Typically, clinical manifestations become evident in early childhood, although age of onset can range from the perinatal period to adulthood. Disease progression is often more rapid when onset of symptoms occurs in early life [77].

Initial studies by Pentchev *et al.* found that fibroblasts from NPC1-deficient patients have a defect in cholesterol esterification despite having normal ACAT activity [78]. Staining of these cells with filipin, which labels unesterified cholesterol, suggested that although LDL-cholesterol is internalized and hydrolyzed normally in these fibroblasts, its movement to the ER is blunted [78]. Consequently, LDL is unable to decrease cholesterol biosynthesis and LDLR activity, both of which are regulated at the ER [79]. Cytochemical techniques confirmed that there is a massive storage of cholesterol within the lysosomes of NPC-deficient fibroblasts [80]. More recent studies have begun to unravel the molecular and cell biological bases of these findings.

*1.B(i) NPC1 and NPC2 Proteins*

Positional cloning techniques have identified the human *NPC1* gene (on chromosome 18q11) and its orthologs in mice, the yeast *Saccharomyces cerevisiae*, the nematode *Caenorhabditis elegans* [81, 82]

and *Drosophila* [83]. Expression of NPC1 in cultured fibroblasts from patients with NPC disease abolished the lysosomal accumulation of cholesterol [81]. NPC1 is an integral membrane protein that is primarily localized to the LE/L, although this protein also appears to cycle through the *trans*-Golgi network [84, 85]. Human NPC1 consists of 1278 amino acids and contains 13 putative transmembrane domains that are separated by three luminal glycosylated loops [81, 86]. Moreover, NPC1 contains a sterol-sensing domain that has a similar sequence to that in HMGCR, SREBP and Patched [81].

Through studies that were designed to characterize the lysosomal proteome, the gene responsible for NPC2 disease was subsequently identified [87]. NPC2 (previously called HE1) is a ubiquitously expressed 151-amino acid, soluble lysosomal protein [87]. Originally, NPC2 was identified as a cholesterol binding protein that is a major secretory component of epididymal fluid [88]. Fluorescence quenching assays showed that NPC2 can transfer cholesterol between phospholipid vesicles *in vitro*. In addition, the transfer of cholesterol from phospholipid vesicles to NPC2 is dramatically increased by the presence of bis(monoacylglycero)phosphate (a LE/L phospholipid that accumulates in NPC-deficient cells) in donor vesicles [89].

Homozygous mutations in either NPC1 or NPC2 result in virtually identical cellular and clinical phenotypes [90]. Likewise, when NPC1-deficient mice are crossed with *Npc2* hypomorphic mice, which retain

0-4% residual NPC2 protein, the phenotype is indistinguishable from that of either NPC1- or NPC2-deficient mice [91], suggesting that these proteins function in tandem, or sequentially, in the same pathway. Binding studies and crystal structures of NPC1 and NPC2 have provided valuable insights into the functions of these proteins. NPC2 binds cholesterol with high affinity in a process that is sensitive to modification of the hydrophobic side-chain of cholesterol [88, 92]. A crystal structure of bovine NPC2 bound to cholesterol sulfate shows that cholesterol binds in a deep hydrophobic pocket, with only the sulfate (substituted for the 3β-OH moiety) of the sterol exposed to solvent [93]. NPC1 also binds cholesterol and fluorescent sterol analogs, as well as oxysterols [92, 94, 95]. More recently, Kwon *et al.* reported the crystal structure of the N-terminal domain of NPC1 and revealed that this domain binds to cholesterol so that the 3β-OH group is buried within the binding pocket and the iso-octyl side-chain is exposed on the surface [96]. Since NPC1 and NPC2 appear to bind cholesterol in opposite orientations, a model for the functions of the two NPC proteins was proposed. In this model, unesterified cholesterol in the interior of the LE/L is initially bound by NPC2 which subsequently transfers the cholesterol to the N-terminal cholesterol-binding domain of NPC1 in the limiting membrane of the LE/L (Fig. 1.1) [96]. This model predicts that NPC1 inserts the iso-octyl side-chain of cholesterol into the lysosomal outer membrane, although this feature remains to be confirmed [96]. In support of this model, NPC2

greatly accelerates the bi-directional transfer of cholesterol from NPC1 to liposome acceptors, particularly those containing the LE/L-specific phospholipid, bis(monoacylglycero)phosphate [97]. The role that the sterol-sensing domain of NPC1 plays in this process remains unclear since mutations in this domain prevent the binding of a photo-activatable analog of cholesterol to NPC1 in intact cells [98]. However, direct binding of this cholesterol analog to the sterol-sensing domain was not demonstrated [98], leaving open the possibility that this domain modulates cholesterol binding to the N-terminal domain of NPC1. An alternative model that has been proposed, and not yet ruled out, for the sequential action of NPC1 and NPC2 is that NPC1 transfers cholesterol to NPC2. No direct interaction between the NPC1 and NPC2 proteins has been detected.

Other experiments, in which NPC1 was expressed in *Escherichia coli,* indicated that NPC1 might be a fatty acid transporter [99]. In these studies, NPC1 was able to transport oleic acid, but not cholesterol or CE, across the *E. coli* membrane [99]. Nevertheless, subsequent work showed that the flux of fatty acids through the NPC1-deficient LE/L is normal, suggesting that fatty acid export from the LE/L does not require NPC1 in mammalian cells [100]. The finding that NPC1 that is expressed in *E. coli* cannot mediate the transbilayer movement of cholesterol might indicate that NPC1 requires the presence of functional NPC2 in order to transport cholesterol.

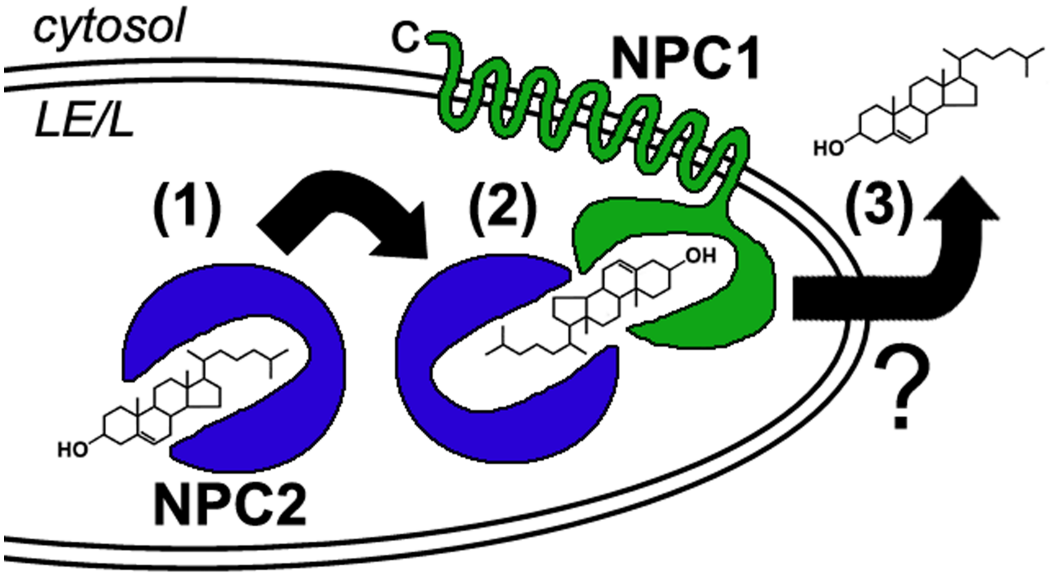


FIGURE 1.1 - **Potential mechanism for NPC1/NPC2-mediated cholesterol efflux out of LE/L.** (1) NPC2 (soluble protein) binds unesterified cholesterol in the LE/L with the isooctyl chain in the binding pocket, an event that may be enhanced by/require cholesterol - lyso-*bis*-phosphatidic acid interactions. (2) NPC2 transfers cholesterol to the N-terminal domain of NPC1 (a multi-pass membrane protein) which binds cholesterol with the hydroxyl group in the binding pocket. (3) Cholesterol is effluxed out of the LE/L by an unknown mechanism.

*1.B(ii) Models of NPC Disease*

NPC disease is studied in a number of different models. Cellular models of NPC disease include human *NPC1*$^{-/-}$ fibroblasts and *Npc1*$^{-/-}$ Chinese hamster ovary cells, both of which have been used extensively. Additionally, the amphipathic steroid 3-β-[2-(diethylamino)ethoxy]androst-5-en-17-one (U18666A), which blocks the egress of cholesterol out of the LE/L, is frequently used to induce an NPC-like phenotype in a variety of different cell types [101]. However, U18666A does not perfectly mimic the NPC-phenotype, and causes other effects not seen in NPC-deficient cells

that include blocking cholesterol synthesis [102, 103].

Several mouse models exist that recapitulate the features of human NPC disease, including accumulation of cholesterol in the LE/Ls of tissues throughout the body, progressive neurodegeneration, ataxia, liver and lung disease, and premature death. The most commonly used mouse model contains a naturally occurring null mutation in *Npc1* on the BALB/c genetic background [82, 104, 105]. However, it is important to note that genetic drift can lead to variations in the severity and progression of the disease [106]. An *Npc2* hypomorphic mouse model also exists, which retains 0-4% NPC2 in various tissues [91]. This NPC2-deficient mouse model has a phenotype that is virtually identical to that in *Npc1*$^{-/-}$ mice [91]. In addition, a feline model exists with a mutation in NPC1 that results in an NPC phenotype similar to that seen in human NPC disease [107-109]. As well, *Drosophila* [83] and *Saccharomyces cerevisae* [110, 111] models have been used to study NPC disease.

*1.B(iii) Abnormal Lipid Trafficking in NPC-deficient Cells*

The mechanisms responsible for the various pathways of inter-organelle trafficking of cholesterol within cells are largely undefined. The endocytic uptake of LDLs, and the subsequent hydrolysis of CE, are normal in NPC1-deficient cells [78]. However, the export of cholesterol and other lipids from the LE/L is defective. Consequently, normal amounts of cholesterol fail to reach the plasma membrane and the ER for regulation of cholesterol homeostasis [78, 79]. Since cholesterol trafficking to the ER

is impaired in NPC-deficient cells, the cells sense a lack of cholesterol. Thus, cholesterol synthesis and LDLR expression are increased despite abnormally elevated cholesterol levels in the LE/L [79]. The mechanism by which cholesterol reaches the ER from the LE/L remains to be defined. Recent findings suggest that cholesterol is first trafficked from the LE/L to the *trans*-Golgi network prior to reaching the ER in a process that is dependent upon a SNARE complex, although other possibilities exist [112]. Endogenously synthesized cholesterol can also accumulate within the LE/L, albeit much more slowly than does LDL-derived cholesterol [113]. Unlike LDL-derived cholesterol, the transport of endogenously synthesized cholesterol to the plasma membrane is not impaired in NPC1-deficient fibroblasts [113, 114]. Presumably through formation of endocytic vesicles and membrane recycling, this source of cholesterol can, however, also become trapped in the LE/L. Furthermore, cholesterol that is taken up through bulk-phase endocytosis also enters the LE/L and, as a consequence, becomes trapped within the LE/L compartment of NPC1-deficient cells [7]. Interestingly, the intracellular transport of cholesterol derived from HDL appears to be unaffected by NPC1-deficiency, suggesting that cholesterol derived from these lipoproteins is processed in the cell through a pathway different from that used by LDL-cholesterol [115].

In addition to cholesterol, a variety of other lipids, including sphingomyelin, sphingosine, bis(monoacylglycero)phosphate, and

complex glycosphingolipids (GSLs, particularly the gangliosides GM2 and GM3) accumulate in the LE/L of NPC-deficient cells (reviewed in [62]). There has been, and still is, debate over which lipid is the first to accumulate in NPC-deficient cells, and which lipids are responsible for the cellular dysfunction underlying NPC disease. Although the majority of data implicate cholesterol accumulation as the primary defect, there is some evidence that points to other lipids. For example, in a drug-induced (U18666A) model of NPC disease the accumulation of sphingosine in the LE/L apparently preceded both calcium depletion of these organelles and cholesterol accumulation [116]. Moreover, calcium stores in the acidic compartment of NPC1-deficient cells were reduced, and the chelation of calcium in the lumen of the endocytic pathway of wild-type cells causes an NPC disease-like phenotype [116]. Although these experiments show that sphingosine is elevated prior to cholesterol in this drug-induced NPC model, these studies do not demonstrate that sphingosine accumulation is the initial event that causes lipid accumulation in the LE/L of NPC1-deficient cells. As U18666A does not precisely mimic NPC deficiency, and has additional effects on cholesterol homeostasis, including inhibition of cholesterol synthesis [102, 103], it is unclear if the changes seen in this U18666A model would also be seen in NPC1-deficient cells, or if they are due to other effects of the drug.

Several studies indicate that GSL accumulation in the LE/L is not the causative event in NPC disease. For example, NPC1-deficient mice

that also have disrupted *Galgt1* and *Siat9* genes, and are unable to synthesize GM2/GD2 or GM3 complex gangliosides, accumulate the same amount of cholesterol in LE/L in the brain and other tissues as do NPC1-deficient mice [106, 117]. Moreover, rather than extending the life of NPC1-deficient mice, deletion of these genes shortened the life-span, most likely because GSLs are important for CNS health and function [106, 117]. Similarly, when mice lacking *N*-acetylgalactosamine transferase (unable to synthesize GM2 and complex gangliosides) were crossed with NPC1-deficient mice, the absence of GM2 did not increase the life-span of the NPC1-deficient mice [118]. Thus, elimination of the GSL storage did not prevent development of the NPC disease phenotype. On the other hand, in another study, elimination of the GSL biosynthetic enzyme N-acetylgalactosamine transferase in NPC1-deficient mice reduced filipin staining of cholesterol in some, but not all, types of neurons in the brain, although cholesterol content was not measured directly [119].

The idea that cholesterol is the initial lipid that accumulates in NPC deficiency is strongly supported by the observation that both NPC1 and NPC2 bind cholesterol [93, 96], while this evidence is lacking for other lipids such as GSLs. Currently, the majority of experimental evidence supports a model in which mutation of either NPC1 or NPC2 initially leads to cholesterol accumulation in the LE/L, which in turn causes sequestration of a variety of other lipids. Cholesterol accumulation in the LE/L can also cause mis-trafficking of GSLs [120] and GSL accumulation

can cause cholesterol entrapment in the LE/L [121]. Cholesterol storage in the LE/L is increased in several sphingolipid storage disorders, including Niemann-Pick Type A disease, and depletion of cholesterol from sphingolipid storage disease cells restored the normal trafficking of a fluorescent GSL analog (BODIPY-lactosylceramide) from the LE/L to the Golgi apparatus [120]. Moreover, when wild-type cells were overloaded with cholesterol, the trafficking of BODIPY-lactosylceramide to the LE/L increased [120]. The affinity of cholesterol for GSLs is indicated by their association in detergent-resistant domains of cell membranes. Thus, in NPC disease, not only is it possible that the initial sequestration of cholesterol leads to the accumulation of GSLs, but these GSLs might subsequently induce the accumulation of even more cholesterol. We speculate that this cyclic buildup of lipids within the LE/L might explain why treatments that focus on reduction of GSL storage can provide some therapeutic benefit in NPC1-deficient models [122]. Devlin *et al.* provide compelling evidence in support of this theory, by demonstrating that although impaired cholesterol trafficking is most likely the primary defect in NPC1-deficient cells, correction of a secondary defect (sphingomyelin accumulation) can substantially improve lipid and protein trafficking [123].

Another lipid that accumulates in the LE/L of NPC1-deficient cells is sphingomyelin. In response to the abnormal cholesterol accumulation in membranes of the LE/L in NPC1-deficient fibroblasts, the activity of acid sphingomyelinase was reduced although the amount of this enzyme was

normal [123]. When normal acid sphingomyelinase activity was restored in the NPC1-deficient fibroblasts, either through cDNA transfection or enzyme replacement, a dose-dependent reduction in lysosomal cholesterol content occurred and the abnormal recycling of the transferrin receptor was partially corrected [123]. Even when normal sphingomyelinase activity was restored, the intensity of filipin staining remained 25-30% higher than normal, most likely due to the primary underlying cholesterol trafficking defect [123]. The same logic might explain the partial success of miglustat treatment of children with NPC disease [124, 125]. Miglustat is a small iminosugar that reversibly inhibits the first step of GSL synthesis (glucosylceramide synthase), improves the clinical symptoms, and modestly increases the life-span of NPC1-deficient mice and cats [122]. This “substrate reduction therapy” is a potentially useful treatment for NPC disease since the residual activity of glucosylceramide synthase would likely produce sufficient GSLs for functioning of the CNS.

There is evidence that cholesterol accumulation in the LE/L can impair vesicular trafficking pathways. Vesicles of the endocytic pathway are transported along the cytoskeleton, a process that is regulated by Rab GTPases (reviewed in [126]). Over-expression of Rab7, which is involved in vesicle trafficking from the early endosomes to LE, or over-expression of Rab9, which is involved in LE to Golgi trafficking, corrected the lipid trafficking defects in NPC1-deficient fibroblasts [127]. Although Rab4

(which is involved in endocytic recycling to the plasma membrane) protein levels are elevated in NPC1-deficient cells, the sequestration of cholesterol in the LE/L prevents the extraction of Rab4 from the endosomal membrane, a key step required for Rab4 function [128]. As a consequence, the Rab4-mediated recycling of lipids and proteins is impaired [128]. Cholesterol depletion of NPC1-deficient cells restored normal BODIPY-lactosylceramide recycling and Rab4 organization [128]. Modulation of pathways that involve Rab4, Rab7 or Rab9 was suggested as a method of overcoming the trafficking defects in NPC-deficient cells. Along these lines, over-expression of Rab9 in NPC1-deficient mice modestly increased life-span and reduced ganglioside storage in the brain [129]. Over-expression of Arf6 (which is involved in regulation of early endosomal membrane internalization and recycling) also reduced lipid accumulation in NPC1-deficient cells [130]. Furthermore, Goldman and Krise have demonstrated that fusion/fission events between the LE and lysosomes are severely impaired in NPC1- and NPC2-deficient cells [131]. Intriguingly, it appears that NPC1 and NPC2 might be involved in different aspects of this process, so that NPC1 is important for the retrograde fusion of LE and lysosomes, while NPC2 plays a role in fission events that might be important for re-formation of lysosomes [132]. Retrograde fusion of lysosomes with LE is thought to be important for egress of membrane-impermeable cargo out of the cell, and impairment of this pathway might cause a build-up of toxic metabolites in the LE/L [132]. Indeed, the

release of molecules such as dextran and sucrose from NPC1-deficient cells is impaired [85, 131, 133]. Thus, lipid accumulation within the LE/L can severely reduce the trafficking of lipids and other molecules through the endocytic pathway.

Mitochondria are crucial for providing cells with energy in the form of ATP, and also play a central role in apoptosis. Due to these important functions, mitochondrial dysfunction has been implicated in cell death in a variety of neurodegenerative disorders. Cholesterol trafficking from the LE/L to mitochondria does not appear to be impaired by NPC1 deficiency [134]. Indeed, the cholesterol content of mitochondria in brains, neurons and hepatocytes from NPC1-deficient mice is increased by NPC1 deficiency [134-137], probably due to the increased amounts of unesterified cholesterol in the LE/L that are available for import into mitochondria. Interestingly, RNA silencing of the endosomal protein MLN64 decreased the cholesterol content of mitochondria, both in the absence and presence of NPC1, indicating that MLN64 can mediate the transport of endosomal cholesterol into mitochondria independent of NPC1 [134]. Since cholesterol regulates membrane fluidity, these changes in mitochondrial cholesterol content might have a direct impact on mitochondrial function and stability, as suggested in several studies. For example, mitochondrial membrane potential, the activity of ATP synthase, and levels of ATP are all decreased in NPC1-deficient mouse brains and neurons [137]. Mitochondria from NPC1-deficient cells also

have decreased levels of glutathione, which serves as an important anti-oxidant defense. Consequently, these cells are more susceptible to killing by tumor necrosis factor-α (TNFα), as well as by oxidative stress induced by amyloid-$\beta_{1-42}$ [135, 136].

*1.B(iv) NPC Deficiency in Liver*

In individuals with NPC disease, cholesterol accumulates in almost all tissues of the body in amounts that are proportional to the rate at which each tissue obtains cholesterol through the LDLR pathway [138]. The liver is responsible for the uptake of ~80% of LDL-cholesterol [138]. Although the rate of LDL-cholesterol uptake by the liver is similar in wild-type and NPC1-deficient mice, the large flux of cholesterol through the liver causes a massive accumulation of cholesterol within the LE/L of livers in NPC1-deficient mice [138]. Consequently, markers of liver damage (alanine aminotransferase and aspartate aminotransferase activities) are substantially increased in NPC1-deficient mice [139]. Moreover, ~50% of infants with NPC disease exhibit hepatomegaly which can lead to liver failure and death [140]. Underscoring the unique role that the liver plays in lipoprotein metabolism, the extent of cholesterol accumulation in NPC1-deficient mouse hepatocytes is much greater than in NPC1-deficient fibroblasts [141]; cholesterol levels in hepatocytes from *Npc1*$^{-/-}$ mice are 5- to 10-fold higher than in *Npc1*$^{+/+}$ mice [141]. Enigmatically, whereas in NPC1-deficient fibroblasts cholesterol esterification is markedly attenuated, cholesterol esterification in NPC1-deficient hepatocytes is

increased [141]. In addition, NPC1 deficiency in hepatocytes increases the expression of ABCA1 and the formation of HDL [142]. It is likely that the massive overload of cholesterol in the LE/L of hepatocytes causes a leakage of excess cholesterol from the LE/L so that cholesterol can be transported to the ER where cholesterol homeostasis is regulated.

*1.B(v) NPC Deficiency in the Brain*

Defects in cholesterol metabolism in the brain have increasingly been linked to neurodegenerative disorders such as AD and Huntington disease. Surprisingly, although cholesterol accumulates in tissues throughout the body in NPC disease, the amount of cholesterol in the brain does not increase, but even *decreases*, with age [138]. Several factors may explain this apparent discrepancy. First, extensive demyelination occurs in the NPC1-deficient brain, and since myelin is particularly rich in cholesterol, the demyelination would likely mask any increase in cholesterol content of other cells in the brain [143]. Second, the rate of cholesterol excretion from the brain is increased in NPC1-deficient mice [143]. However, as in other NPC1-deficient cells, cholesterol does accumulate in the LE/L of neurons of newborn NPC1-deficient mice [63] and in the brains of young NPC1-deficient mice, prior to extensive demyelination [143]. In addition, increased filipin (cholesterol) staining was observed in NPC1-deficient brain slices compared to wild-type brains [144]. However, these studies did not determine if other lipids also accumulated in brains of young NPC1-deficient mice.

Since the BBB isolates the brain from cholesterol in the circulation, treatments that modulate cholesterol homeostasis in other tissues would not necessarily be expected to translate into improvement of neurological symptoms of diseases that involve defects in cholesterol metabolism. Thus, when NPC1-deficient mice were crossed with LDLR knockout mice, the neuropathological features of NPC disease did not improve [145]. The lack of a beneficial effect of cholesterol-lowering treatments in the brain might be due to contributions of other lipoprotein receptors in the brain, or to the accumulation of endogenously synthesized cholesterol within neurons. In support of the latter explanation, NPC1-deficient mouse sympathetic neurons [63], embryonic hippocampal neurons [62], and CGCs (Fig. 3.23*A*) showed the typical punctate filipin staining pattern of cholesterol sequestration in the LE/L, even in neurons that had been isolated from newborn mice or cultured for 20 days in the complete absence of serum lipoproteins. Pharmacological attempts at lowering plasma cholesterol also failed to improve the NPC phenotype [146], possibly because some cholesterol-lowering drugs cannot cross the BBB. On the other hand, when cholesterol synthesis was blocked using a squalene synthase inhibitor in young NPC1-deficient mice prior to formation of the BBB, cholesterol accumulation in neurons, and astrocyte activation, were attenuated [147]. Importantly, however, blocking cholesterol synthesis at this early stage of mouse development might disrupt the myelination process, which could negate any beneficial effects

of this treatment for NPC1 deficiency [147]. When cholesterol homeostasis was altered using an LXR agonist, the life-span of NPC1-deficient mice was extended and the neurodegeneration was delayed [75]. While the LXR agonist did not reduce cholesterol concentration or synthesis in the brain, excretion of cholesterol from the CNS was increased [75]. Thus, modulation of cholesterol metabolism in NPC-deficient brains might reduce the severity and progression of NPC disease. Nevertheless, the importance of adequate levels of cholesterol for brain development and function, along with the problem of overcoming the BBB, represent some of the many technical difficulties associated with altering cholesterol metabolism in the CNS.

*Neurons*

Neurodegeneration in NPC disease occurs in a progressive and neuron-selective manner, and is particularly evident in Purkinje cells of the cerebellum. In NPC1-deficient mice, Purkinje cell death is first evident around three weeks after birth, with nearly all Purkinje cells dying by eleven weeks [148, 149]. Neuronal loss is also evident in other brain regions including the substantia nigra, pons, regions of the brainstem, thalamus, and prefrontal cortex [150-152]. NPC1-deficiency in the brain causes a variety of neuronal abnormalities that could lead to neuronal dysfunction and/or death. The reason for the selective neurodegeneration in NPC disease has yet to be elucidated. Recent experiments have shown that in *Npc1*$^{-/-}$ mice, the levels and activity of the lysosomal

enzymes, cathepsins B and D, are elevated to a greater extent in the cerebellum than in the hippocampus, which is relatively protected from neurodegeneration [153]. Furthermore, cytosolic levels of cathepsins and apoptotic molecules are higher in the cerebellum than in the hippocampus [153]. Experiments with chimeric mice, that contain both *Npc1*$^{+/+}$ and *Npc1*$^{-/-}$ cells, showed that the death of NPC1-deficient Purkinje cells was not prevented by the presence of wild-type glia [154]. Nor did NPC1-deficient glia induce death of wild-type Purkinje cells, suggesting that death of Purkinje cells is cell autonomous [154]. In support of these findings, Elrick *et al.* recently generated mice that lacked NPC1 in only the Purkinje cells [155]. The same extent of Purkinje cell death occurred in these mice as in NPC1 global null mice [155]. Interestingly, however, although these mice showed progressive motor impairment, they did not exhibit other typical manifestations of NPC disease such as weight loss and early death [155]. These important studies demonstrate that the premature death of NPC1-deficient mice is not due (solely) to the death of Purkinje cells.

The mechanism by which Purkinje cells, and other neurons, degenerate in NPC disease remains unclear. Increased levels of markers of autophagy (beclin-1 and microtubule-associated protein 1 light chain 3-II) were detected in brains of *Npc1*$^{-/-}$ mice [156, 157], and electron microscopy revealed autophagic vesicles in *Npc1*$^{-/-}$ Purkinje cells [154]. Autophagy is the process through which cells degrade long-lived proteins

and organelles via lysosomes. During periods of starvation, autophagy is crucial for providing cells with energy through digestion of non-essential cellular components [158]. Signs of autophagy have been detected in other neurodegenerative disorders including AD, Parkinson disease and Huntington disease, leading to speculation that excessive or impaired autophagy leads to neuronal cell death. In NPC disease, the induction of autophagy may serve as a mechanism for counteracting the abnormal accumulation of lipids within the LE/L, or as a starvation response to the sequestration of lipids in LE/L. Although it is possible that accumulation of lipids within lysosomes impairs their ability to bind to autophagosomes for degradation of engulfed material, degradation of long-lived proteins was increased in NPC1-deficient human fibroblasts, suggesting that the autophagy pathway was intact [157]. It remains to be determined whether or not autophagy contributes to neuronal death in NPC disease.

Apoptosis of neurons has also been observed in NPC disease. TUNEL-positive staining of nuclei in the cerebral cortex and cerebellum was evident in NPC patients and NPC1-deficient mice [159]. Moreover, the level of mRNAs encoding TNFα and players in the TNFα death pathway in the brain were higher in *Npc1*$^{-/-}$ mice than in *Npc1*$^{+/+}$ mice [159]. The expression of other markers of apoptosis, including mRNAs encoding caspases 1 and 3 [148], as well as activation of the c-Abl/p73 pro-apoptotic pathway [160], was also increased in the cerebellum of NPC1-deficient mice. Treatment of *Npc1*$^{-/-}$ mice with imatinib, an inhibitor

of c-Abl, reduced Purkinje cell death, improved neurological symptoms and modestly extended the life-span [160].

In addition to neuronal death in NPC disease, other neuronal functions are likely to be impaired by NPC deficiency. The transport of cholesterol from cell bodies to distal axons of isolated neurons is reduced by NPC1 deficiency [161]. Correspondingly, the cholesterol content of cell bodies of *Npc1*$^{-/-}$ neurons is increased whereas the cholesterol content of distal axons is reduced [63]. Moreover, the NPC1 protein is present not only in the LE/L of cell bodies of sympathetic neurons but also in recycling endosomes of pre-synaptic nerve terminals [162]. This observation might explain the defects in synaptic functions in NPC1-deficient neurons [163, 164]. NPC1-deficient neurons in humans, felines, and mice show additional abnormalities such as dendritic and axonal alterations that include ectopic dendrites and axonal spheroids [165]. Furthermore, NPC disease exhibits some similarities to AD as neurofibrillary tangles and hyperphosphorylation of tau are evident in both Alzheimer patients and in NPC disease patients [166, 167]. However, neurofibrillary tangles are absent in NPC1-deficient mice despite tau being hyperphosphorylated [150, 168].

*Astrocytes*

Although much focus has been directed at neuronal death in NPC disease, the brain also contains many glial cells which are crucial for brain

function. Astrocytes, the major glial cell type in the CNS, play important roles in supporting neuronal functions, particularly at the synapse [169]. As in other NPC1-deficient cells, *Npc1*$^{-/-}$ mouse astrocytes sequester cholesterol within LE/L [50], and reactive astrocytes have been detected throughout the brains of 4-week-old *Npc1*$^{-/-}$ mice, particularly in the cerebellum and thalamus [170]. The finding that NPC1 protein is localized predominantly in astrocytic processes in monkey brains suggests that mutations in NPC1 might impair astrocyte function [171]. Surprisingly, despite these astrocyte abnormalities, the quantity and composition of apolipoprotein E-containing lipoproteins secreted by *Npc1*$^{+/+}$ and *Npc1*$^{-/-}$ mouse astrocytes are similar, and the lipoproteins secreted by astrocytes of both *Npc1* genotypes promote axon growth to the same extent [50]. On the other hand, when *Npc1*$^{+/+}$ neurons were cultured on *Npc1*$^{-/-}$ astrocytes, neurite growth was reduced compared to that of *Npc1*$^{+/+}$ neurons cultured on *Npc1*$^{+/+}$ astrocytes [172]. In addition, the expression of neurosteroid biosynthetic enzymes, and the secretion of the neurosteroid estradiol, were lower in *Npc1*$^{-/-}$ astrocytes than in *Npc1*$^{+/+}$ astrocytes [172]. Estradiol levels were also lower in NPC1-deficient mouse brains, and administration of estradiol to *Npc1*$^{-/-}$ mice alleviated some of the symptoms of NPC disease [172]. These results imply that impaired neurosteroid synthesis in NPC1-deficient astrocytes might contribute to neuronal death in NPC disease. In other experiments, NPC1 was over-expressed in astrocytes of NPC1-deficient mice using the glial fibrillary acidic protein promoter [173].

Neurodegeneration and the neuronal storage of cholesterol in the mice were decreased and life-span was increased compared to those parameters in the *Npc1*$^{-/-}$ mice [173]. However, the expression of NPC1 in astrocytes of *Npc1*$^{-/-}$ mice did not prevent Purkinje cell loss [173], suggesting that astrocyte dysfunction alone does not account for the extensive neuron loss in NPC disease.

*Oligodendrocytes*

Oligodendrocytes are the glial cells that form myelin sheaths around axons in the brain and are, therefore, essential for proper neuronal function. The NPC1-deficient mouse brain exhibits extensive demyelination, especially in the corpus callosum, where myelin is essentially absent by 8 weeks of age [143, 174]. Pre-myelinating oligodendrocytes and oligodendrocyte progenitor cells are abundant in *Npc1*$^{-/-}$ mouse brain regions that show hypomyelination, including the corpus callosum and cerebral cortex [175]. The abundance of these precursor cells and the lack of mature oligodendrocyte markers in hypomyelinated regions suggest that NPC1 deficiency causes a defect in myelination [175]. This abnormal myelination might be due to axonal damage, which occurs early during development of the NPC1-deficient mouse brain [152]. On the other hand, inclusion bodies have been detected in *Npc1*$^{-/-}$ oligodendrocytes, suggesting that defects in myelination might be due to oligodendrocyte dysfunction [176]. As is the case for oligodendrocytes in the CNS, immortalized Schwann cells of the

peripheral nervous system showed punctate filipin staining [177], and hypomyelination of peripheral nerves was observed in 70-day-old *Npc1*$^{-/-}$ mice [178]. Furthermore, myelination in the peripheral nervous system of *Npc1*$^{-/-}$ mice was impaired following sciatic nerve crush injury [179]. In *Npc1*$^{+/+}$ mice, thick myelin sheaths surrounded the axons 4 weeks after the crush injury, whereas NPC1-deficient mice had thinner sheaths [179]. Eventually, however, 10 weeks after the injury, the extent of myelination in the *Npc1*$^{-/-}$ mice was comparable to that in *Npc1*$^{+/+}$ mice [180]. These alterations in myelination might contribute to the neuronal dysfunction and degeneration characteristic of NPC disease.

*Microglia*

Microglia are the resident macrophages of the CNS, functioning as the primary immunocompetent and phagocytic cells (reviewed in [181]). Microglia are believed to originate from the myeloid lineage, infiltrating the brain during embryonic development, and ultimately differentiating into mature, ramified microglia [182]. Discovered by del Rio Hortega, microglia comprise approximately 10% of the glial cells in an adult brain [183]. In a healthy brain, ramified microglia are in close association with neurons and other glial cells, continuously monitoring their local environment with extended cellular processes [184]. Microglia are typically the first cells to respond to disruptions in the CNS that include cellular damage, dysfunction, or death. Upon stimulus, microglia can quickly become activated and change from a resting ramified morphology to a motile

ameboid cell type [185, 186]. Activated microglia are capable of migrating to the site of injury [186, 187], proliferating [188], and phagocytosing dying cells and debris [189]. The initial activation of microglia typically leads to an inflammatory response, causing microglia to release a variety of molecules including pro-inflammatory cytokines [190, 191], glutamate [192], reactive oxygen species [193], and nitric oxide [194]. This inflammatory response is an attempt to prevent further damage to the CNS by removing damaged cells and/or offending metabolites. However, molecules produced during an inflammatory response are potentially cytotoxic, and thus microglia must tightly control inflammation as excessive or prolonged inflammation can lead to neuron death. As such, microglia are also capable of producing anti-inflammatory cytokines and a variety of neuroprotective molecules including growth factors [195-197]. This allows microglia to shift from a classical pro-inflammatory state to a more neuroprotective state once damaged cells are removed, promoting the repair and regeneration of damaged tissue [198]. These wide ranging capabilities allow microglia to provide the first line of defense against a variety of insults to the CNS.

Although microglia play a critical role in maintaining a healthy brain, there is increasing evidence that chronic activation, or microglial dysfunction, can contribute to cell death in a variety of neurodegenerative disorders. In disorders such as AD, Parkinson disease, amyotrophic lateral sclerosis, and the lysosomal storage disorder Sandhoff disease, the

number of active microglia is markedly increased [199-202]. Moreover, pro-inflammatory cytokines, as well as other neurotoxic molecules, are elevated in affected brain regions [202-205]. Along these lines, minocycline, a tetracycline derivative which inhibits microglial activation [206], is found to delay disease progression in animal models of Parkinson disease and amyotrophic lateral sclerosis [207], while anti-inflammatory treatment has shown some beneficial effects in AD patients [201]. Importantly, in amyotrophic lateral sclerosis and Sandhoff mouse models, replacing mutant microglia with wild-type microglia by bone marrow transplant delays the onset and slows the course of disease [202, 208]. Thus, microglia appear to be an active component in these disorders, although it remains unclear what is causing the microglia dysfunction. As microglia respond to damaged neurons, it is very likely that neurons degenerating during the course of the disorder recruit microglia which exacerbate the damage. The increased cellular damage caused by excessive microglial activation could lead to further microglial activation and neurodegeneration, creating a highly damaging cycle. Other evidence suggests microglia may be even more intimately involved in the neurodegenerative process. For example, increases in active microglia were found to precede neuron loss in Sandhoff disease [202]. Furthermore, pathogenic amyloid β-peptide (in AD) and prion protein are both capable of activating microglia in primary cultures, leading to increased production of cytotoxic molecules [209-211]. Thus, microglial

dysfunction, as well as expression of defective proteins within the CNS, may impair normal responses of microglia, or lead to microglial activation. Ultimately, activation or dysfunction of microglia could contribute to neurodegeneration directly, as well as by altering functions/survival of other neuron-supporting glial cells. Since microglia play a key role in maintaining CNS health, altered states of microglial activation or microglial dysfunction could also impair beneficial actions such as production of anti-inflammatory cytokines and growth factors, as well as cell migration and phagocytosis. Impairment in these microglial abilities would be predicted to be detrimental to neuron survival, particularly during periods of cellular stress or damage.

NPC1-null microglia show intracellular inclusions similar to those seen in other NPC1-null cells [174, 176]. In the NPC1-null brain, there are increased numbers of microglia showing an active morphology [170, 174, 212]. These microglia are found in regions such as the thalamus and cerebellum, prior to any detectable neurodegeneration, eventually spreading throughout the brain as the disease progresses [170]. This observation suggests microglia may play a role initiating neurodegeneration, although neuronal damage that is undetectable by the techniques employed in this paper may be responsible for activating the microglia [170]. Moreover, neuronal dysfunction, or death of other brain cells such as oligodendrocytes, could also be initiating microglial activation. The mRNA encoding the proinflammatory cytokine TNFα and

other mRNAs involved in the TNFα death pathway are increased in the cerebellum of NPC1-null mice [75, 148, 159]. Additionally, interleukin-6 and the toll-like receptor 4 (which can lead to production of interleukin-6 and other cytokines) are increased in microglia and other glial cells in the cerebellum of NPC1-null mice [213]. Notably, deletion of interleukin-6 in NPC1-null mice prevents activation of glia and causes a moderate increase in life-span, without increasing Purkinje cell survival [213]. Treatment of NPC1-null mice with an LXR agonist decreases Purkinje cell loss, prolongs life, and causes microglia to shift from an active state to a resting morphology [75]. Other studies found degenerating Purkinje cells in areas that show microglial infiltration. Treatment of NPC1-null mice with allopregnanolone delivered in methyl-β-cyclodextrin results in decreased Purkinje cell loss, increased survival, as well as decreased microglial infiltration and inflammatory markers [214, 215]. Although it remains unclear whether these effects are mediated by the allopregnanolone or the vehicle itself, the findings might implicate microglia in NPC disease progression.

These experiments, however, do not provide direct evidence that microglia are causing neuron death in NPC disease. Indeed, other groups have reported results that suggest microglia are not involved in NPC disease progression. Treatment of NPC1-null mice with minocycline did not lead to increased survival, although the authors did not show that the treatments actually inactivated microglia [216]. Additionally, treatments

with minocycline are not always well tolerated by mice due to the acidity of the compound, and thus effects of the compound may be masked by the stress induced by injecting the mice (unpublished data K. Peake *et al.*). Findings by Ko *et. al.*, using a chimeric mouse model, show NPC1-expressing Purkinje cells survive in the presence of NPC1-null microglia, and NPC1-expressing microglia are not capable of rescuing NPC1-null Purkinje cells [154]. Furthermore, when NPC1 is eliminated exclusively in Purkinje cells, Purkinje cell death still proceeds at a rate that is comparable to that seen in *Npc1*$^{-/-}$ mice [155]. These results suggest that Purkinje cell death in *Npc1*$^{-/-}$ mice may be cell autonomous. However, in these experiments, active microglia are still present when NPC1 is absent in Purkinje cells [155]. Thus, microglia may accelerate Purkinje cell death. Additionally, it remains possible that active microglia may be leading to death of neurons other than Purkinje cells in the NPC brain. In support of non-cell autonomous death, Chen *et. al.* call attention to experiments where NPC1 was expressed in NPC1-null mice under control of the mouse prion promoter [172, 217]. This treatment prevented Purkinje cell death, although there is evidence that the prion-promoter may not drive transgene expression in Purkinje cells [172, 218-220]. Furthermore, NPC1-null astrocytes release less estradiol, resulting in decreased neurite growth in neuron-astrocyte co-cultures, and administration of estradiol to NPC1-null mice increased Purkinje cell survival, delayed onset of symptoms, and increased life-span [172]. Thus, the role of microglia in

NPC disease remains controversial. Further work is needed to elucidate what is leading to microglial activation in NPC disease, and to determine if this actually translates to neurotoxicity. Furthermore, as microglia secrete beneficial molecules and clean up cellular debris by phagocytosis, it is also possible that microglial contribution to the NPC phenotype may not be direct, but instead through lack of trophic support or other beneficial functions.

*1.B(vi) Therapies for NPC Disease*

No treatments are currently available for NPC disease other than those used to alleviate the symptoms caused by disease progression. Recently, however, miglustat (an inhibitor of glucosylceramide synthase, the first step in GSL synthesis) was approved in Europe for the treatment of adult and pediatric patients with NPC disease. Miglustat was initially approved for treatment of patients with Gaucher disease, a lysosomal GSL storage disorder [221]. Administration of miglustat to animal models of NPC disease, including mice and cats, reduced ganglioside accumulation in the brain, delayed neurological symptoms, and modestly increased life-span [122]. Data from initial clinical trials suggest that long-term treatment of NPC patients with miglustat is well tolerated in adult and juvenile patients, and can stabilize some of the neurological symptoms [124, 125].

Another therapeutic strategy that was proposed for NPC disease was the administration of neurosteroids [222]. Cholesterol is a precursor of

the neurosteroids (i.e. steroids that are synthesized in the brain) that are important for neuron growth and development. In brains of NPC1-deficient mice, levels of pregnenolone and the neurosteroid allopregnanolone (ALLO), as well as the activities of the enzymes involved in ALLO synthesis, are lower than in wild-type mice [222]. Remarkably, a single injection of ALLO in 7-day-old NPC1-deficient mice delayed the onset of neurological symptoms and increased life-span. Purkinje cell survival was also increased, while levels of GM1 and GM2 gangliosides were reduced [222]. Other studies reported that ALLO reduced microglial activation and astrocyte proliferation, and increased myelination [214, 223]. At the cellular level, ALLO decreased the amount of filipin-labeled cholesterol, as well as markers of autophagy and the levels of lysosomal enzymes [223]. Although a $GABA_A$ receptor antagonist blocked the beneficial effect of ALLO on Purkinje cell survival, the stereoisomer of ALLO, *ent*-ALLO (which is not a $GABA_A$ receptor agonist) promoted neuronal survival to the same extent as ALLO [215, 222]. On the basis of these findings, Langmade *et al.* proposed that induction of pregnane X receptor-dependent gene expression by treatment of NPC1-deficient mice with ALLO or *ent*-ALLO mediated the beneficial effects of the neurosteroid [215]. However, it is difficult to rationalize why ALLO would improve the neurodegenerative phenotype through the pregnane X receptor, since expression of this receptor was undetectable in the brain [75]. Recently, the reported beneficial effects of ALLO have come under intense scrutiny

due to effects caused by the vehicle, cyclodextrin (CD), that was used in the experiments with ALLO described above.

*Cyclodextrin*

CDs are cyclic oligosaccharides composed of glucose molecules linked by α-1,4 glycosidic bonds. The molecule has a hydrophilic exterior and a relatively hydrophobic interior capable of solubilizing a variety of hydrophobic molecules, including cholesterol (reviewed in [224]). Due to these properties, CD has been used in a host of different applications that include drug delivery [225], food processing [226], the manipulation of cellular membranes [227], and gene delivery [228, 229]. CD is formed through enzymatic degradation of starch that most commonly results in the generation of rings composed of six (α), seven (β), or eight (γ) glucose units [230]. The number of glucose units determines the size of the CD cavity, and thus is an important factor in determining the specificity of binding of CD to specific lipids [231, 232]. Along these lines, αCD binds phospholipids with a high affinity whereas βCD binds cholesterol with a high affinity [233], while the larger cavity of γCD allows it to bind to a variety of lipids with lower specificity [231, 232].

The ability of βCD to bind to cholesterol has made it of particular interest in the field of NPC research. Although βCD is able to bind cholesterol, it has several properties that make it unsuitable for any practical therapeutic applications. For instance, the hydroxyl groups of the

glucose molecules comprising the CD ring structure are responsible for the solubility of CD. In βCD, interactions among the different hydroxyl groups actually render it relatively insoluble compared to αCD and γCD [225, 230, 234]. Moreover, βCD shows signs of toxicity when administered to animal models [235, 236]. As such, βCD has been modified to generate several derivatives in which the hydroxyl groups are replaced, to various degrees, with alternative groups. One such derivative is methyl-β-CD (MβCD). MβCD is significantly more soluble than βCD due to the substitution of methoxy groups for several of the hydroxyl groups on the glucose ring [237]. Not only is MβCD more soluble than βCD, it also binds cholesterol with a higher affinity [238]. This property is exploited in studies that use MβCD to extract cholesterol from cell membranes *in vitro*. Unfortunately, this property also causes MβCD to be rather toxic, both in cell cultures and *in vivo* [239, 240]. The toxicity of MβCD correlates with the ability of CD to extract cholesterol from plasma membranes of cells *in vitro* [240]. Another derivative of βCD substitutes hydroxypropyl groups for several of the hydroxyl groups in the oligosaccharide ring structure [241]. 2-hydroxypropyl-β-CD (HPCD) also shows much greater solubility than βCD, although this is somewhat lower than the solubility of MβCD [241]. Moreover, HPCD does not bind cholesterol with as high affinity as seen with MβCD [240, 242]. Unlike MβCD, however, HPCD shows significantly lower toxicity *in vitro* and *in vivo* [243]. Indeed, HPCD was actually

approved by the Food and Drug Administration for use in humans as a vehicle for the delivery of several different drugs.

The impact βCD has on cellular cholesterol depends on several factors, including the concentration of βCD, the ratio of βCD to cholesterol, and the length of time cells are exposed to βCD [224]. Moreover, different cell types show varying sensitivities to βCD treatment [224]. Most experiments use βCD, as well as MβCD and HPCD derivatives, to remove cholesterol from the plasma membrane of cells. In these experiments, high concentrations (e.g. 5-10 mM) of βCD are used, and the cells are exposed to βCD for a short period of time (e.g. 10 min) [227]. In other experiments, when βCD is given to cultures along with high concentrations of cholesterol, βCD enriches the cholesterol content of these cells [227]. Importantly, when low concentrations of βCD are used, βCD can mediate the transfer of cholesterol between different hydrophobic compartments [244, 245]. As such, βCD has been used to transfer cholesterol from membranes that are relatively cholesterol-rich, to cholesterol-poor acceptor membranes [244, 245]. It is this property of βCD that makes it of particular interest for use in the treatment of NPC disease.

Interestingly, recent work of Liu *et al.* found that treatment of NPC1-deficient mice with HPCD delayed the neurodegeneration and prolonged the life of the mice by ~3-4 weeks, independent of ALLO administration [106]. A single dose of HPCD given to 7-day-old NPC1-deficient mice reduced the accumulation of unesterified cholesterol, increased the

amount of CE, and decreased cholesterol synthesis in the liver, spleen and, to a lesser extent, the brain [246]. Weekly administration of HPCD corrected cholesterol metabolism in nearly all organs of NPC1-deficient mice, although the lungs did not show improvement and neurodegeneration was not entirely prevented [247]. In addition, chronic administration of HPCD to mice delayed clinical onset of the disease and increased life-span of both NPC1- and NPC2-deficient mice [248]. Filipin staining and immunohistochemical analysis revealed that chronic HPCD treatment of mice reduced the amount of unesterified cholesterol, as well as the gangliosides GM1 and GM2, in NPC1- and NPC2-deficient mouse brains [248]. Although the mechanism underlying this remarkable effect of HPCD has not been completely elucidated, the current model is that HPCD enters the endocytic pathway through bulk-phase endocytosis and releases cholesterol and other lipids that are trapped in the LE/L so that the cholesterol reaches the ER [246]. In support of this model, in NPC1-deficient mouse brains and livers, the levels of the mRNAs encoding SREBP2 and its target genes were decreased by HPCD administration, whereas the mRNAs encoding LXR target genes were increased [246]. In addition, when NPC1-deficient cultured human fibroblasts were treated with HPCD *in vitro*, ACAT-mediated cholesterol esterification was increased, indicating that cholesterol had been released from the LE/L and transported to the ER [249]. If, on the other hand, cholesterol had been stripped from the plasma membrane by HPCD, one would have expected

that cholesterol synthesis would have increased as compensation for the loss of cholesterol. Thus, the finding that cholesterol synthesis was decreased, not increased, by HPCD treatment suggests that the primary effect of HPCD is mobilization of cholesterol from the LE/L rather than the plasma membrane [246]. The idea that CD can extract cholesterol from LE/L is supported by recent work indicating that dextran-conjugated MβCD localizes to intracellular filipin-stained organelles and reduces cholesterol accumulation in NPC1-deficient cells [250]. Although experiments by Davidson *et al.* suggest that the administration of ALLO alone to NPC1-deficient mice, without HPCD has no beneficial effects, the administration of HPCD with ALLO is more beneficial than HPCD alone [248]; these results remain controversial. Thus, further investigations are needed to clarify the role, if any, of ALLO in the improvement of the NPC phenotype.

*Future Therapies*

Although the recent development of potential therapies for NPC disease has shown promising advances, one of the major obstacles that remains is the efficient and rapid diagnosis of NPC disease which would allow treatment to be initiated as early as possible. NPC disease has a significant delay in diagnosis after onset of symptoms, with one recent study finding that the average delay in diagnosis was 4.3 years with a range of 3 months to 19 years [251]. Most of the experiments in which these compounds are administered to animals were performed prior to the onset of neurological symptoms. While these treatments yielded

encouraging results, when the same compounds were administered at later stages of disease progression, the results were not as positive. For example, significant improvements occurred when HPCD was administered to 7-day-old mice prior to the onset of overt neurodegenerative symptoms [246]. However, when a single dose of HPCD was given to 49-day-old mice, the amount of cholesterol that accumulated in tissues throughout the body was reduced but life-span was not extended [252]. The latter observation might be explained by the fact that HPCD can enter the brain from the circulation in 7-day-old mice, prior to formation of the BBB, whereas access of HPCD to the brain might be impeded in adult mice with an intact BBB. In addition, beneficial effects might occur only if HPCD were chronically administered, particularly at later stages of disease progression. However, it appears that there is a critical therapeutic window, after which irreversible damage occurs, so that any therapy for the disease will only prevent further progression. Thus, better screening processes and increased awareness of NPC disease are needed, as early treatment will likely have the greatest benefit. Nonetheless, recent therapeutic advances such as treatments with miglustat and HPCD provide options that show promise in slowing the progression of NPC disease. Due to the complex nature of NPC disease, a combination of various treatments will probably have the greatest therapeutic effect.

## *1.C RATIONALE FOR THE HYPOTHESES*

The consequences of NPC1 deficiency in the nervous system are very complex and incompletely understood. Experimental evidence indicates that the neurological phenotype of NPC disease, and the extensive death of neurons, likely arise from an interplay among the different cell types in the brain: neurons, astrocytes, microglia and oligodendrocytes. While microglia are implicated in NPC disease, the presence of activated microglia in the *Npc1*$^{-/-}$ mouse brain does not necessarily indicate that *Npc1*$^{-/-}$ microglia are contributing to neurodegeneration. As the primary role of microglia is to maintain brain health, it is possible the increase in active microglia is simply an attempt to prevent neuronal death in the NPC1-deficient brain. However, much evidence suggests that while the initial inflammatory response is beneficial to neuron survival, chronic microglial activation and inflammation ultimately lead to increased neurodegeneration, not just of damaged neurons, but also of healthy cells surrounding the site of damage. Moreover, evidence suggests microglia may be active prior to detectable neurodegeneration in the *Npc1*$^{-/-}$ mouse brain [170]. As microglia can secrete a variety of potentially neurotoxic molecules, it is a distinct possibility that the high level of activated microglia in the NPC mouse brain is indeed exacerbating the neuronal death in NPC disease. It is also possible that the absence of NPC1 in microglia can alter their function, making them more reactive, or conversely, less able to carry out normal

microglia functions that may promote neuron survival. In order to investigate these possibilities, we used primary microglia cultures that allow us to explore the consequences of NPC1-deficiency in microglia. We hypothesize that microglial dysfunction plays an important role in neurodegeneration in NPC disease.

The therapeutic options for NPC disease are limited. Recent studies that treated *Npc1*$^{-/-}$ mice with HPCD have yielded promising results, significantly increasing the life-span and ameliorating many of the facets of NPC disease. Additionally, the US Food and Drug Administration has already approved HPCD for use in humans as a vehicle for drug delivery, and have given HPCD an orphan drug designation for compassionate treatment of several children with NPC disease. While HPCD has been shown to decrease neurodegeneration in *Npc1*$^{-/-}$ mice, it is unclear how HPCD is mediating these effects in the CNS. The brain is not only composed of neurons, but also glial cells including astrocytes, microglia, and oligodendrocytes. HPCD can have varying effects on different cell types [224]. Neurons are highly polarized, specialized cells, and thus HPCD may have different effects on neurons compared to other cells such as glia. As astrocytes play a major role in cholesterol metabolism in the CNS, it is possible that HPCD is correcting the cholesterol trafficking defect in astrocytes, and that the attenuation of neuron death is secondary to this action. Moreover, high concentrations of CD, as well as prolonged exposure to CD, can also lead to cholesterol

depletion and cell death. It remains unclear what concentrations of HPCD can be tolerated by neurons, and whether neurons are more sensitive than other cells such as glia to HPCD. In order to investigate the effects HPCD has on cells of the CNS, we cultured neurons and astrocytes from *Npc1*$^{-/-}$ and *Npc1*$^{+/+}$ mice, and treated these cultures with varying concentrations of HPCD. We hypothesize that low concentrations of HPCD will correct the cholesterol trafficking defect in *Npc1*$^{-/-}$ neurons and astrocytes whereas higher doses will be detrimental.

## 2. EXPERIMENTAL PROCEDURES

### *2.A MATERIALS*

Dulbecco's Modified Eagle Medium (DMEM) high glucose, Ham's F12 medium, Neurobasal™ medium, Neurobasal™ 'A' medium, fetal bovine serum (FBS), B-27 supplement, and 0.25% trypsin-EDTA were purchased from Invitrogen. L-glutamine, poly-D-lysine hydrobromide, and trypsin (type XII-S from bovine pancreas) were purchased from Sigma, while deoxyribonuclease I (DNAse I) was from Worthington Biochemical Corporation (Lakewood, NJ). 25-$cm^2$ flasks, 75-$cm^2$ flasks, 96-well plates, and 100x20 mm tissue culture dishes were purchased from BD Falcon (BD Biosciences, Bedford, MA), while 60x15 mm tissue culture dishes were purchased from Corning Incorporated (Corning, NY). (2-Hydroxypropyl)-β-cyclodextrin (H107) was purchased from Sigma and U18666A was from Biomol Research Laboratories (Plymouth Meeting, PA). Potassium chloride, sodium acetate, and potassium dihydrogen orthophosphate (monobasic) were from BDH Incorporated (Toronto, ON), sodium chloride was from EMD Chemicals (Gibbstown, NJ), sodium phosphate dibasic was from Anachemia (Montreal, QC), and oleic acid was from Sigma. [1-$^{14}$C]oleic acid was from Perkin Elmer (Boston, MA), while [$^{3}$H]acetic acid sodium salt and CytoScint™ was from MP Biomedicals (Solon, OH). Chloroform, methanol, n-heptane, isopropyl ether, isopropanol, and acetic acid were from Fisher Scientific (Ottawa, ON) while anhydrous ethanol was from Commercial Alcohols (Brampton,

ON). Bovine serum albumin (BSA), saponin, and filipin complex were from Sigma, paraformaldehyde was from Fisher Scientific (Ottawa, ON), while Hoechst 33258 pentahydrate (bis-benzimide), Texas Red® goat anti-rabbit IgG (H+L) secondary antibody and Alexa Fluor® 488 chicken anti-mouse IgG (H+L) secondary antibody were from Invitrogen. Rabbit anti-Iba1 (ionized calcium binding adaptor molecule 1) antibody was from Wako Pure Chemical Industries Ltd. (Osaka, Japan), mouse anti-NeuN antibody (MAB377) was from Chemicon International (Jaffrey, NH), mouse anti-MAP2 antibody (HM-2, Ab11267) was from Abcam (Cambridge, MA), while goat anti-TNFα (R-19, sc-1349) and mouse anti-TNFR1 (H-5, sc-8436) antibodies were from Santa Cruz Biotechnology (Santa Cruz, CA). DNAse I (amplification grade), Oligo$(dT)_{12-18}$ primer, SuperScript® II, Platinum® qPCR SuperMix-UDG, and SYBR Green I nucleic acid gel stain were from Invitrogen, while PCR-grade dNTPs (deoxynucleoside triphosphates) were from Roche (Laval, QC).

*2.B CELL CULTURE*

*2.B(i) $Npc1^{+/+}$ and $Npc1^{-/-}$ mice*

A breeding colony of Balb/cNctr-$Npc^{N/+}$ mice was established at the University of Alberta with breeding pairs obtained from Jackson Laboratories (Bar Harbor, ME). The mice were maintained under temperature-controlled conditions with a 12-h light:12-h dark cycle and were supplied with a 9% fat breeders diet (Purina LabDiet, Richmond, IN)

and water *ad libitum*. Mice homozygous or heterozygous for the *Npc1* mutation will be referred to as *Npc1*$^{-/-}$ and *Npc1*$^{+/-}$, respectively, while wild-type mice will be termed *Npc1*$^{+/+}$. Since *Npc1*$^{-/-}$ mice are unable to produce offspring, *Npc1*$^{+/-}$ mice were used for breeding. Prior to brains of the mice being dissected for cell culture, *Npc1* genotypes of the mouse pups were determined by PCR analysis of genomic DNA isolated from tail clippings using the REDExtract-N-Amp$^{TM}$ Tissue PCR Kit (Sigma). The PCR reaction was carried out as described [82], using the forward primer 5'-GGTGCTGGACAGCCAAGTA-3' and the reverse primer 5'-GATGGTCTGTTCTCCCATG-3' (IDT Technologies, San Diego, CA). All experiments were approved by the Health Sciences Animal Welfare Committee of the University of Alberta.

*2.B(ii) Isolation and culture of cortical glia*

Glial cells were isolated from the cerebral cortices of 1-3 day-old *Npc1*$^{+/+}$ and *Npc1*$^{-/-}$ mice, as well as 2d-old Sprague-Dawley rats [253]. Isolated cortices were cleaned of meninges and blood vessels, finely chopped, and digested in 0.25% trypsin (Invitrogen) containing 1 mg/mL DNAse I (Worthington). Cells were dissociated by trituration through a Pasteur pipette in DMEM containing 10% FBS. Glial cells were pelleted by centrifugation at 950 rpm, and resuspended in fresh DMEM containing 10% FBS. Glial cells from mice were plated at a density of two cortices per 75-cm$^2$ flask and one cortex per 25-cm$^2$ flask or 100x20 mm culture dish. Glial cells from rats were plated at a density of one cortex per 75-cm$^2$

flask. Cultures were maintained at 37°C and 5% $CO_2$ in DMEM containing 10% FBS, with media being replaced every 3-5 days.

*2.B(iii) Isolation and culture of cortical astrocytes*

Astrocyte-enriched cultures were isolated from glia according to the protocol of Hayashi *et al.* [59]. Following 3-4 weeks of culture, confluent glial cells were washed several times in phosphate-buffered saline (PBS), harvested by treatment with 0.125% trypsin (Sigma), and replated at a density of 1:3 in DMEM containing 10% FBS. These cultures were highly enriched in astrocytes, (>90%), as previously shown [50, 59]. Cultures were maintained at 37°C and 5% $CO_2$ in DMEM containing 10% FBS, with media being renewed every 3-5 days. Astrocytes were used for experiments within 7-14 days following replating.

*2.B(iv) Isolation and culture of cortical microglia*

Mouse microglia were isolated using the mild trypsinization method described by Saura *et al.* [254]. Following 3-4 weeks of culture in flasks, confluent glial cells were washed with DMEM:Ham's F12 medium (1:1) and then incubated at 37°C with DMEM:Ham's F12 medium (1:1) containing 0.0625% trypsin (Invitrogen) for 30-60 min until the astrocyte layer lifted. Medium, along with the astrocyte layer, was aspirated from the dish. For quantitative real-time PCR (qPCR) analysis, microglia were washed once with DMEM:Ham's F12 medium (1:1) containing 10% FBS, followed by a another wash with DMEM:Ham's F12 medium (1:1).

Microglia were then fed fresh DMEM:Ham's F12 medium (1:1) and incubated at 37°C and 5% $CO_2$ for 24 h. For other microglia experiments, following removal of the astrocyte layer, microglia were incubated with 0.25% trypsin (Invitrogen) at room temperature and subsequently scraped. DMEM:Ham's F12 medium (1:1) containing 10% FBS was added to the cell suspension, cells were centrifuged at 950 rpm to pellet the cells, and microglia were resuspended in fresh DMEM:Ham's F12 medium (1:1) containing 10% FBS. Microglia were plated in 96-well plates at a density of 62,500 cells/well.

Rat microglia were isolated using the shaking method [255]. Flasks containing mixed glia were shaken at 100 rpm at 37°C for 5 min to remove microglia loosely bound to the top of the astrocyte layer. The medium was then collected and microglia were pelleted by centrifugation at 950 rpm. Microglia were resuspended in DMEM containing 10% FBS and plated in 96-well plates at a density of 62,500 cells/well.

*2.B(v) Isolation and culture of cerebellar granule cells*

CGCs were cultured according to the protocol of Michikawa and Yanagisawa [256], with the medium being adapted to CGCs. Briefly, cerebella were dissected from 7-8 day-old mice, cleaned of meninges and blood vessels, finely chopped, and digested in 0.25% trypsin (Invitrogen) containing 1 mg/mL DNAse I (Worthington). Cells were dissociated by trituration through a fire-polished Pasteur pipette in Neurobasal™ medium

containing 10% heat-inactivated FBS. Dissociated cells were pelleted by centrifugation at 950 rpm, resuspended in Neurobasal™ medium supplemented with 2% B27, 0.5 mM glutamine, and 20 mM potassium chloride, and passed through a 40 μm nylon cell strainer (BD Falcon, BD Biosciences, Bedford, MA) to remove any clumped cells. Trypan blue-excluding cells were counted using a haemocytometer and plated in 96-well plates (31,250 cells/well), 100x20 mm dishes ($2.1x10^6$ cells/dish), 75-$cm^2$ flasks ($3.1x10^6$ cells/flask), or 60x15 mm dishes ($1.0x10^6$ cells/dish) coated with 10 μg/mL poly-D-lysine hydrobromide. Cells were maintained at 37°C and 5% $CO_2$ without refeeding until used for experiments.

*2.B(vi) Isolation and culture of cortical neurons*

Cortical neurons were cultured according to the protocol of Michikawa and Yanagisawa [256]. Briefly, cerebral cortices were dissected from 0-1 day-old mice, cleaned of meninges and blood vessels, finely chopped, and digested in 0.25% trypsin (Invitrogen) containing 1 mg/mL DNAse I (Worthington). Cells were dissociated by trituration through a fire-polished Pasteur pipette in Neurobasal™ 'A' medium containing 10% heat-inactivated FBS. Dissociated cells were pelleted by centrifugation at 950 rpm, resuspended in Neurobasal™ 'A' medium supplemented with 2% B27 and 0.5 mM glutamine, and passed through a 40 μm nylon cell strainer (BD Falcon, BD Biosciences, Bedford, MA) to remove any clumped cells. Trypan blue-excluding cells were counted using a haemocytometer and plated in 96-well plates (31,250 cells/well)

coated with 10 µg/mL poly-D-lysine hydrobromide. Cells were maintained at 37°C and 5% $CO_2$ for 3 d until use in co-culture experiments.

## *2.C MICROGLIA EXPERIMENTS*

### *2.C(i) Immunohistochemical staining of mouse brain slices*

Brains from 7-wk-old *Npc1*$^{+/+}$ and *Npc1*$^{-/-}$ mice were prepared according to Amritraj *et al.* [153]. Briefly, mice were anesthetized with 4% chloral hydrate, perfused with PBS, and subsequently perfused with 4% (w/v) paraformaldehyde. Brains were sectioned on a cryostat (20 µM) and processed using the free-floating procedure [257, 258]. Sections were washed with PBS and incubated with anti-Iba1 antibody (1:1000) overnight at room temperature. Subsequently, sections were washed with PBS and incubated with Texas Red®-conjugated secondary antibody for 2 h at room temperature. Sections were then washed with PBS, mounted on slides in glycerol mounting media (1M Tris-Chloride pH 8.0, water, glycerol [1:4:5]) and imaged using a Leica DM IRE2 fluorescence microscope (Leica Microsystems, Bannockburn, IL). The excitation wavelength was 596 nm. Images were captured using Open Lab 3.1.4 Software (PerkinElmer, Waltham, MA) and post-processing of images was done using Adobe Photoshop CS4 (San Jose, CA).

### *2.C(ii) U18666A treatment of Npc1*$^{+/+}$ *microglia*

*Npc1*$^{+/+}$ rat microglia were isolated using the shaking method while *Npc1*$^{+/+}$ mouse microglia were isolated by the mild trypsinization method.

Microglia were plated in 96-well plates and allowed to rest overnight. Cultures were re-fed with fresh medium containing vehicle (anhydrous ethanol) or 3 μM U18666A and incubated at 37°C. Following 6 h of treatment, phase images were taken with a Leica DM IRE2 fluorescence microscope (Leica Microsystems, Bannockburn, IL). Images were captured using Open Lab 3.1.4 Software (PerkinElmer, Waltham, MA) and post-processing of images was done using Adobe Photoshop CS4 (San Jose, CA).

*2.C(iii) Filipin staining and phase images*

*Npc1*$^{+/+}$ and *Npc1*$^{-/-}$ microglial cultures were isolated using the mild trypsinization method, plated in 96-well plates, and allowed to rest overnight. Microglia were washed with PBS, fixed for 15 min in 4% (w/v) paraformaldehyde, and stained for 1.5 h with 0.15 mg/mL filipin complex at room temperature. Following staining, cells were washed with PBS and examined with a Leica DM IRE2 fluorescence microscope (Leica Microsystems, Bannockburn, IL). The excitation wavelength was 351 nm. Phase images were also taken of the cells. Images were captured using Open Lab 3.1.4 Software (PerkinElmer, Waltham, MA) and post-processing of images was done using Adobe Photoshop CS4 (San Jose, CA).

*2.C(iv) Measurement of TNFα secretion*

*Npc1*$^{+/+}$ and *Npc1*$^{-/-}$ microglia were isolated using the mild trypsinization method, plated in 96-well plates, and allowed to rest overnight. Medium was removed, and cells were incubated with fresh DMEM/Ham's F12 medium (1:1) containing 10% FBS for 24 h. Media were collected and stored at -20°C. TNFα concentrations were determined using a TNFα ELISA kit (Biosource, Camarillo, CA) according to the manufacturer's instructions. Samples were measured using a Spectra Max 250 plate reader (Molecular Devices, Sunnyvale, CA), and concentrations of TNFα were calculated from a standard curve generated from known TNFα concentrations.

*2.C(v) Immunocytochemical staining*

*Npc1*$^{+/+}$ and *Npc1*$^{-/-}$ microglia used for TNFα ELISA experiments were also used for immunocytochemical analysis. Following removal of conditioned media, cells were washed with PBS and fixed for 15 min in 4% (w/v) paraformaldehyde. Cells were then washed with PBS and permeabilized for 1 h at room temperature with PBS containing 1% BSA and 0.05% saponin. Following permeabilization, cells were incubated with anti-TNFα (1:50) or anti-TNFR1 (1:50) antibodies diluted in PBS containing 1% BSA and 0.05% saponin for 1 h at room temperature. Cells were then washed with PBS and incubated with the appropriate (Texas Red®-conjugated or Alexa Fluor® 488-conjugated) secondary antibody

(1:200) for 45 min at room temperature in the dark. Cells were rinsed with PBS and examined using a Leica DM IRE2 fluorescence microscope (Leica Microsystems, Bannockburn, IL). The excitation wavelength was 596 nm for Texas Red® or 495 nm for Alexa Fluor® 488. Images were captured using Open Lab 3.1.4 Software (PerkinElmer, Waltham, MA) and post-processing of images was done using Adobe Photoshop CS4 (San Jose, CA).

*2.C(vi) RNA isolation and quantitative real-time PCR analysis*

Newly isolated *Npc1*$^{+/+}$ and *Npc1*$^{-/-}$ microglia were cultured for 24 h in DMEM:Ham's F12 medium (1:1) in 75-cm$^2$ flasks. Flasks were washed with ice-cold PBS, and total RNA was isolated using the RNeasy Mini Kit (Invitrogen) and stored at -80°C. RNA was treated with DNAse I (amplification grade, Invitrogen) to prevent DNA contamination, and cDNA was synthesized from 0.5 µg total RNA using oligo(dT)$_{12-18}$ random primers and Superscript II reverse transcriptase according to the manufacturer's instructions. qPCR reactions were performed using Platinum® Quantitation PCR supermix, SYBR Green I and 250 nmol of gene-specific primers. Reactions were carried out in 25 µL total volume in 0.2 mL tubes (Axygen, Union City, CA). Transcripts were detected by qPCR with a Rotor-Gene 3000 instrument (Montreal Biotech, Montreal, QC) and data were analyzed with Rotor-Gene 6.0.19 software. Relative concentrations of transcripts were determined using the standard curve method. Intron-spanning primers were designed using OLIGO 6.71

software (Cascade, CO) and specificity was confirmed using the NCBI BLAST nucleotide query tool, by melt curve analysis, and by agarose gel electrophoresis. All primers were synthesized by IDT Technologies (San Diego, CA) with the sequences shown in Table 2.1. Results are presented relative to the control gene glyceraldehyde-3-phosphate dehydrogenase (GAPDH).

**Table 2.1 -** Mouse qPCR primers designed to quantify mRNA levels of genes involved in microglial functions

| Gene | Primer Sequence |
|---|---|
| Tumor necrosis factor-α (TNFα) | F: 5'- GTCTACTGAACTTCGGGGTGA -3'<br>R: 5'- CACTTGGTGGTTTGCTACGAC -3' |
| Interleukin-1β (IL1β) | F: 5'- GAAGTTGACGGACCCCAAAA -3'<br>R: 5'- CCACGGGAAAGACACAGGTAG -3' |
| Inducible nitric oxide synthase (iNOS) | F: 5'- AAGCCCCGCTACTACTCCATC -3'<br>R: 5'- GCCACTGACACTTCGCACAA-3' |
| NADPH oxidase (NADPHox) | F: 5'- GACTGGACGGAGGGGCTAT -3'<br>R: 5'- ACTTGAGAATGGAGGCAAAGG -3' |
| Interleukin-10 (IL10) | F: 5'- GCTGGACAACATACTGCTAAC -3'<br>R: 5'- CCGCATCCTGAGGGTCTTC -3' |
| Transforming growth factor-β (TGFβ) | F: 5'- CGCCATCTATGAGAAAACCA -3'<br>R: 5'- CCAAGGTAACGCCAGGAAT-3' |
| Glutaminase (GLTase) | F: 5'- GTTTGCCGCATACACTGGAG -3'<br>R: 5'- ACATGGAGGGCTGTTCTGGA-3' |
| Macrophage colony-stimulating factor receptor (M-CSFR) | F: 5'- CAAGATTGGGGACTTTGGACT -3'<br>R: 5'- AGAGGAGGATGCCGTAGGA -3' |
| Glyceraldehyde-3-phosphate dehydrogenase (GAPDH) | F: 5'- GAGCCAAACGGGTCATCATC -3'<br>R: 5'- CATCACGCCACAGCTTTCCA -3' |

*2.C(vii) Microglia-neuron co-cultures*

*Npc1*$^{+/+}$ and *Npc1*$^{-/-}$ CGCs were cultured in 96-well plates for 7 d prior to use in co-cultures. *Npc1*$^{+/+}$ and *Npc1*$^{-/-}$ microglia were isolated using the mild trypsinization method and plated directly on to CGC cultures at densities that were either 25% or 50% of the CGC density

(7,800 cells/well or 15,600 cells/well respectively). Co-cultures were fed Neurobasal™ medium supplemented with 2% B27, 0.5 mM glutamine, and 20 mM potassium chloride. Following 24 h of co-culture, cells were fixed with 4% (w/v) paraformaldehyde. Cells were then washed with PBS and permeabilized for 1 h at room temperature with PBS containing 1% BSA and 0.05% saponin. Following permeabilization, cells were incubated with anti-MAP2 (1:500) and anti-Iba1 (1:500) antibodies diluted in PBS containing 1% BSA and 0.05% saponin for 1 h at room temperature. Cells were then washed with PBS and incubated with Alexa Fluor® 488- and Texas Red®-conjugated secondary antibodies (1:200) for 45 min at room temperature in the dark. Cells were rinsed with PBS, stained for 12 min with 0.5 μg/mL Hoechst 33258, and examined using a Leica DM IRE2 fluorescence microscope (Leica Microsystems, Bannockburn, IL). The excitation wavelength was 495 nm for Alexa Fluor® 488, 596 nm for Texas Red® and 351 nm for Hoechst staining. Images were captured using Open Lab 3.1.4 Software (PerkinElmer, Waltham, MA) and the number of apoptotic cells staining with the neuronal marker MAP2 was quantified.

Microglia-cortical neuron co-cultures were used in a similar fashion with a few modifications. *Npc1*$^{+/+}$ and *Npc1*$^{-/-}$ cortical neurons were cultured in 96-well plates for 3 d prior to use in co-cultures. *Npc1*$^{+/+}$ and *Npc1*$^{-/-}$ microglia were isolated using the mild trypsinization method and plated directly on to cortical neuron cultures at a density of 10,000 cells/well in Neurobasal™ 'A' medium lacking supplements. Following

48 h of co-culture, cells were immunostained with anti-NeuN antibodies and nuclei were labeled with Hoechst 33258 as above. The number of apoptotic cells staining with the neuronal marker NeuN was quantified.

*2.C(viii) Treatment of neurons with microglia-conditioned media*

For treatment of CGCs with microglia-conditioned media, *Npc1*$^{+/+}$ and *Npc1*$^{-/-}$ microglia were isolated using the mild trypsinization method, plated in 96-well plates, and allowed to rest overnight. The medium was replaced with Neurobasal™ medium supplemented with 2% B27, 0.5 mM glutamine, and 20 mM potassium chloride, which was incubated with the cells for 24 h at 37°C and 5% $CO_2$. Following 24 h, the conditioned medium was removed and frozen at -20°C until use. Medium in 7-d-old *Npc1*$^{+/+}$ and *Npc1*$^{-/-}$ CGC cultures was replaced with microglia-conditioned media and CGCs were incubated for 24 h. Following conditioned media treatment, CGC cultures were fixed with 4% (w/v) paraformaldehyde, stained for 12 min with 0.5 μg/mL Hoechst 33258, and observed using a Leica DM IRE2 fluorescence microscope (Leica Microsystems, Bannockburn, IL). The excitation wavelength was 351 nm. Images were captured using Open Lab 3.1.4 Software (PerkinElmer, Waltham, MA) and the number of apoptotic cells was quantified.

Treatment of cortical neurons with microglia-conditioned media was conducted in a similar fashion with a few modifications. *Npc1*$^{+/+}$ and *Npc1*$^{-/-}$ microglia were isolated using the mild trypsinization method, plated

in 96-well plates, and allowed to rest overnight. The medium was replaced with Neurobasal™ 'A' medium without supplements, and incubated with the cells for 48 h at 37°C and 5% $CO_2$. Following 48 h, the conditioned medium was removed and frozen at -20°C until use. Medium from 3-d-old *Npc1*$^{+/+}$ and *Npc1*$^{-/-}$ cortical neuron cultures was replaced with microglia-conditioned media and neurons were incubated for 48 h. Following conditioned media treatment, cortical neurons were fixed and stained with Hoechst stain as above. The number of apoptotic neurons was quantified.

*2.C(ix) Phagocytosis assay*

*Npc1*$^{+/+}$ and *Npc1*$^{-/-}$ microglia were isolated using the mild trypsinization method, plated in 96-well plates, and allowed to rest overnight. Medium was then replaced with fresh medium containing 1.0 µm fluorescent carboxylate-modified polystyrene latex beads (Sigma, L4655) at a concentration of $3.1x10^6$ beads/well (50 beads/microglia). Cells were incubated with beads at 37°C for 2 h, followed by three washes with ice-cold PBS. Microglia were examined using a Leica DM IRE2 fluorescence microscope (Leica Microsystems, Bannockburn, IL). The excitation wavelength for the beads was 505 nm. Phase and fluorescent images were captured using Open Lab 3.1.4 Software (PerkinElmer, Waltham, MA) and the number of beads associated with microglia was quantified. To control for beads that were bound to the microglia, but not internalized, we performed identical experiments with the cultures

incubated at 4°C to block phagocytosis. The number of beads associated with microglia incubated at 4°C was subtracted from the number of beads associated with microglia at 37°C.

*2.C(iix) Statistical analysis*

The statistical significance of differences (** $p < 0.01$; *** $p < 0.001$) was determined using the Student's *t* test.

*2.D CYCLODEXTRIN EXPERIMENTS*

*2.D(i) Cyclodextrin treatments*

Stock solutions of 2-hydroxypropyl-β-cyclodextrin (H107, Sigma) were made in double-distilled water and sterilized using a 0.22 μm Millex-GV syringe driven filter unit (Millipore, Bedford, MA). For all experiments, vehicle (double-distilled water), 0.1 mM HPCD, and 1.0 mM HPCD were incubated with the cells for 24 h. Additionally, 10 mM HPCD was incubated with cells for 24 h in cell survival experiments. For CGC experiments, the appropriate agent was added directly to the medium in the culture dishes. For astrocyte experiments, cultures were fed fresh DMEM containing 10% FBS 24 h prior to the start of the treatment. The medium was then replaced with DMEM containing the appropriate treatment in the absence of serum.

*2.D(ii) Staining with filipin and Hoechst*

CGCs and replated astrocytes were cultured 7 d in 96-well plates prior to being given the indicated treatment. Following treatment, cells were washed with PBS, fixed for 15 min in 4% (w/v) paraformaldehyde, and stained for 12 min with 0.5 μg/mL Hoechst 33258 or 1.5 h with 0.15 mg/mL filipin complex at room temperature. Following staining, cells were washed with PBS and examined using a Leica DM IRE2 fluorescence microscope (Leica Microsystems, Bannockburn, IL). The excitation wavelength was 351 nm for both Hoechst and filipin staining. Phase images were also taken of the cells. Images were captured using Open Lab 3.1.4 Software (PerkinElmer, Waltham, MA) and post-processing of images was done using Adobe Photoshop CS4 (San Jose, CA).

*2.D(iii) Metabolic labeling of cholesterol and cholesteryl esters*

CGCs and replated astrocytes were cultured for 7 d in 60x15 mm dishes before administration of the indicated treatment for 24 h. For cholesterol labeling experiments, cultures were then incubated with fresh medium containing the appropriate agent, 5 μCi/mL [$^{3}$H]acetate and 100 μM sodium acetate for an additional 4 h. For CE formation, cultures were incubated with fresh medium containing the indicated additive, 0.2 μCi/mL [$^{14}$C]oleate, 100 μM oleic acid, and 0.5% BSA for 4 h, in the presence or absence of 2 μg/mL of the ACAT-specific inhibitor Sandoz 58-035 (Sigma). In preliminary experiments with CGCs, very little

radioactivity was detectable in CE. Consequently, in subsequent experiments we added 0.2 μCi/mL [$^{14}$C]oleate, 100 μM oleic acid, and 0.5% BSA alongside the initial treatment for 24 h, in the presence or absence of 2 μg/mL Sandoz 58-035 (Sigma). Following radiolabeling, cells were washed twice with ice-cold PBS, scraped in double-distilled water, sonicated, and protein concentrations determined using a BCA™ protein assay kit (Thermo Scientific, Rockford, IL). Lipids were extracted with chloroform/methanol (2:1), washed with methanol/water (1:1), and separated by thin-layer chromatography on TLC silica gel 60 plates (EMD Chemicals Inc., Gibbstown, NJ) in the solvent system heptane/isopropyl ether/acetic acid/isopropanol (65:35:4:2). Bands corresponding to standards of cholesterol, CE, and phospholipids were scraped, mixed with CytoScint scintillation fluid, and radioactivity measured using an LS 6500 Multi-Purpose Scintillation Counter (Beckman Coulter, Brea, CA). Results are presented as dpm/mg protein.

*2.D(iv) RNA isolation and quantitative real-time PCR analysis*

CGCs were cultured 7 d in 75-cm$^2$ flasks and replated astrocytes were cultured 14 d in 100x20 mm dishes, prior to being given the indicated treatment. Dishes were washed with ice-cold PBS, and total RNA was isolated using the RNeasy Mini Kit (Invitrogen) and stored at -80°C. RNA was treated with DNAse I (amplification grade, Invitrogen) to prevent DNA contamination, and cDNA was synthesized from 1.25 μg total RNA using oligo(dT)$_{12\text{-}18}$ random primers and Superscript II reverse transcriptase

according to the manufacturer's instructions. qPCR reactions were performed using Platinum® Quantitation PCR supermix, SYBR Green I and 250 nmol of gene-specific primers. Reactions were carried out in both 20 µL and 25 µL total volumes, in 0.1 mL (Corbett, Sydney, AU) and 0.2 mL tubes (Axygen, Union City, CA), respectively. Transcripts were detected by qPCR with a Rotor-Gene 3000 instrument (Montreal Biotech, Montreal, QC) and data were analyzed with Rotor-Gene 6.0.19 software. Relative concentrations of transcripts were determined using the standard curve method. Intron-spanning primers were designed using OLIGO 6.71 software (Cascade, CO) and specificity was confirmed using the NCBI BLAST nucleotide query tool, by melt curve analysis, and by agarose gel electrophoresis. All primers were synthesized by IDT Technologies (San Diego, CA) with the sequences given in Table 2.2. ACAT1 primers were kindly provided by Dr. Rene Jacobs (University of Alberta, Edmonton, AB). All results are presented relative to the control gene GAPDH.

**Table 2.2 -** Mouse qPCR primers designed to quantify mRNA levels of genes involved in cholesterol metabolism

| Gene | Primer Sequence |
|---|---|
| Sterol regulatory element binding protein 2 (SREBP2) | F: 5'- CAGGCGACCAGGAAGAAGA -3'<br>R: 5'- CACGGAACTGCTGGAGAATG -3' |
| 3-hydroxy-3-methylglutaryl coenzyme A reductase (HMGCR) | F: 5'- TGGGCATGAACATGATCTCTA -3'<br>R: 5'- GGCTTCACAAACCACAGTC -3' |
| Low-density lipoprotein receptor (LDLR) | F: 5'- CCGTCTCTATTGGGTTGATT -3'<br>R: 5'- GAGTCGATTGGCACTGAAA -3' |
| ATP-binding cassette transporter A1 (ABCA1) | F: 5'- AGTTTCTGCCCTCTGTGGTC -3'<br>R: 5'- GGGTCGGGAGATGAGATGT -3' |
| ATP-binding cassette transporter G1 (ABCG1) | F: 5'- ACCCGCCTGTCATGTTCTTT -3'<br>R: 5'- ACTGGGCTGGTGGATGGTA -3' |
| Glyceraldehyde-3-phosphate dehydrogenase (GAPDH) | F: 5'- GAGCCAAACGGGTCATCATC -3'<br>R: 5'- CATCACGCCACAGCTTTCCA -3' |

*2.D(v) Statistical analysis*

The statistical significance of differences between vehicle and 0.1 mM HPCD treatments or vehicle and 1.0 mM HPCD treatments (* $p < 0.05$; ** $p < 0.01$; *** $p < 0.001$) were determined using Student's *t* test.

## 3. RESULTS

### *3.A ROLE OF MICROGLIA IN NPC DISEASE*

#### *3.A(i) Microglia with an active morphology accumulate in the Npc1$^{-/-}$ mouse brain*

Microglia have been implicated in a number of neurodegenerative disorders. In order to investigate the involvement of microglia in NPC disease, we performed immunohistochemical analysis of brain slices from the cerebellum and cerebral cortex of *Npc1*$^{+/+}$ and *Npc1*$^{-/-}$ mice. Sections were taken from 7-week-old mice, as this is a time point when overt signs of NPC neurological disease are apparent, and the slices were immunostained for the microglial marker Iba1. In the *Npc1*$^{+/+}$ cerebellum and cortex, microglia were present in a ramified, resting morphology (Fig. 3.1*A* and 3.2*A*). In the *Npc1*$^{-/-}$ cerebellum and cortex, there was a dramatic increase in the number of microglia (Fig. 3.1*B* and 3.2*B*). Moreover, these microglia had swollen cell bodies and shortened processes (Fig. 3.1*B* and 3.2*B*), suggesting that the microglia were activated. Thus, microglia number and morphology are dramatically altered in the NPC mouse brain.

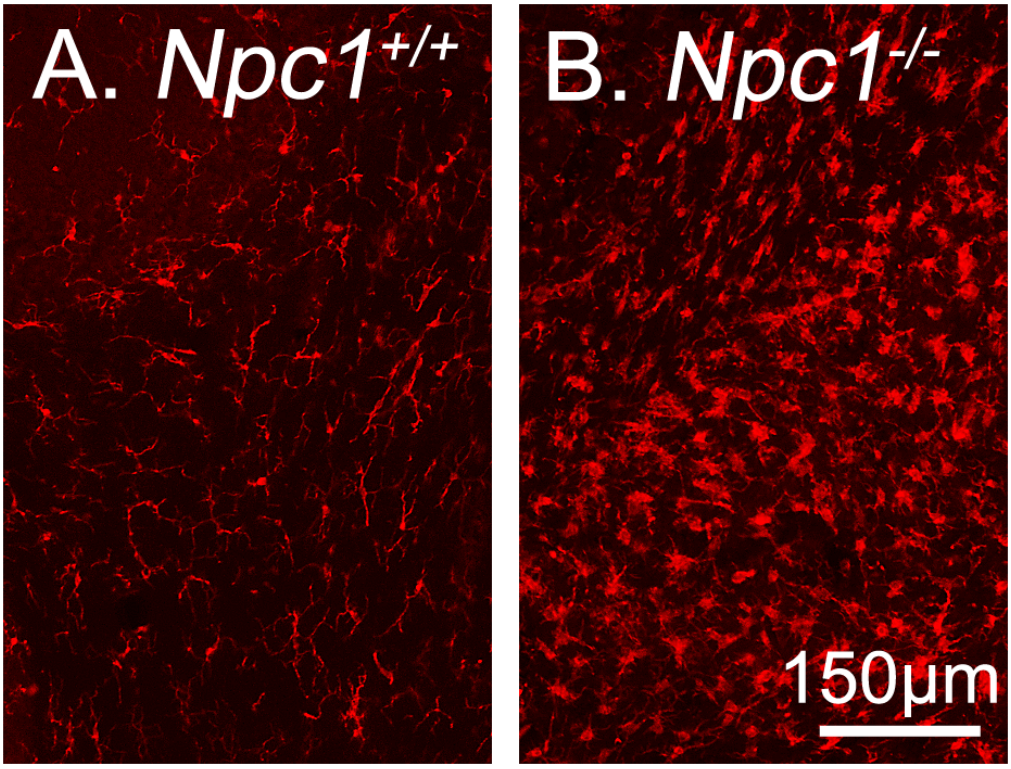


FIGURE 3.1 - **Active microglia accumulate in the 7-week-old *Npc1*$^{-/-}$ mouse cerebellum.** Immunohistochemical staining of microglia in cerebellar slices from 7-wk-old *Npc1*$^{+/+}$ (A) and *Npc1*$^{-/-}$ (B) mice. Brains from 7-wk-old mice were fixed, and cerebella were sectioned and labeled with Iba1, a microglial marker. Results are representative images from three independent mice.

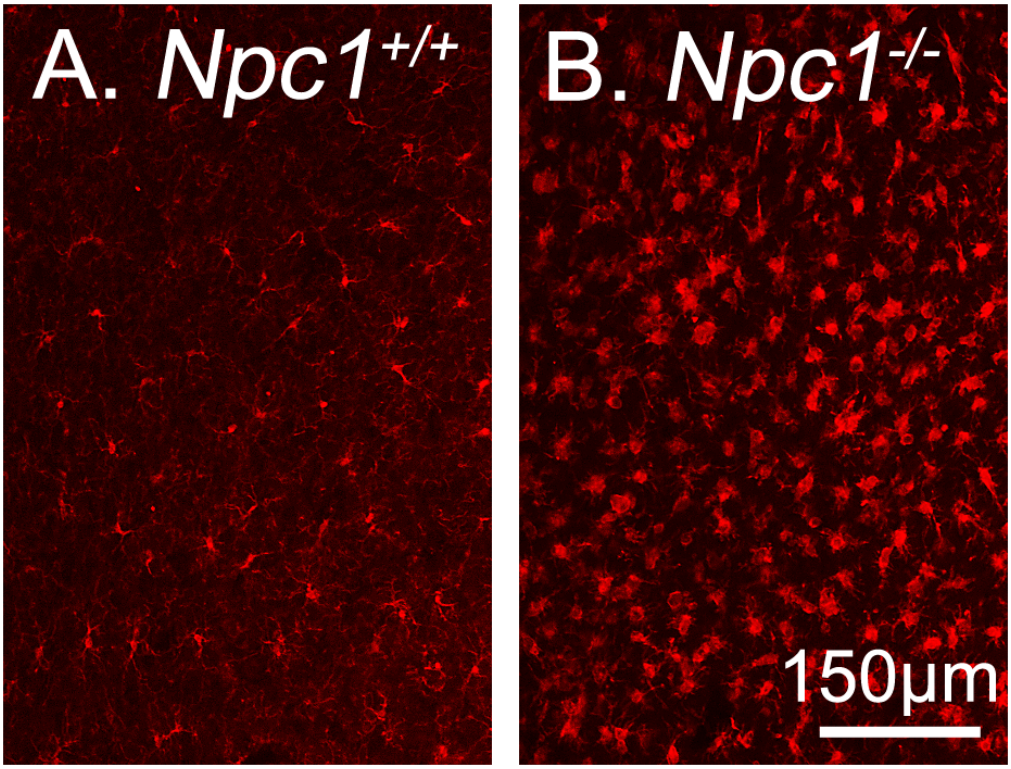


FIGURE 3.2 - **Active microglia accumulate in the 7-week-old *Npc1*$^{-/-}$ mouse cortex.** Immunohistochemical staining of microglia in cortical slices from 7-wk-old *Npc1*$^{+/+}$ (A) and *Npc1*$^{-/-}$ (B) mice. Brains from 7-wk-old mice were fixed, and cerebral cortices were sectioned and labeled with Iba1, a microglial marker. Results are representative images from three independent mice.

*3.A(ii) U18666A induces an active morphology in Npc1$^{+/+}$ microglia*

We used primary microglia cultures to determine if impaired cholesterol transport through the LE/L altered the morphology of the microglia. Microglia isolated from *Npc1*$^{+/+}$ rats were treated with U18666A, a compound that blocks cholesterol transport out of the LE/L, inducing an NPC-like accumulation of unesterified cholesterol within the LE/L. Microglia show several different morphologies *in vitro*: ramified (resting), ameboid (phagocytic), and spherical (fully activated) (Fig. 3.3) [259]. Vehicle treated microglia showed a variety of morphologies, mainly consisting of ramified and ameboid cells, with few spherical microglia (Fig. 3.4*A*). Addition of U18666A to the microglia cultures caused a dramatic shift in morphologies, with the majority of microglia showing a spherical morphology within 6 h of treatment (Fig. 3.4*B*). Identical experiments were also conducted with *Npc1*$^{+/+}$ microglia isolated from mice. Similar changes occurred, with U18666A causing the morphology to shift to a spherical, fully activated morphology, compared to vehicle treatment (Fig. 3.5). These results suggest that altering cholesterol efflux from LE/L in microglia can potentially lead to microglial activation. It is important to note, however, that U18666A has other effects in addition to inhibiting cholesterol export from LE/Ls, including inhibition of cholesterol synthesis [102, 103], that could be responsible for the changes in microglia morphology.

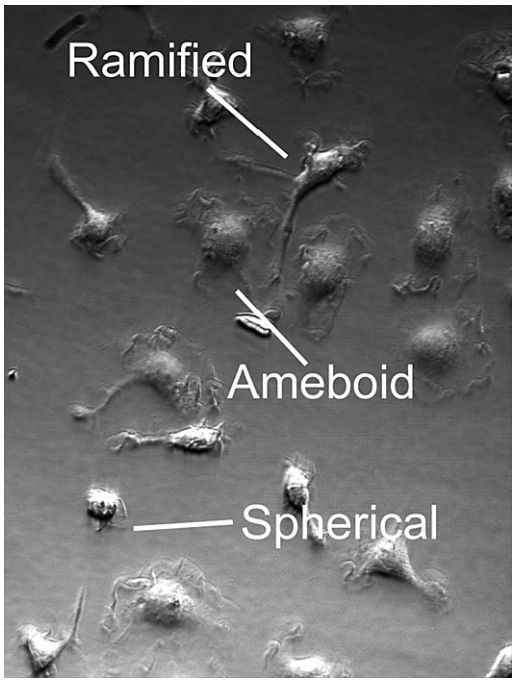


FIGURE 3.3 - **Microglia cultured *in vitro* show several different morphologies.** Phase images of primary microglia cultures showing a ramified (resting), ameboid (phagocytic), and spherical (fully activated) morphology. Primary microglia were isolated from glia cultures by mild trypsinization, replated, and allowed to rest overnight prior to being imaged.

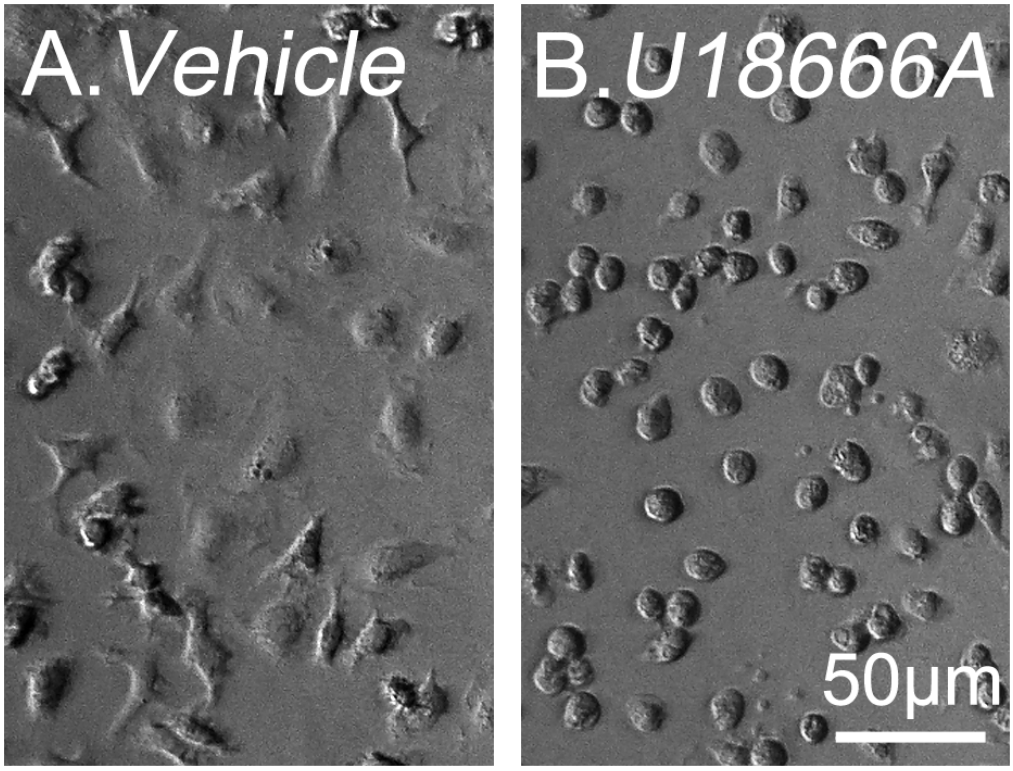


FIGURE 3.4 - **U18666A treatment of *Npc1*$^{+/+}$ rat microglia induces an active morphology.** Primary cultures of *Npc1*$^{+/+}$ rat microglia were treated with vehicle (A) or U18666A (B) for 6 h prior to being imaged. Primary microglia were isolated from glia cultures by mild trypsinization, replated, and allowed to rest overnight before treatment. Results are representative images from one cell preparation analyzed in triplicate.

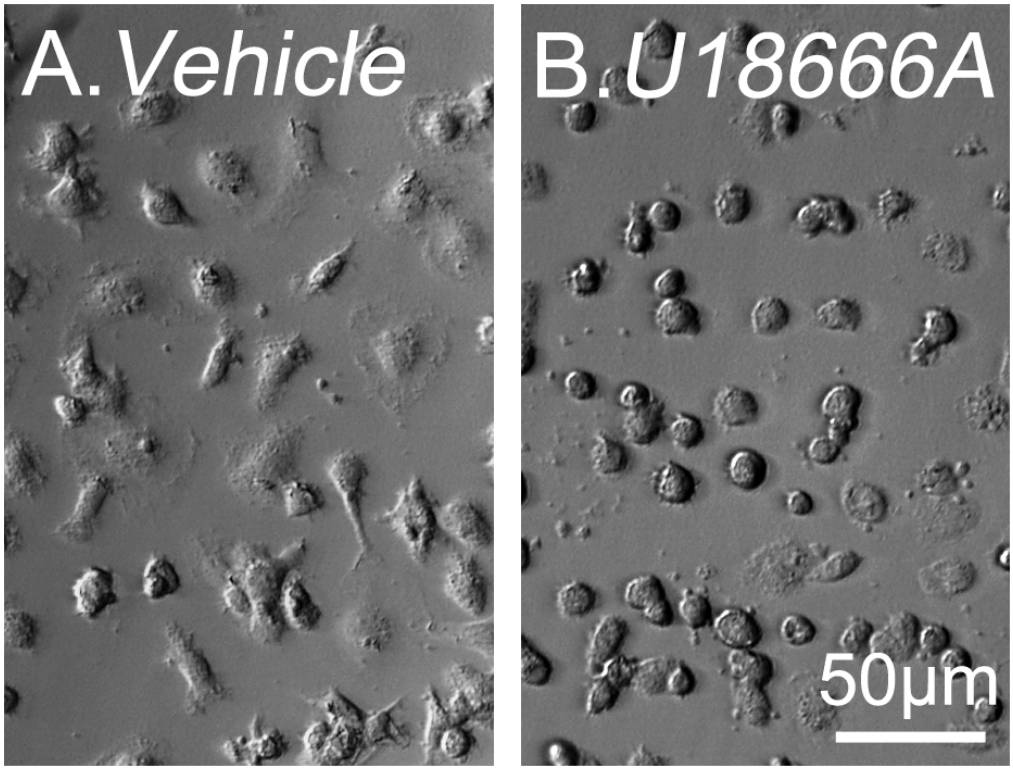


FIGURE 3.5 - **U18666A treatment of *Npc1*$^{+/+}$ mouse microglia induces an active morphology.** Primary cultures of *Npc1*$^{+/+}$ mouse microglia were treated with vehicle (A) or U18666A (B) for 6 h prior to being imaged. Primary microglia were isolated from glia cultures by mild trypsinization, replated, and allowed to rest overnight before treatment. Results are representative images from three independent cell preparations analyzed in duplicate.

*3.A(iii) Npc1$^{-/-}$ microglia have an altered morphology and an altered cholesterol distribution*

Since perturbation of cholesterol trafficking through the endosomal system had such drastic effects on *Npc1*$^{+/+}$ microglia, we isolated microglia from *Npc1*$^{-/-}$ mice to determine if these cells exhibited any obvious abnormalities. Unlike U18666A-treated microglia, *Npc1*$^{-/-}$ microglia cultures had a variety of different morphologies and appeared similar to *Npc1*$^{+/+}$ microglia cultures, except that *Npc1*$^{-/-}$ microglia appeared to be larger than *Npc1*$^{+/+}$ microglia (Fig. 3.6).

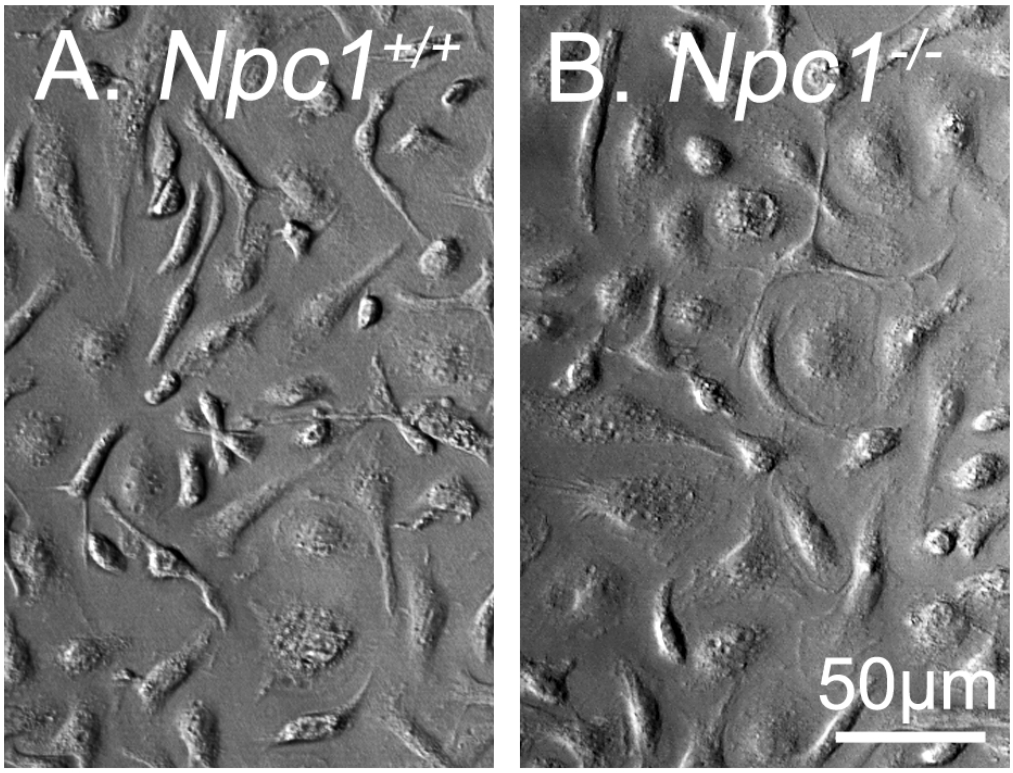


FIGURE 3.6 – ***Npc1*$^{-/-}$ microglia appear to be larger than *Npc1*$^{+/+}$ microglia.** Phase images of primary *Npc1*$^{+/+}$ (A) and *Npc1*$^{-/-}$ (B) microglia isolated from glia cultures by mild trypsinization, replated, and allowed to rest overnight prior to being imaged. Results are representative images from three independent cell preparations.

When unesterified cholesterol was labeled using filipin, *Npc1*$^{-/-}$ microglia showed a punctate intracellular staining pattern, which is characteristic of other NPC-deficient cells, while *Npc1*$^{+/+}$ microglia showed diffuse cholesterol staining (Fig. 3.7). *Npc1*$^{+/+}$ microglia also showed some intracellular cholesterol staining (Fig. 3.7*A*), which is most likely present in the endosomal recycling compartment, a region that has been shown to be enriched in cholesterol [260]. These experiments show that cholesterol distribution is indeed altered in *Npc1*$^{-/-}$ microglia. While this sequestration might cause a slight change in microglial morphology, this change is not nearly as dramatic as that induced with U18666A treatment.

*3.A(iv) Npc1*$^{-/-}$ *microglia show increased TNFα immunostaining, but not increased TNFα secretion*

TNFα mRNA levels are increased in the brains of *Npc1*$^{-/-}$ mice [148, 159]. Since microglia are considered to be the primary source of TNFα in the brain [261], we performed immunocytochemical staining of microglia cultures using a TNFα antibody. *Npc1*$^{-/-}$ microglia showed markedly increased TNFα immunostaining compared to *Npc1*$^{+/+}$ microglia (Fig. 3.8). We also compared immunostaining of the TNF-receptor 1 (TNFR1) in *Npc1*$^{+/+}$ and *Npc1*$^{-/-}$ microglial cultures; this TNFα receptor is involved in the TNFα-mediated death pathway. *Npc1*$^{-/-}$ microglia showed increased immunostaining for the TNFR1 compared to *Npc1*$^{+/+}$ microglia (Fig. 3.9). Surprisingly, however, the amount of TNFα secreted into the medium of *Npc1*$^{-/-}$ microglia was not higher than that of *Npc1*$^{+/+}$ microglia (Fig. 3.10).

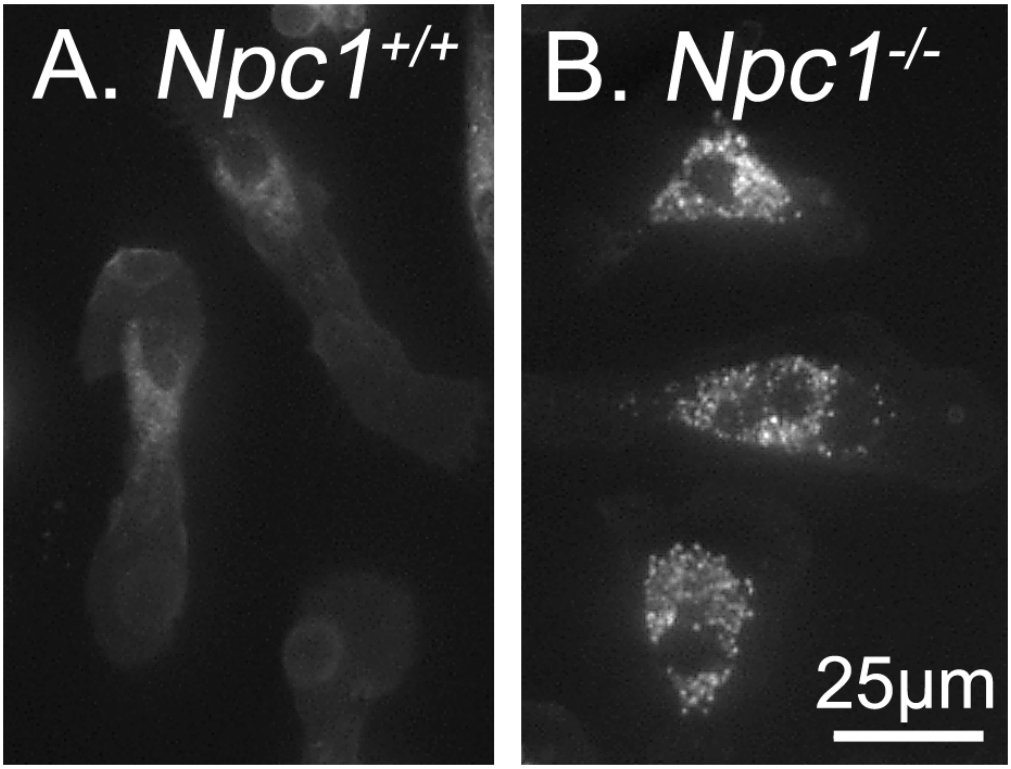


FIGURE 3.7 - ***Npc1*$^{-/-}$ microglia show an altered unesterified cholesterol staining pattern.** Filipin staining of unesterified cholesterol in *Npc1*$^{+/+}$ (A) and *Npc1*$^{-/-}$ (B) microglia cultures. Primary microglia were isolated from glia cultures by mild trypsinization, replated, and allowed to rest overnight prior to being stained. Results are representative images from three independent cell preparations.

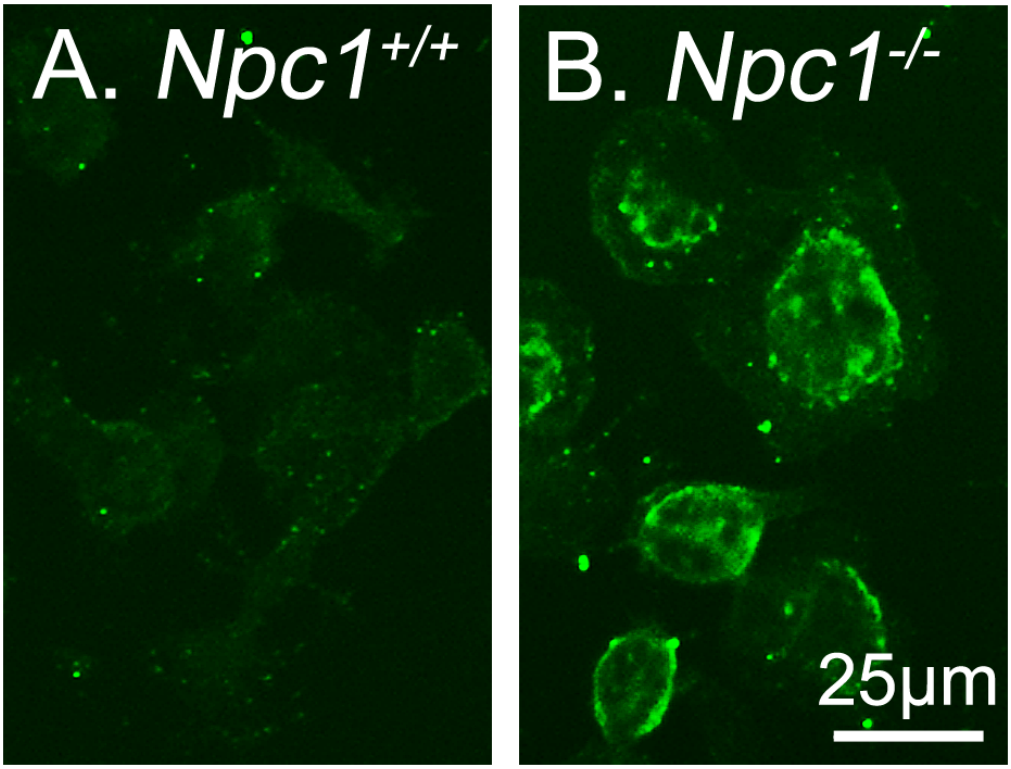


FIGURE 3.8 - ***Npc1*$^{-/-}$ microglia show increased immunostaining for TNFα.** Immunocytochemical staining of TNFα in *Npc1*$^{+/+}$ (A) and *Npc1*$^{-/-}$ (B) microglia cultures. Primary microglia were isolated from glia cultures by mild trypsinization, replated, and allowed to rest overnight prior to being immunostained. Results are representative images from three independent cell preparations.

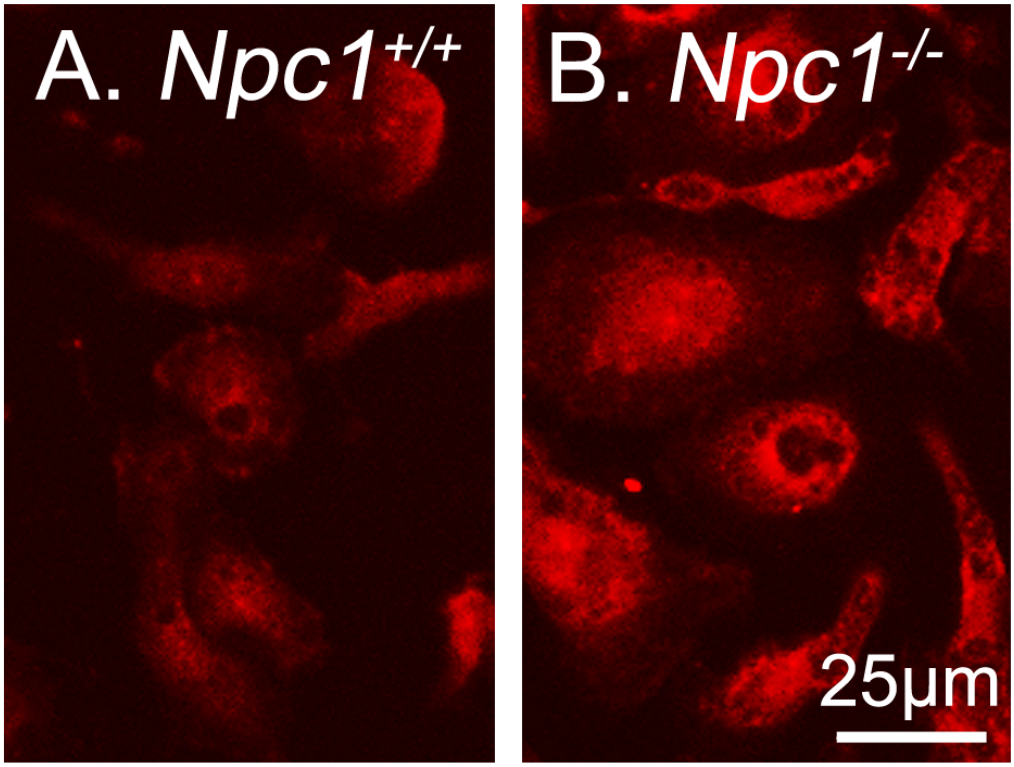


FIGURE 3.9 - ***Npc1*$^{-/-}$ microglia show increased immunostaining for TNFR1.** Immunocytochemical staining of TNFR1 in *Npc1*$^{+/+}$ (A) and *Npc1*$^{-/-}$ (B) microglia cultures. Primary microglia were isolated from glia cultures by mild trypsinization, replated, and allowed to rest overnight prior to being immunostained. Results are representative images from three independent cell preparations.

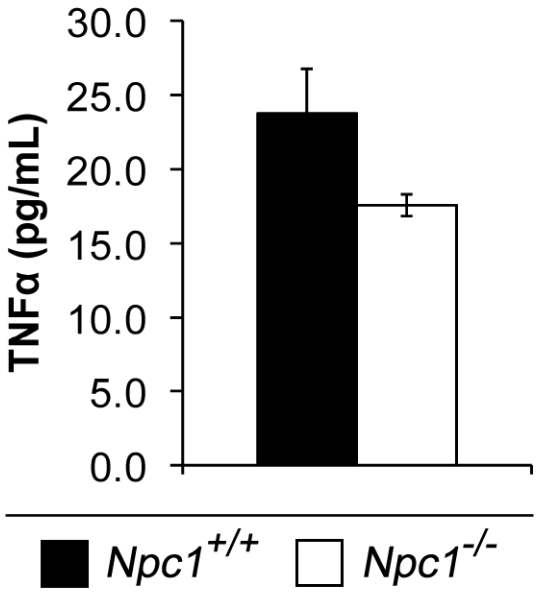


FIGURE 3.10 - ***Npc1*$^{+/+}$ and *Npc1*$^{-/-}$ microglia secrete similar levels of TNFα *in vitro*.** Amount of TNFα secreted into the media by *Npc1*$^{+/+}$ (black bars) and *Npc1*$^{-/-}$ (white bars) microglia. Primary microglia were isolated from glia cultures by mild trypsinization, replated, and allowed to rest overnight. Microglia were refed with fresh medium and, following a 24 h incubation, the amount of TNFα in the medium was determined by ELISA. Values are means ± SE of three independent microglia preparations analyzed in duplicate. Data were analyzed using the Student's *t* test.

*3.A(v) NPC1 deficiency in microglia decreases the level of mRNA encoding the anti-inflammatory cytokine IL10, but does not change levels of mRNAs encoding pro-inflammatory cytokines or oxidative stress genes*

Microglia produce not only pro-inflammatory cytokines, but also a range of other molecules including those involved in oxidative stress, as well as anti-inflammatory cytokines. We performed qPCR analysis of primary microglia in order to compare the mRNA levels of these factors in *Npc1*$^{-/-}$ microglia and *Npc1*$^{+/+}$ microglia. The levels of mRNAs encoding the pro-inflammatory cytokines, TNFα and interleukin-1β (IL1β), were not

different between *Npc1*$^{-/-}$ and *Npc1*$^{+/+}$ microglia (Fig. 3.11*A*). Similarly, levels of mRNAs encoded by genes involved in oxidative stress such as inducible nitric oxide synthase (iNOS) [which produces nitric oxide [262]], and NADPH oxidase (NADPHox) [which produces superoxide [263]], were similar in *Npc1*$^{-/-}$ and *Npc1*$^{+/+}$ microglia (Fig. 3.11*B*). However, levels of mRNAs encoding the anti-inflammatory cytokine interleukin-10 (IL10) were significantly lower in *Npc1*$^{-/-}$ microglia, while mRNA levels of another anti-inflammatory cytokine, transforming growth factor-β (TGFβ), were no different between *Npc1*$^{-/-}$ and *Npc1*$^{+/+}$ microglia (Fig. 3.11*C*). Additionally, we quantified mRNAs encoding glutaminase (GLTase), [which produces glutamate that can lead to excitotoxic death [264]], as well as the macrophage colony-stimulating factor receptor (M-CSFR), [which is involved in microglial proliferation and activation [265]]. However, there were no differences in the expression of these genes between *Npc1*$^{-/-}$ and *Npc1*$^{+/+}$ microglia (Fig. 3.11*D*). These results suggest that protective functions, or the suppression of an inflammatory response, may be impaired in *Npc1*$^{-/-}$ microglia.

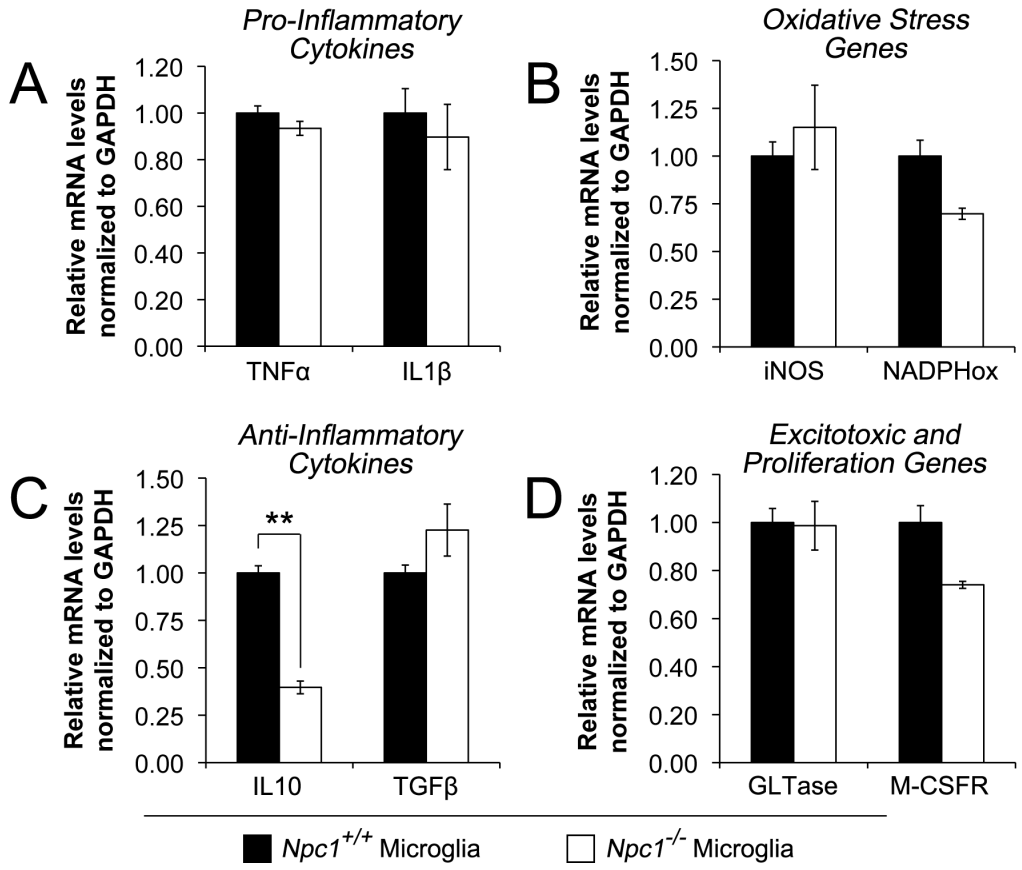


FIGURE 3.11 - ***Npc1*$^{-/-}$ microglia have decreased mRNA levels of the anti-inflammatory cytokine IL10.** Quantitative real-time PCR analysis of mRNAs encoding pro-inflammatory cytokines (A), oxidative stress genes (B), anti-inflammatory cytokines (C), as well as genes involved in excitotoxicity and proliferation (D) in *Npc1*$^{+/+}$ (black bars) and *Npc1*$^{-/-}$ (white bars) microglia cultures. mRNA levels were quantified relative to mRNA encoding GAPDH. Microglia were isolated by mild trypsinization and allowed to rest for 24 h prior to isolating RNA. Data are means ± SE of three independent microglia preparations analyzed in triplicate. Data were analyzed using the Student's *t* test (** $p<0.01$).

*3.A(vi) Npc1$^{-/-}$ microglia do not increase neuronal apoptosis in microglia-neuron co-cultures*

To determine if the alterations we observed in *Npc1*$^{-/-}$ microglia could lead to neuron death, we performed several experiments in which neurons were co-cultured with microglia. Different densities of microglia were plated directly on to cultures of CGCs. Different combinations of cells and genotypes were plated, such that *Npc1*$^{+/+}$ and *Npc1*$^{-/-}$ neurons were independently co-cultured with *Npc1*$^{+/+}$ and *Npc1*$^{-/-}$ microglia. Following 24 h of co-culture, cells were fixed with paraformaldehyde, and stained with specific markers for neurons (MAP2) and microglia (Iba1). The number of apoptotic neurons was quantified by Hoechst staining (Fig 3.12). Interestingly, *Npc1*$^{-/-}$ microglia, plated at both low and high densities, did not increase apoptosis in *Npc1*$^{+/+}$ or *Npc1*$^{-/-}$ CGCs, compared to *Npc1*$^{+/+}$ microglia (Fig. 3.13). In fact, a high density of *Npc1*$^{-/-}$ microglia caused a significant decrease in apoptosis of *Npc1*$^{+/+}$ CGCs (Fig. 3.13*B*). Notably, the level of apoptosis in *Npc1*$^{+/+}$ and *Npc1*$^{-/-}$ CGCs cultured without microglia was similar (Fig. 3.14), and these levels of apoptosis were also comparable to those in the co-culture experiments. Thus, *Npc1*$^{-/-}$ microglia do not appear to be causing increased neuronal apoptosis, at least within the limits our co-culture system.

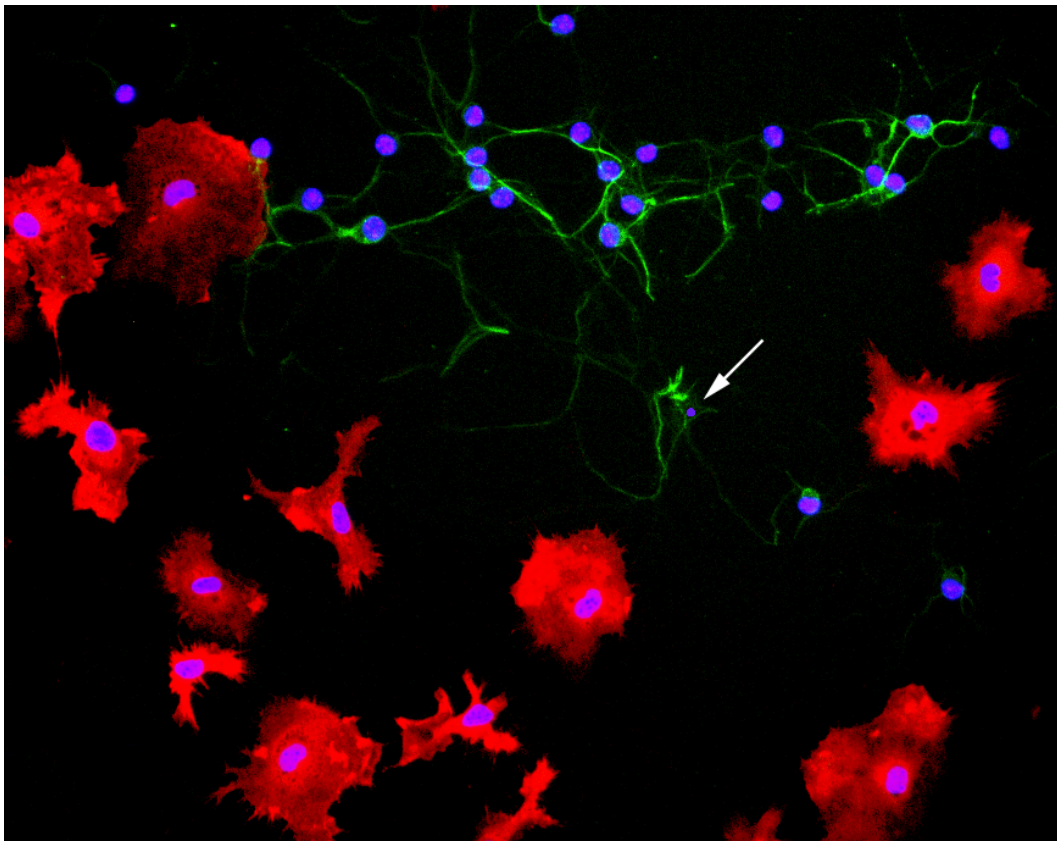

FIGURE 3.12 – **Microglia-cerebellar granule cell co-cultures.** Following 24 h of co-culture, cells were fixed with paraformaldehyde, and stained with specific markers for neurons (MAP2, green) and microglia (Iba1, red). Nuclei were labeled by Hoechst staining (blue) for quantitation of the number of apoptotic neurons (condensed or fragmented nuclei, arrow).

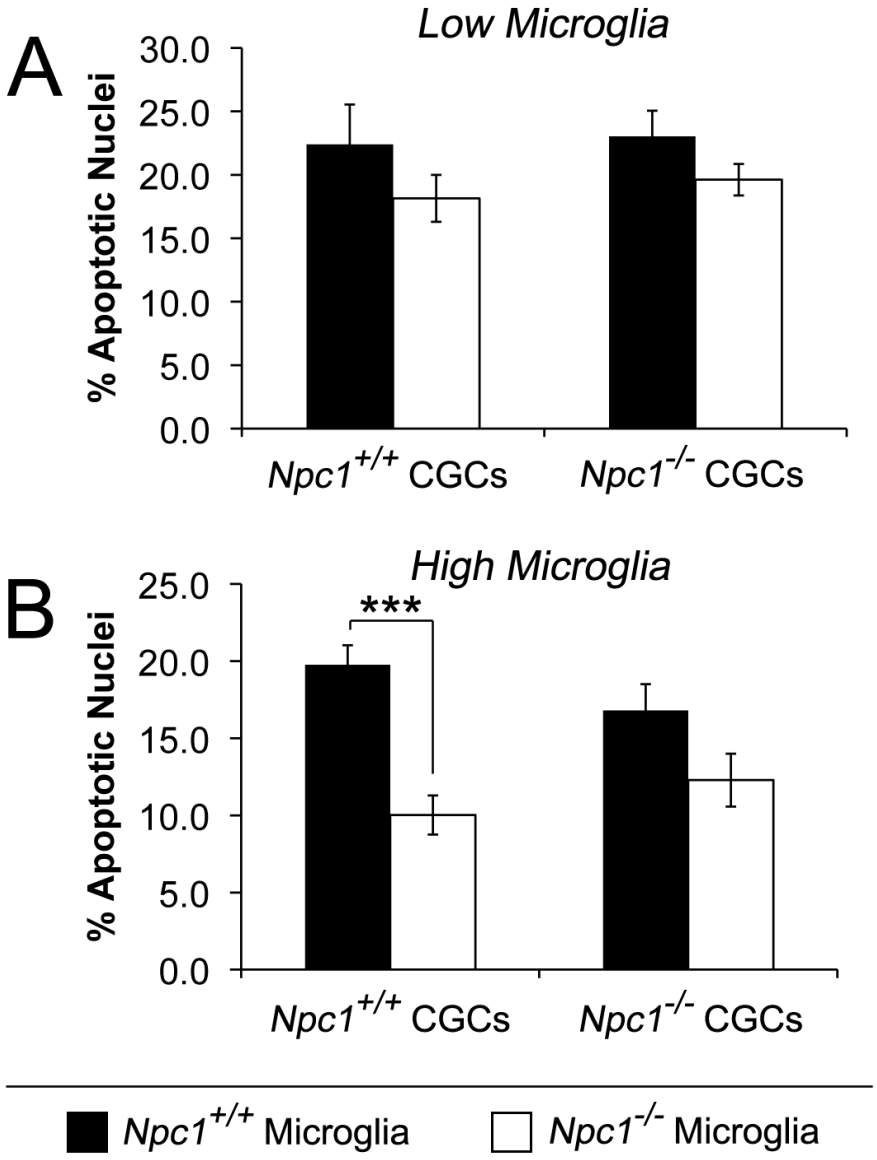


FIGURE 3.13 - ***Npc1*$^{-/-}$ microglia do not increase CGC apoptosis in microglia-neuron co-cultures.** Number of apoptotic *Npc1*$^{+/+}$ and *Npc1*$^{-/-}$ neurons (CGCs) directly co-cultured with *Npc1*$^{+/+}$ (black bars) and *Npc1*$^{-/-}$ (white bars) microglia. Microglia were plated at densities that were either 25% [low] (A) or 50% [high] (B) of the total number of neurons. Primary microglia were isolated from glia cultures by mild trypsinization, and replated in neuronal medium at the indicated densities on 7-d-old CGC cultures. Following 24 h of co-culture, cells were fixed and neurons were labeled with Map2, microglia with Iba1, and nuclei with Hoechst stain. Data are the mean percentages of apoptotic nuclei in > 1000 cells quantified from two independent CGC preparations co-cultured with three independent microglia preparations, performed in duplicate. Error bars represent SE. Data were analyzed using the Student's *t* test (*** $p<0.001$).

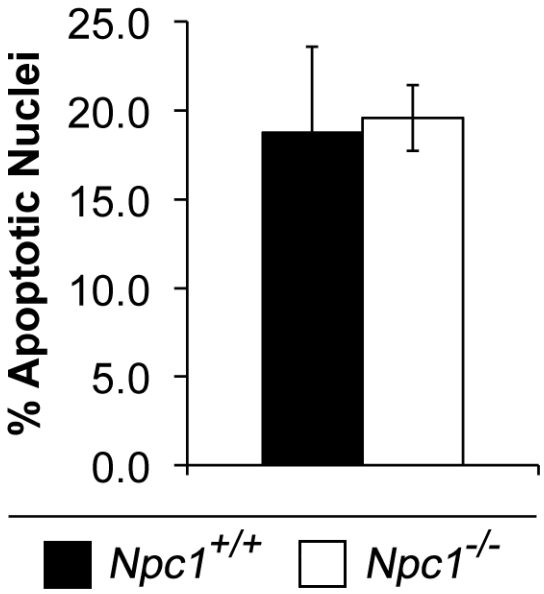


FIGURE 3.14 - ***Npc1*$^{+/+}$ and *Npc1*$^{-/-}$ CGCs have similar levels of apoptosis *in vitro*.** Extent of apoptosis in 7-d-old *Npc1*$^{+/+}$ (black bars) and *Npc1*$^{-/-}$ (white bars) CGC cultures. CGCs were cultured for 7 d, fixed with paraformaldehyde, and the nuclei were labeled with Hoechst stain. Data are the mean percentages of apoptotic nuclei in > 500 cells quantified from two independent CGC preparations, performed in duplicate. Error bars represent standard error. Data were analyzed using the Student's *t* test.

We performed several other experiments where a similar trend was observed. These included experiments in which medium was incubated on microglia cultures for 24 h and then the conditioned medium was added to neurons for an additional 24 h, in order to determine if microglia secreted any factors that were toxic to neurons. Medium conditioned by *Npc1*$^{-/-}$ microglia, however, caused no increase in apoptosis in *Npc1*$^{-/-}$ or *Npc1*$^{+/+}$ CGC cultures compared to *Npc1*$^{+/+}$ microglia-conditioned medium (Fig. 3.15). As our neuron culture conditions are normally optimized for survival, it is possible growth factors added to the culture medium might prevent microglial factors from inducing apoptosis. Thus, we also performed co-culture experiments using microglia and cortical neurons cultured in Neurobasal™ 'A' medium without the addition of any supplements. Under these conditions, *Npc1*$^{-/-}$ microglia cultured directly with *Npc1*$^{+/+}$ and *Npc1*$^{-/-}$ cortical neurons, did not increase neuronal apoptosis compared to *Npc1*$^{+/+}$ microglia co-cultures (Fig. 3.16). Similarly, the level of apoptosis in *Npc1*$^{+/+}$ and *Npc1*$^{-/-}$ cortical neurons incubated with *Npc1*$^{-/-}$ microglia-conditioned medium (lacking supplements) was not different from that of neurons cultured with *Npc1*$^{+/+}$ microglia-conditioned medium (Fig. 3.17). These results suggest that factors in the media were not preventing *Npc1*$^{-/-}$ microglia from inducing apoptosis in neuron cultures. Furthermore, these results also imply that the ability of *Npc1*$^{-/-}$ microglia to prevent apoptosis under these culture conditions was not impaired.

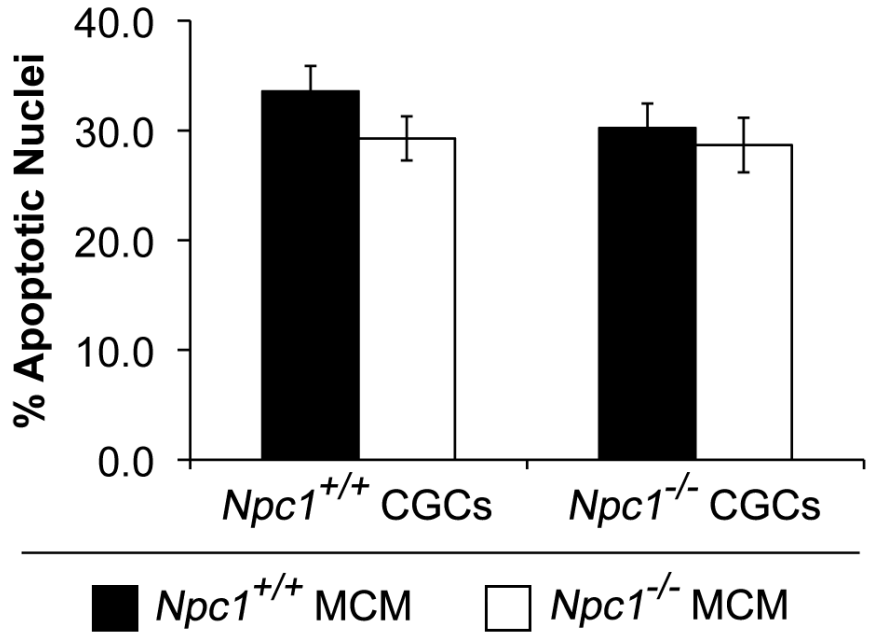


FIGURE 3.15 - ***Npc1*$^{-/-}$ microglia-conditioned medium does not increase apoptosis in CGC cultures.** Extent of apoptosis in *Npc1*$^{+/+}$ and *Npc1*$^{-/-}$ CGCs incubated with *Npc1*$^{+/+}$ (black bars) and *Npc1*$^{-/-}$ (white bars) microglia-conditioned medium. Neuronal medium was incubated on microglia cultures for 24 h prior to being incubated on 7-d-old CGC cultures. Following 24 h of conditioned medium treatment, neurons were fixed with paraformaldehyde and the nuclei labeled with Hoechst stain. Data are the mean percentages of apoptotic nuclei in > 2000 cells quantified from one CGC preparation treated with conditioned medium from one microglia preparation, performed in triplicate. Error bars represent standard error. Data were analyzed using the Student's *t* test.

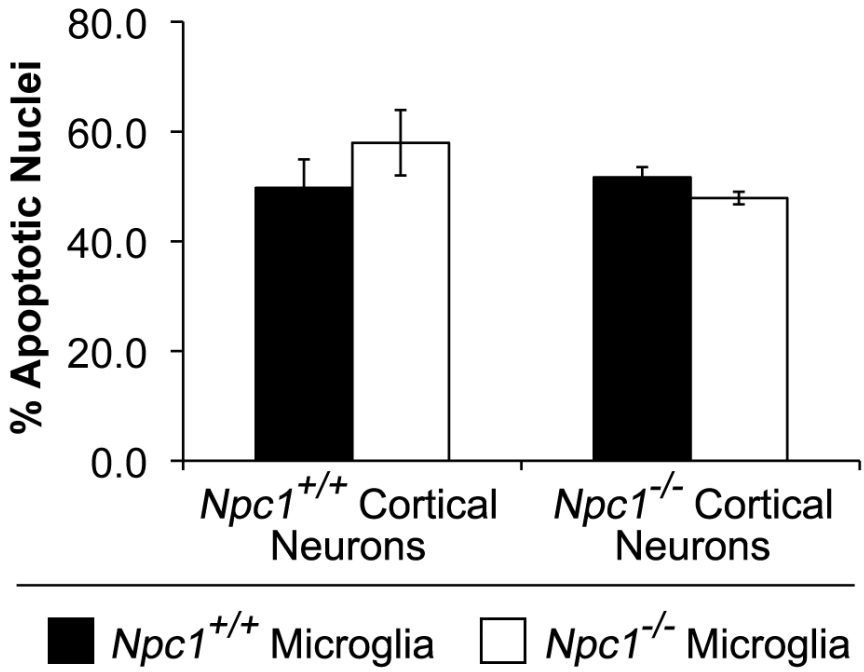


FIGURE 3.16 - ***Npc1*$^{-/-}$ microglia do not increase cortical neuron apoptosis when co-cultured in medium lacking neuronal supplements.** Extent of apoptosis in *Npc1*$^{+/+}$ and *Npc1*$^{-/-}$ cortical neurons directly co-cultured with *Npc1*$^{+/+}$ (black bars) and *Npc1*$^{-/-}$ (white bars) microglia. Microglia were plated at a density that was 30% of the total number of neurons. Primary microglia were isolated from glia cultures by mild trypsinization and replated in neuronal medium lacking supplements at the appropriate density on 3-d-old cortical neuron cultures. Following 48 h of co-culture, cells were fixed and neurons were labeled with NeuN, microglia with Iba1, and nuclei with Hoechst stain. Data are the mean percentages of apoptotic nuclei in > 1000 cells quantified from one cortical neuron preparation co-cultured with one microglia preparation, performed in triplicate. Error bars represent standard error. Data were analyzed using the Student's *t* test.

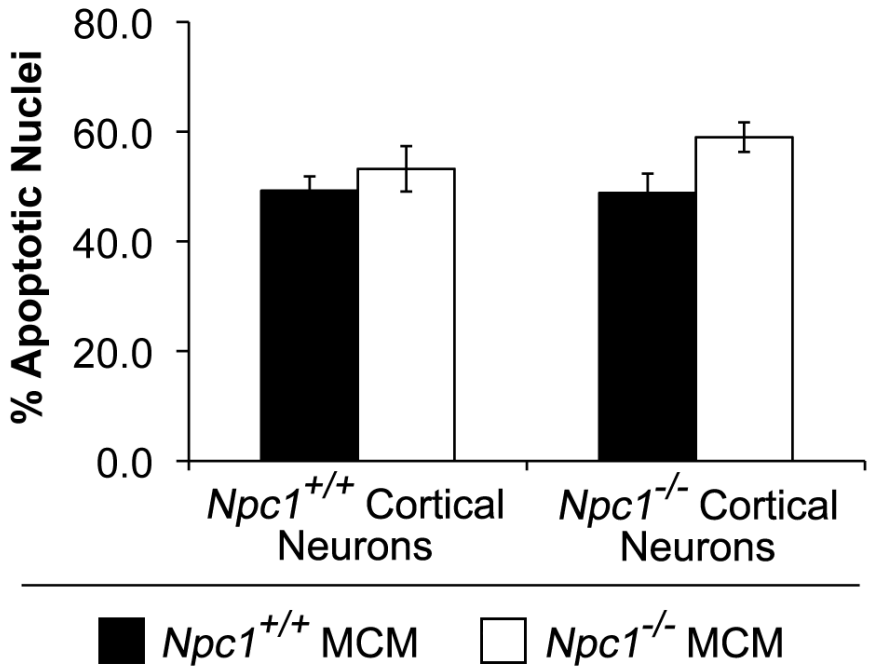


FIGURE 3.17 - ***Npc1*$^{-/-}$ microglia-conditioned medium lacking neuronal supplements does not increase apoptosis in cortical neuron cultures.** Extent of apoptosis in *Npc1*$^{+/+}$ and *Npc1*$^{-/-}$ cortical neurons incubated with *Npc1*$^{+/+}$ (black bars) and *Npc1*$^{-/-}$ (white bars) microglia-conditioned medium. Neuronal medium lacking supplements was incubated on microglia cultures for 48 h prior to being incubated on 3-d-old cortical neuron cultures. Following 48 h of conditioned medium treatment, neurons were fixed with paraformaldehyde, and the nuclei labeled with Hoechst stain. Data are the mean percentages of apoptotic nuclei in > 4000 cells quantified from one cortical neuron preparation treated with conditioned medium from one microglia preparation, performed in triplicate. Error bars represent standard error. Data were analyzed using the Student's *t* test.

*3.A(vii) Phagocytosis is not impaired in Npc1$^{-/-}$ microglia*

Microglia are the resident phagocytic cells of the CNS, engulfing degenerating cells and other debris [189]. It is possible that the sequestration of cholesterol within *Npc1*$^{-/-}$ microglia could impair their phagocytic abilities. Conversely, if *Npc1*$^{-/-}$ microglia were in a more activated state, their ability to phagocytose may instead be increased. Microglia were incubated for 2h with fluorescent latex beads, after which the cells were extensively washed and the number of beads internalized by the microglia quantified. As a control for beads that may have been attached to the cells, but not actually internalized, some cultures were incubated at 4°C in order to block phagocytosis. *Npc1*$^{-/-}$ and *Npc1*$^{+/+}$ microglia exhibited similar levels of phagocytosis of the beads (Fig. 3.18). Thus, phagocytosis does not appear to be impaired in *Npc1*$^{-/-}$ microglia. Nevertheless, other phagocytic pathways, such as the uptake of apoptotic cells, may be disrupted in NPC1-deficient microglia.

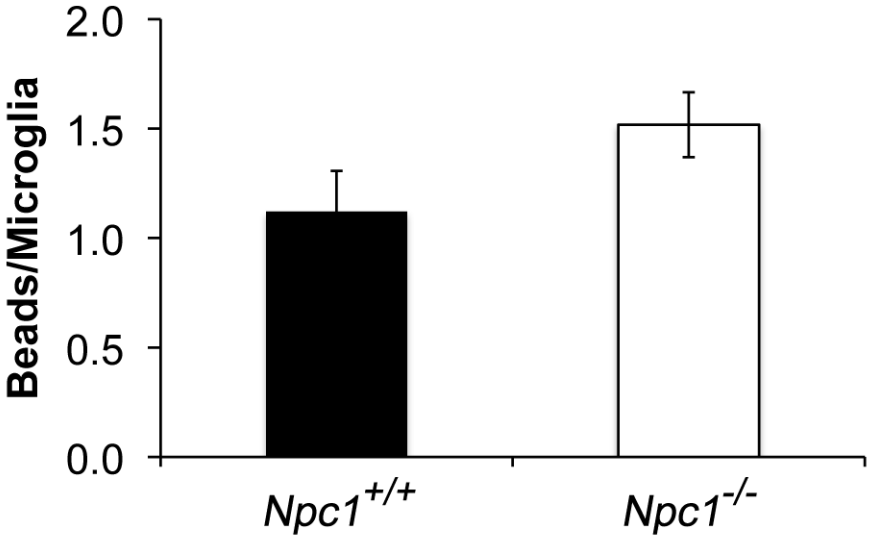


FIGURE 3.18 – **Phagocytosis is not impaired in *Npc1*$^{-/-}$ microglia.** Phagocytosis of carboxylate-modified polystyrene latex beads in *Npc1*$^{+/+}$ (black bars) and *Npc1*$^{-/-}$ (white bars) microglia cultures. Primary microglia were isolated from glia cultures by mild trypsinization, replated, and allowed to rest overnight. Beads were added to the culture medium and incubated on the microglia cultures for 2 h at 37°C. As a control, beads were also incubated on microglia cultures for 2 h at 4°C to block phagocytosis. Cultures were extensively washed with ice-cold PBS and the number of beads/microglia quantified. Values are the means ± SE from three independent experiments (> 600 microglia). Data were analyzed using the Student's *t* test.

## *3.B MODULATION OF CHOLESTEROL HOMEOSTASIS IN NEURONS AND GLIA BY CYCLODEXTRIN*

### *3.B(i) Low concentrations of cyclodextrin are not toxic to neuron and astrocyte cultures*

βCD can have a variety of effects on cells depending upon the concentrations used and the duration of the exposure. Higher concentrations typically deplete the cells of cholesterol, ultimately leading to cell death, while lower concentrations can facilitate cholesterol transfer between hydrophobic compartments [227, 240, 244, 245]. These effects depend not only upon the ratio of βCD to cholesterol, but also depend upon the cell type, with some cells being more sensitive to βCD than others [224]. In order to determine which doses of HPCD could be tolerated by our cell cultures, we assessed the morphology and measured apoptosis in *Npc1*$^{-/-}$ mouse CGC and astrocyte cultures treated for 24 h with various concentrations of HPCD (Fig. 3.19 and 3.20). Neither 0.1 mM nor 1.0 mM HPCD altered cellular morphology compared to vehicle in CGC or astrocyte cultures (Fig. 3.19, *A*-*C* and *E*-*G*). Additionally, these doses of HPCD did not cause any significant increases in apoptosis compared to vehicle (Fig. 3.20). Treatment of cultures with 10 mM HPCD, however, completely destroyed the CGCs such that no cells remained (Fig. 3.19*D*). While these effects were not as drastic in astrocyte cultures, 10 mM HPCD did markedly alter the astrocyte morphology (Fig. 3.19*H*), and thus this concentration was not used for any further experiments.

Similar results were also seen when the same doses of HPCD were administered to *Npc1*$^{+/+}$ CGC and cortical astrocyte cultures (Fig. 3.21 and 3.22).

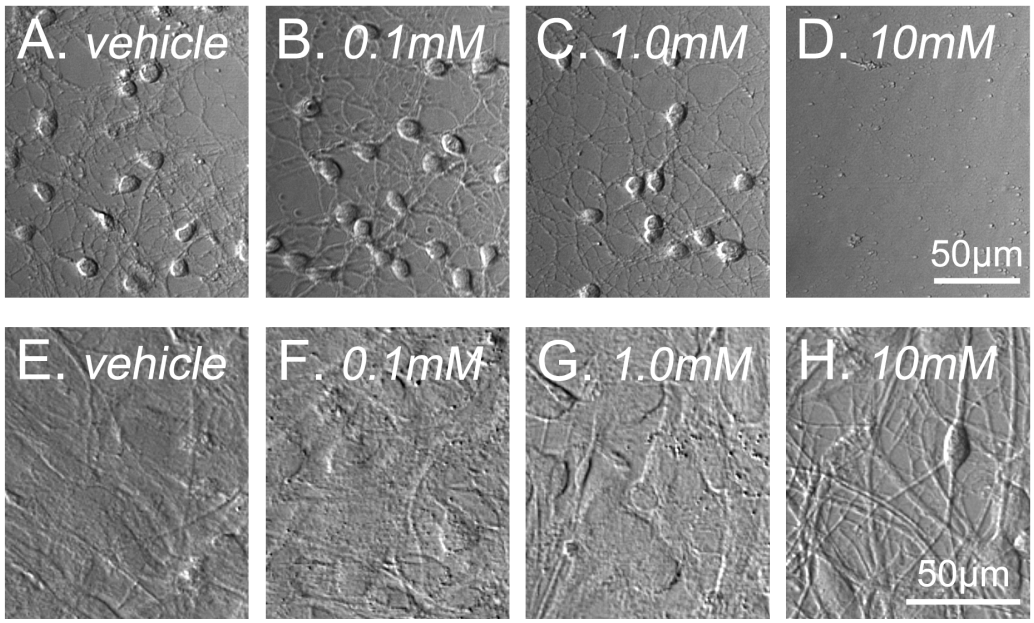


FIGURE 3.19 - **Lower doses of HPCD are not toxic to *Npc1*$^{-/-}$ neurons and astrocytes *in vitro*.** Phase images of 7-d-old *Npc1*$^{-/-}$ cerebellar granule cells (A-D) and *Npc1*$^{-/-}$ astrocytes (E-H) treated for 24 h with vehicle (A,E), 0.1 mM HPCD (B,F), 1.0 mM HPCD (C,G), or 10 mM HPCD (D,H). Results are representative images from three independent cell preparations.

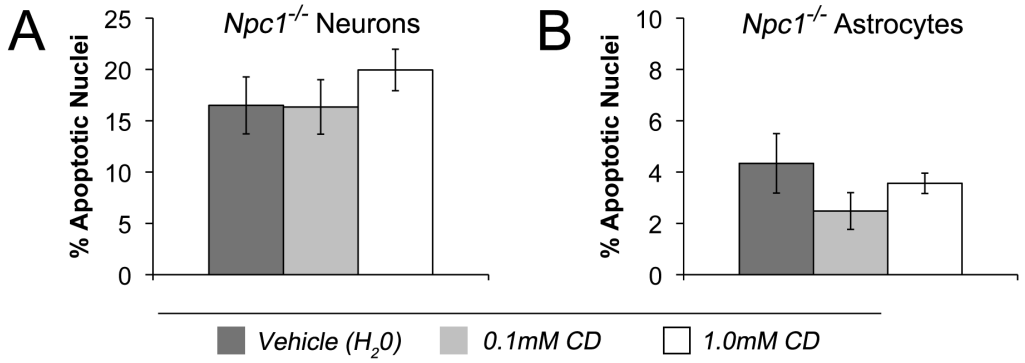


FIGURE 3.20 - **Lower doses of HPCD do not increase apoptosis in *Npc1*$^{-/-}$ neurons and astrocytes *in vitro*.** Apoptosis was quantified in cultured *Npc1*$^{-/-}$ cerebellar granule cells (A) and astrocytes (B). Following 24 h of treatment, cells were fixed with paraformaldehyde, Hoechst stained, and the percentage of apoptotic nuclei quantified for vehicle (dark grey bars), 0.1 mM HPCD (light grey bars), and 1.0 mM HPCD (white bars). Data are the mean percentages of apoptotic nuclei in > 750 cells quantified from three independent cell preparations performed in duplicate. Error bars represent standard error. Data were analyzed using the Student's *t* test.

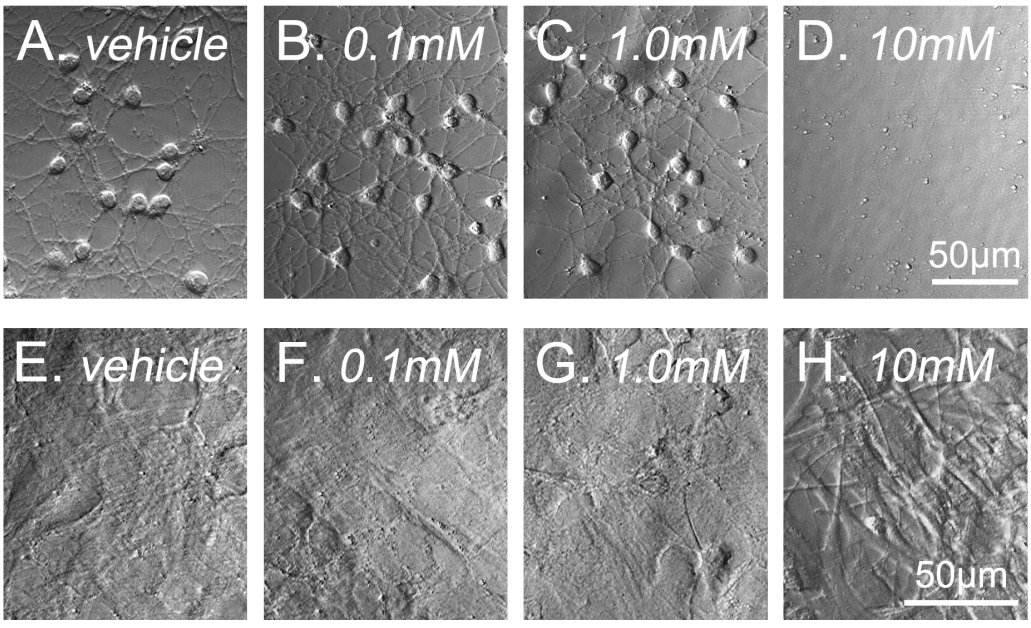


FIGURE 3.21 - **Lower doses of HPCD are not toxic to *Npc1*$^{+/+}$ neurons and astrocytes *in vitro*.** Phase images of 7-d-old *Npc1*$^{+/+}$ cerebellar granule cells (A-D) and *Npc1*$^{+/+}$ astrocytes (E-H) treated for 24 h with vehicle (A,E), 0.1 mM HPCD (B,F), 1.0 mM HPCD (C,G), or 10 mM HPCD (D,H). Results are representative images from one cell preparation analyzed in triplicate.

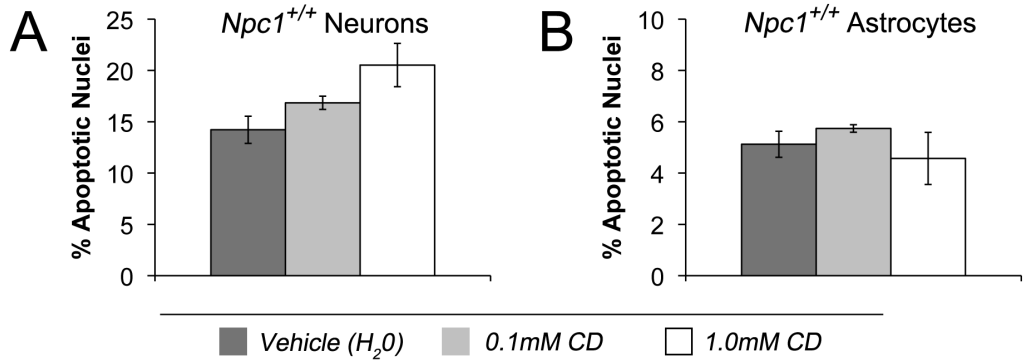


FIGURE 3.22 - **Lower doses of HPCD do not increase apoptosis in *Npc1*$^{+/+}$ neurons and astrocytes *in vitro*.** Apoptosis was quantified in cultures of *Npc1*$^{+/+}$ cerebellar granule cells (A) and astrocytes (B). Following 24 h of treatment, cells were fixed with paraformaldehyde, Hoechst stained, and the percentage of apoptotic nuclei quantified for vehicle (dark grey bars), 0.1 mM HPCD (light grey bars), and 1.0 mM HPCD (white bars). Data are the mean percentages of apoptotic nuclei in > 800 cells quantified from one cell preparation performed in triplicate. Error bars represent standard error. Data were analyzed using the Student's *t* test.

*3.B(ii) Cyclodextrin reduces punctate cholesterol staining in Npc1*$^{-/-}$ *neurons and astrocytes*

*Npc1*$^{-/-}$ CGCs and astrocytes show a punctate intracellular staining pattern for unesterified cholesterol, similar to that in other NPC1-deficient cells (Fig. 3.23, *A* and *D*). Treatment of *Npc1*$^{-/-}$ CGCs and astrocytes with 0.1 mM and 1.0 mM HPCD resulted in decreased punctate filipin staining of unesterified cholesterol (Fig. 3.23, *B,C* and *E,F*). The 1.0 mM HPCD treatment seemed to reduce punctate filipin staining slightly more than 0.1 mM HPCD in both neurons and astrocytes. Interestingly, 0.1 mM and 1.0 mM HPCD appeared to increase filipin staining of cholesterol in the plasma membrane compared to vehicle treatment, an effect that was particularly evident in the CGC cultures (Fig. 3.23). *Npc1*$^{+/+}$ CGCs and

astrocytes showed filipin staining predominantly in the plasma membrane, consistent with the plasma membrane containing the majority of cholesterol in cells (Fig. 3.24, *A* and *D*). Administration of 0.1 mM or 1.0 mM HPCD to *Npc1*$^{+/+}$ CGC and astrocyte cultures caused no changes in filipin staining compared to vehicle (Fig. 3.24).

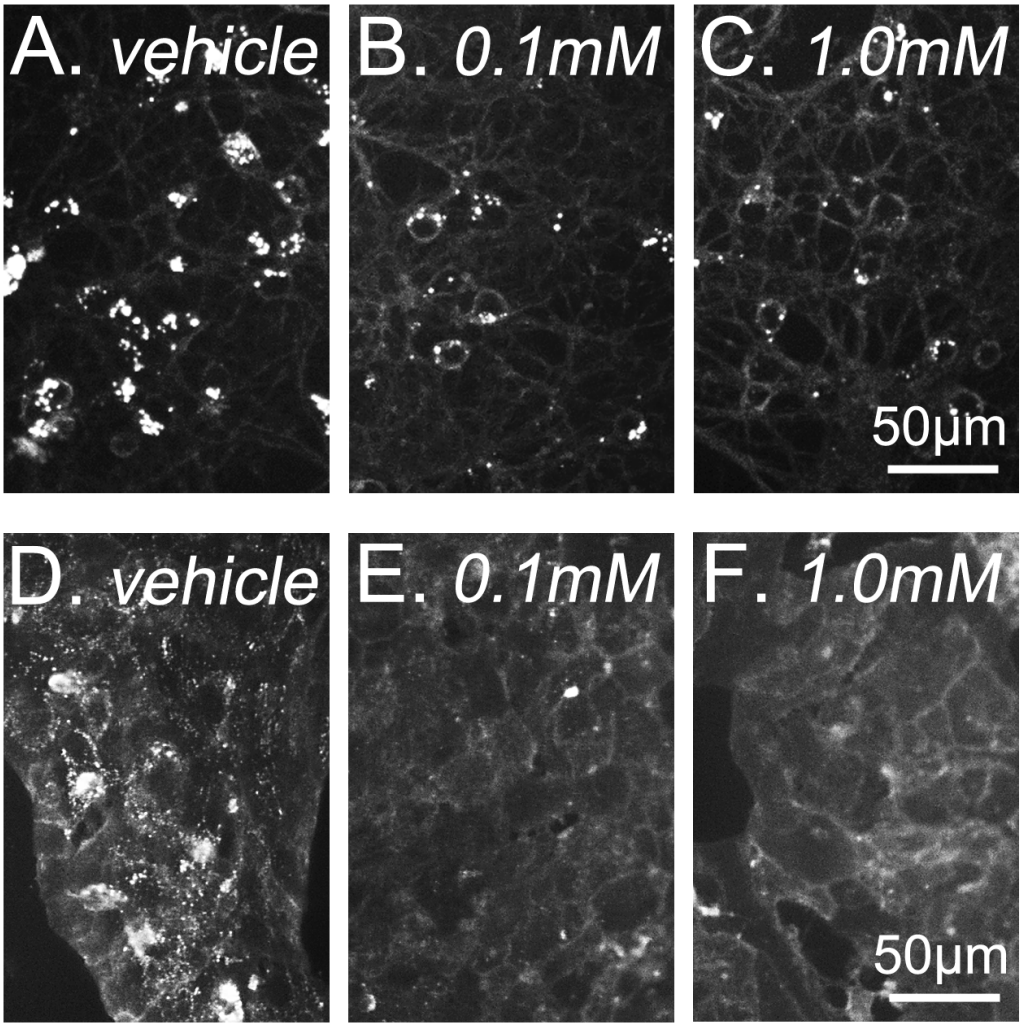


FIGURE 3.23 - **HPCD treatment reduces intracellular cholesterol accumulation in *Npc1*$^{-/-}$ neurons and astrocytes *in vitro*.** Filipin staining of unesterified cholesterol in 7-d-old *Npc1*$^{-/-}$ cerebellar granule cells (A-C) and *Npc1*$^{-/-}$ astrocytes (D-F) treated for 24 h with vehicle (A,D), 0.1 mM HPCD (B,E), or 1.0 mM HPCD (C,F). Results are representative images from three independent cell preparations.

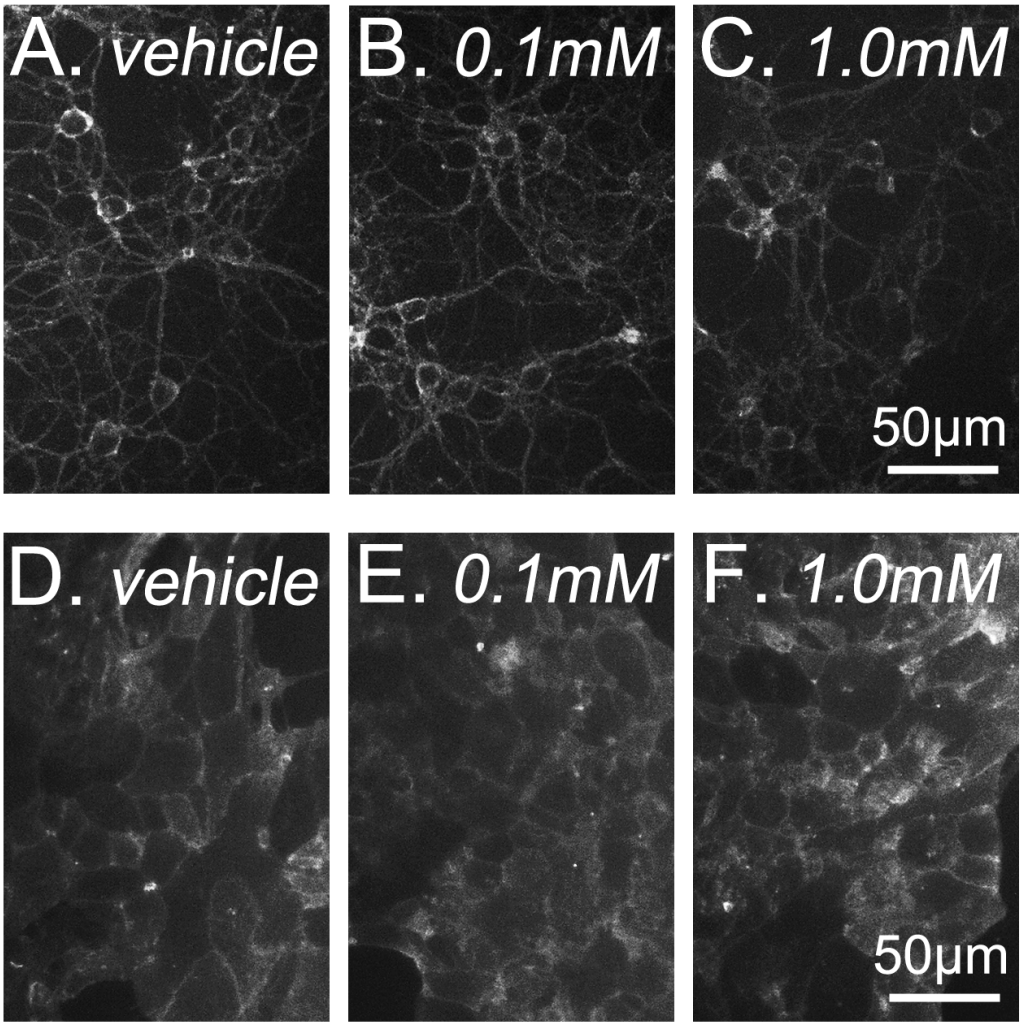


FIGURE 3.24 - **HPCD treatment does not alter cholesterol staining in *Npc1*$^{+/+}$ neurons and astrocytes *in vitro*.** Filipin staining of unesterified cholesterol in 7-d-old *Npc1*$^{+/+}$ cerebellar granule cells (A-C) and *Npc1*$^{+/+}$ astrocytes (D-F) treated for 24 h with vehicle (A,D), 0.1 mM HPCD (B,E), or 1.0 mM HPCD (C,F). Results are representative images from one cell preparation analyzed in triplicate.

*3.B(iii) A low dose of cyclodextrin reduces incorporation of radiolabel into newly synthesized cholesterol in Npc1*$^{-/-}$ *neurons and astrocytes*

In NPC1-deficient cells, the sequestration of lipids within LE/Ls prevents cholesterol from reaching the ER [78, 79], where degradation of

HMGCR is increased, SREBP2 processing is decreased, and ultimately cholesterol synthesis is decreased. As a consequence, many NPC1-deficient cells show increased cholesterol synthesis, despite massive cholesterol accumulation within LE/Ls [79]. In order to assess cholesterol synthesis, cells were given the indicated treatment for 24 h followed by a 4 h incubation with [$^3$H]acetate (the primary building block of cholesterol) and the incorporation of [$^3$H]acetate into unesterified cholesterol was measured. Unlike many *Npc1*$^{-/-}$ cells, which show increased cholesterol synthesis, we found both *Npc1*$^{+/+}$ and *Npc1*$^{-/-}$ CGCs incorporated similar amounts of [$^3$H]acetate into newly synthesized cholesterol (Fig. 3.25*A*). Likewise, the amount of radiolabeled cholesterol was comparable in *Npc1*$^{+/+}$ and *Npc1*$^{-/-}$ astrocytes (Fig. 3.25*B*). These findings parallel those of Liu *et al*., who found no differences in cholesterol synthesis in whole brains from *Npc1*$^{+/+}$ and *Npc1*$^{-/-}$ mice [246]. It is also worth noting that while CGCs incorporated similar amounts of [$^3$H]acetate into cholesterol and phospholipids, astrocytes incorporated much higher levels of [$^3$H]acetate into phospholipids compared to cholesterol (Fig. 3.25, *A* and *B*).

If HPCD treatment liberated sequestered cholesterol from LE/Ls into the cytoplasm and made the cholesterol available to the cell, one would expect that cholesterol synthesis would be reduced. Indeed, treatment of *Npc1*$^{-/-}$ CGCs and astrocytes with 0.1 mM HPCD significantly decreased the incorporation of radiolabel into cholesterol compared to

vehicle treatment (Fig. 3.26). Administration of 0.1 mM HPCD to *Npc1*$^{+/+}$ CGCs and astrocytes, however, did not decrease the incorporation of radiolabel into cholesterol compared to vehicle treatment (Fig. 3.27). In fact, *Npc1*$^{+/+}$ CGC cultures showed a slight, but statistically significant increase in radiolabeled cholesterol with 0.1 mM HPCD treatment compared to vehicle, most likely due to cellular cholesterol levels being partially depleted by the HPCD (Fig. 3.27*A*). This effect did not occur in *Npc1*$^{+/+}$ astrocytes, which showed no difference in the incorporation of [$^{3}$H]acetate into cholesterol between 0.1 mM HPCD and vehicle treatment (Fig. 3.27*B*). When cultures were treated with the higher dose of 1.0 mM HPCD, the incorporation of radiolabel into cholesterol was no longer suppressed, but was dramatically increased compared to vehicle treated cultures. This effect was seen in both *Npc1*$^{+/+}$ and *Npc1*$^{-/-}$ CGCs and astrocytes (Fig. 3.26 and 3.27). These findings suggest that even though 1.0 mM HPCD reduces punctate filipin staining of cholesterol (i.e. reduces sequestration in LE/L) in *Npc1*$^{-/-}$ CGCs and astrocytes, this dose of HPCD ultimately also removes excess cholesterol from the cell surface, forcing the cells to increase cholesterol synthesis. Importantly, HPCD treatment, regardless of concentration, did not alter incorporation of [$^{3}$H]acetate into phospholipids (Fig. 3.26 and 3.27), implying that HPCD treatment does not alter [$^{3}$H]acetate uptake into the cells, nor does it alter the rate of phospholipid synthesis.

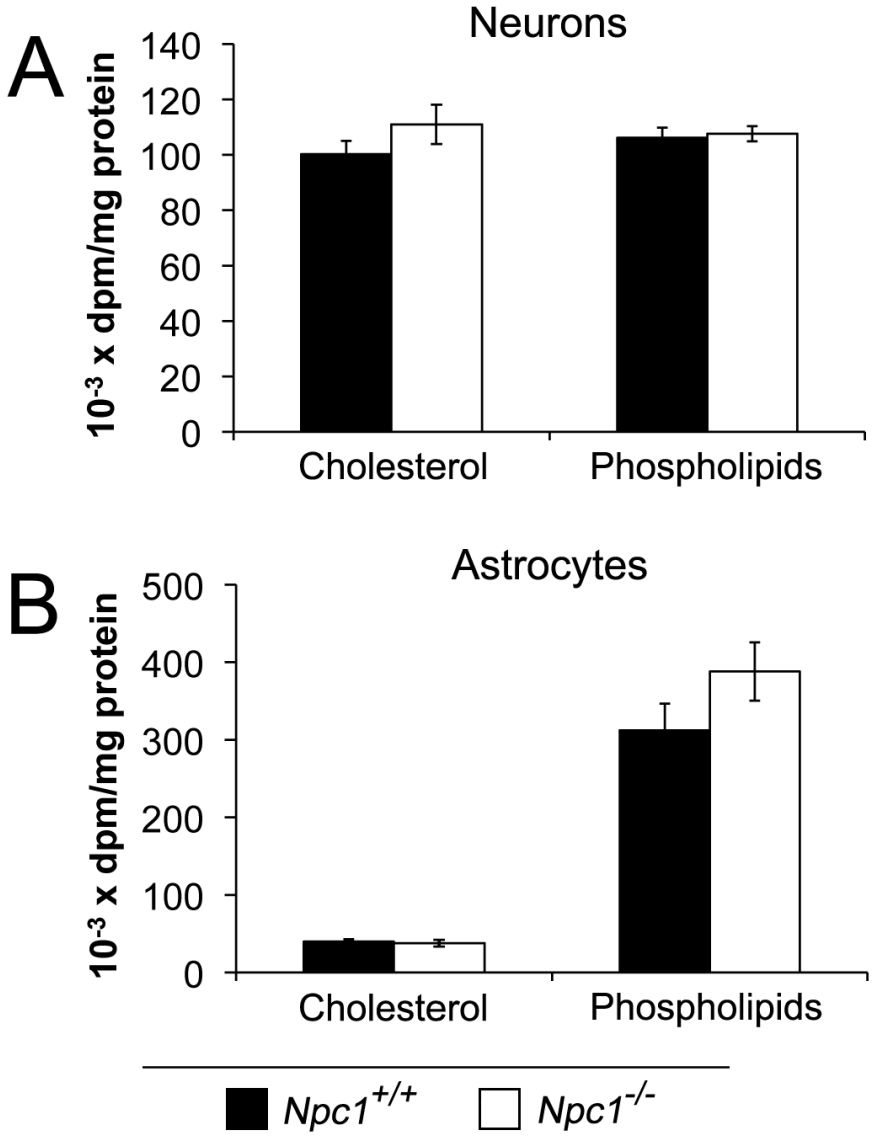


FIGURE 3.25 - **Incorporation of [$^3$H]acetate into newly synthesized cholesterol is the same in *Npc1*$^{-/-}$ and *Npc1*$^{+/+}$ neurons as well as in *Npc1*$^{-/-}$ and *Npc1*$^{+/+}$ astrocytes *in vitro*.** Incorporation of [$^3$H]acetate into newly synthesized cholesterol and phospholipids in cerebellar granule cells (A) and astrocytes (B), isolated from *Npc1*$^{+/+}$ (black bars) and *Npc1*$^{-/-}$ (white bars) mice. Following 24 h treatment with vehicle, cells were incubated an additional 4 h with [$^3$H]acetate, lipids were extracted, separated by thin layer chromatography, and radioactivity was measured in cholesterol and phospholipids. Data for cerebellar granule cells are means from three independent cell preparations performed in duplicate. Data for astrocytes are means from four independent cell preparations. Error bars represent standard error. Data were analyzed using the Student's *t* test.

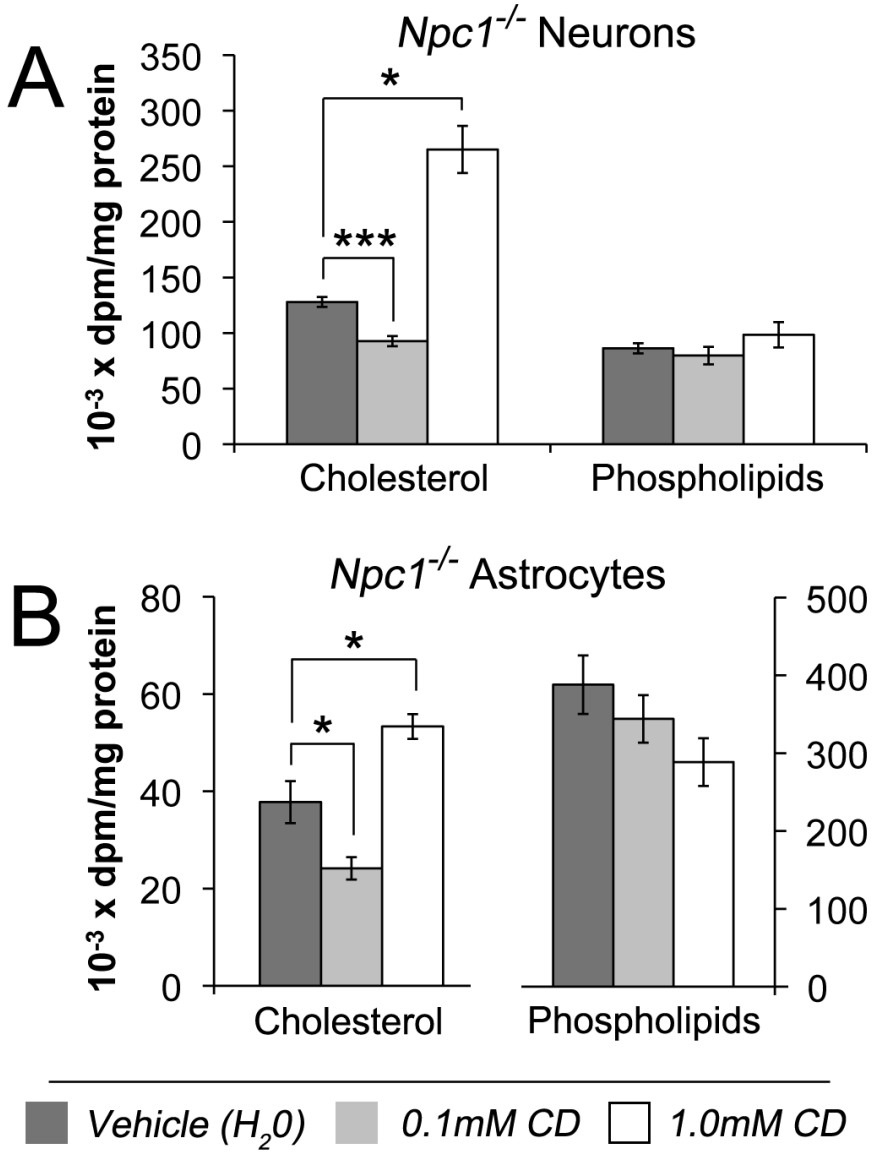


FIGURE 3.26 - **A low dose of HPCD reduces the incorporation of [$^3$H]acetate into cholesterol in *Npc1*$^{-/-}$ neurons and astrocytes *in vitro*.** Incorporation of [$^3$H]acetate into newly synthesized cholesterol and phospholipids in *Npc1*$^{-/-}$ cerebellar granule cells (A) and *Npc1*$^{-/-}$ astrocytes (B) treated for 24 h with vehicle (dark grey bars), 0.1 mM HPCD (light grey bars), or 1.0 mM HPCD (white bars). Following the 24 h treatment, cells were incubated an additional 4 h with [$^3$H]acetate, lipids were extracted, separated by thin layer chromatography, and radioactivity was measured in cholesterol and phospholipids. Data for cerebellar granule cells are means from three independent cell preparations. Data for astrocytes are means from four independent cell preparations. Error bars represent standard error. Data were analyzed using the Student's *t* test (* $p<0.05$; *** $p<0.001$).

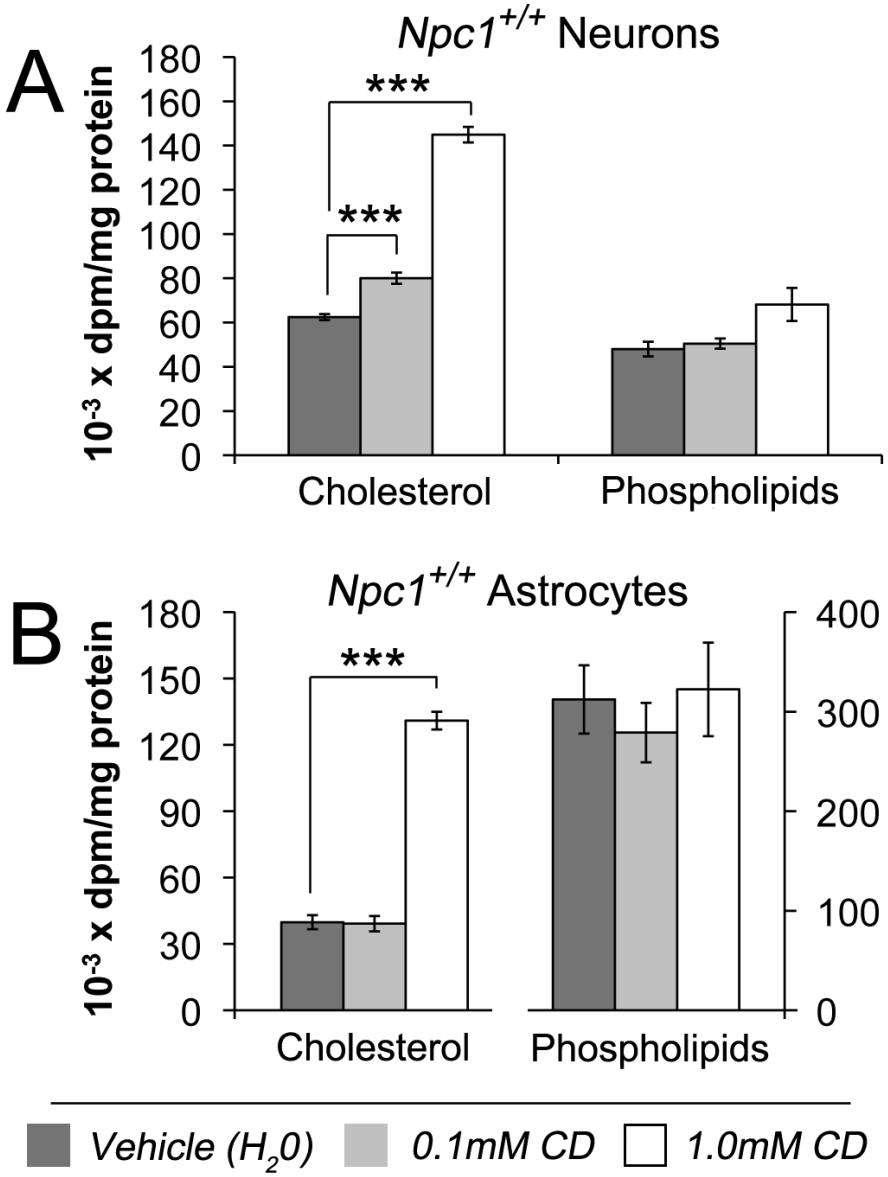


FIGURE 3.27 - **A low dose of HPCD increases the incorporation of [$^3$H]acetate into cholesterol in *Npc1*$^{+/+}$ neurons but not in *Npc1*$^{+/+}$ astrocytes *in vitro*.** Incorporation of [$^3$H]acetate into newly synthesized cholesterol and phospholipids in *Npc1*$^{+/+}$ cerebellar granule cells (A) and *Npc1*$^{+/+}$ astrocytes (B) treated for 24 h with vehicle (dark grey bars), 0.1 mM HPCD (light grey bars), or 1.0 mM HPCD (white bars). Following the 24 h treatment, cells were incubated an additional 4 h with [$^3$H]acetate, lipids were extracted, separated by thin layer chromatography, and radioactivity was measured in cholesterol and phospholipids. Data for cerebellar granule cells are means from three independent cell preparations. Data for astrocytes are means from four independent cell preparations. Error bars represent standard error. Data were analyzed using the Student's *t* test (* $p<0.05$; *** $p<0.001$).

*3.B(iv) A low dose of cyclodextrin increases ACAT-mediated cholesteryl esterification in Npc1$^{-/-}$ astrocytes*

Excess cholesterol that reaches the ER is esterified and stored as CE in a reaction that is catalyzed by the ER protein ACAT [6, 11]. This process is greatly impaired in NPC1-deficient fibroblasts due to cholesterol being trapped in the LE/L. In order to determine whether sequestered cholesterol in *Npc1*$^{-/-}$ neurons and astrocytes was released from the LE/L and became available for esterification by ACAT, cells were given the indicated treatment for 24 h followed by a 4 h incubation with [$^{14}$C]oleate (which gets covalently linked to cholesterol by ACAT), and the incorporation of radiolabel into CE was determined. When *Npc1*$^{-/-}$ astrocytes were treated with 0.1 mM HPCD, there was a significant increase in radiolabeled CE, while 1.0 mM HPCD resulted in a significant decrease in radiolabeled CE, compared to vehicle treatment (Fig. 3.28*A*). In order to ensure that ACAT activity was responsible for catalyzing the CE formation, *Npc1*$^{-/-}$ astrocytes were incubated with the ACAT-specific inhibitor Sandoz 58-035 along with the HPCD. The addition of Sandoz 58-035 greatly attenuated CE formation in *Npc1*$^{-/-}$ astrocytes (Fig. 3.28*A*). Treatment of *Npc1*$^{+/+}$ astrocytes with either 0.1 mM or 1.0 mM HPCD showed no differences in radiolabeled CE compared to vehicle treated controls (Fig. 3.29*A*). There were also no differences in the amount of radiolabel that was incorporated into phospholipids in *Npc1*$^{+/+}$ or *Npc1*$^{-/-}$ astrocytes treated with vehicle, 0.1 mM or 1.0 mM HPCD, suggesting

treatment did not effect the uptake of [$^{14}$C]oleate into the cells and that phospholipid synthesis was not altered by HPCD treatment (Fig. 3.28*B* and 3.29*B*). Moreover, Sandoz 58-035 did not reduce the incorporation of radiolabel into phospholipids (Fig. 3.28*B* and 3.29*B*). These results provide further evidence that cholesterol trapped in the LE/L of NPC1-deficient astrocytes is able to reach the ER, the site of ACAT, following treatment with a low dose of HPCD.

Very little radiolabeled CE was detected with the same assay in *Npc1*$^{-/-}$ CGCs (data not shown) consistent with very low levels of CE in neurons. Recent experiments by Abi-Mosleh *et al.* found the rate of CE formation in *NPC1*$^{-/-}$ human fibroblasts increased for 10 h following HPCD treatment, and subsequently decreased, an effect that was attributed to the depletion of trapped LE/L cholesterol [249]. It is possible that the amount of cholesterol trapped in *Npc1*$^{-/-}$ CGCs is relatively low compared to astrocytes, and thus we were not able to detect CE formation by treating the cultures with HPCD for 24 h prior to adding radiolabel to the culture medium. In subsequent attempts to measure CE formation in CGCs, we incubated the cultures with [$^{14}$C]oleate, alongside either vehicle or 0.1 mM HPCD for 24 h. Regardless of the treatment, however, very little radiolabeled CE was detected in *Npc1*$^{-/-}$ CGCs, with levels of radioactivity approximately equaling background levels measured by the scintillation counter (Fig. 3.30). Additionally, Sandoz 58-035 treatment of *Npc1*$^{-/-}$ CGCs did not reduce the radiolabeling of CE (Fig. 3.30). The

minimal formation of CE in neurons does not appear to be due to NPC1-deficiency, as very little radiolabelled CE was present in *Npc1*$^{+/+}$ CGC cultures (Fig. 3.31). Radiolabel was detectable in phospholipids in both *Npc1*$^{-/-}$ and *Npc1*$^{+/+}$ CGCs, indicating that [$^{14}$C]oleate entered the cells, but CE formation is either very low or absent in these neuron cultures (Fig. 3.30 and 3.31). In support of the conclusion that very little CE synthesis occurs in the neurons, qPCR analysis showed low levels of ACAT1 mRNA in *Npc1*$^{-/-}$ and *Npc1*$^{+/+}$ CGCs compared to that in astrocyte cultures (Fig. 3.32).

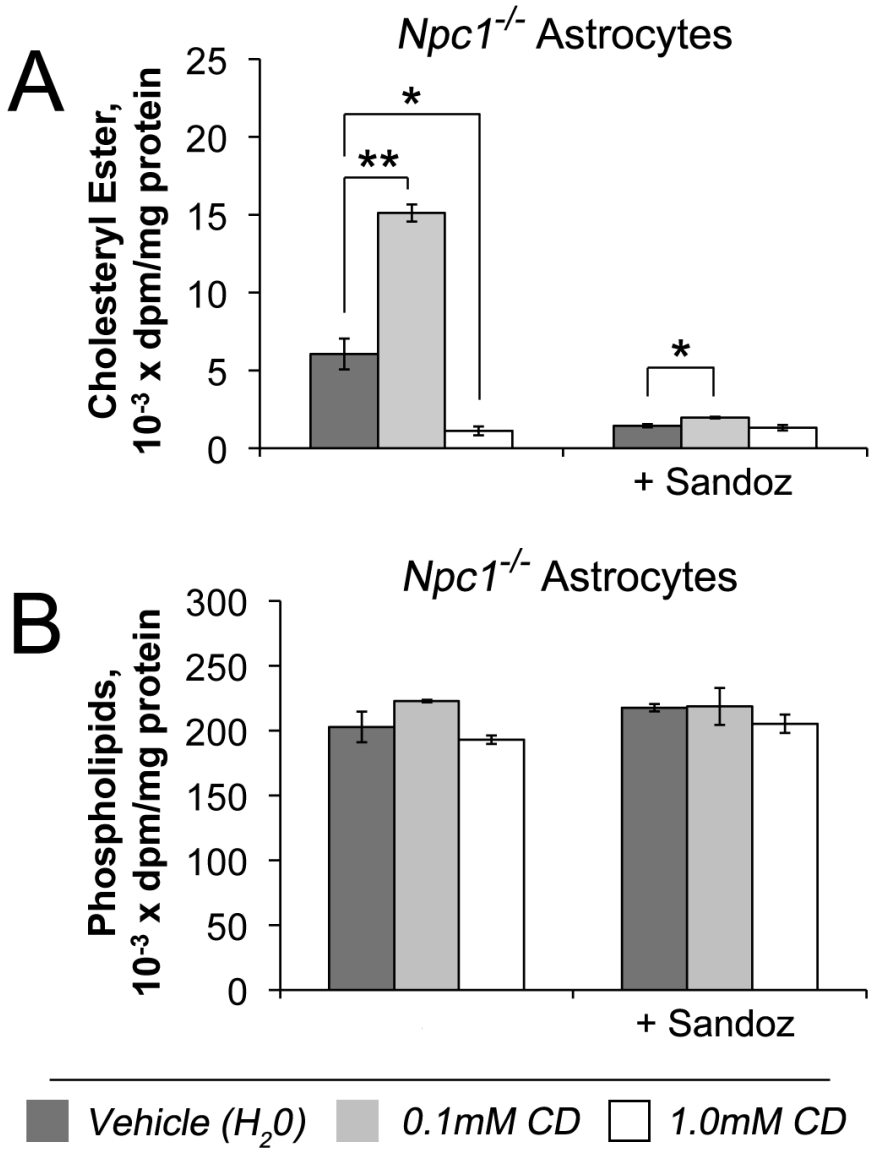


FIGURE 3.28 - **A low dose of HPCD increases the rate of cholesteryl ester formation in *Npc1*$^{-/-}$ astrocytes *in vitro*.** Incorporation of [$^{14}$C]oleate into newly formed cholesteryl esters (A) and phospholipids (B) in *Npc1*$^{-/-}$ astrocytes treated for 24 h with vehicle (dark grey bars), 0.1 mM HPCD (light grey bars), or 1.0 mM HPCD (white bars). Following the 24 h treatment, cells were incubated an additional 4 h with [$^{14}$C]oleate in the presence or absence of the ACAT inhibitor Sandoz 58-035, lipids were extracted, separated by thin layer chromatography, and radioactivity was measured in cholesteryl esters and phospholipids. Data are means from three independent cell preparations. Error bars represent standard error. Data was analyzed using the Student's *t* test (* $p<0.05$; ** $p<0.01$).

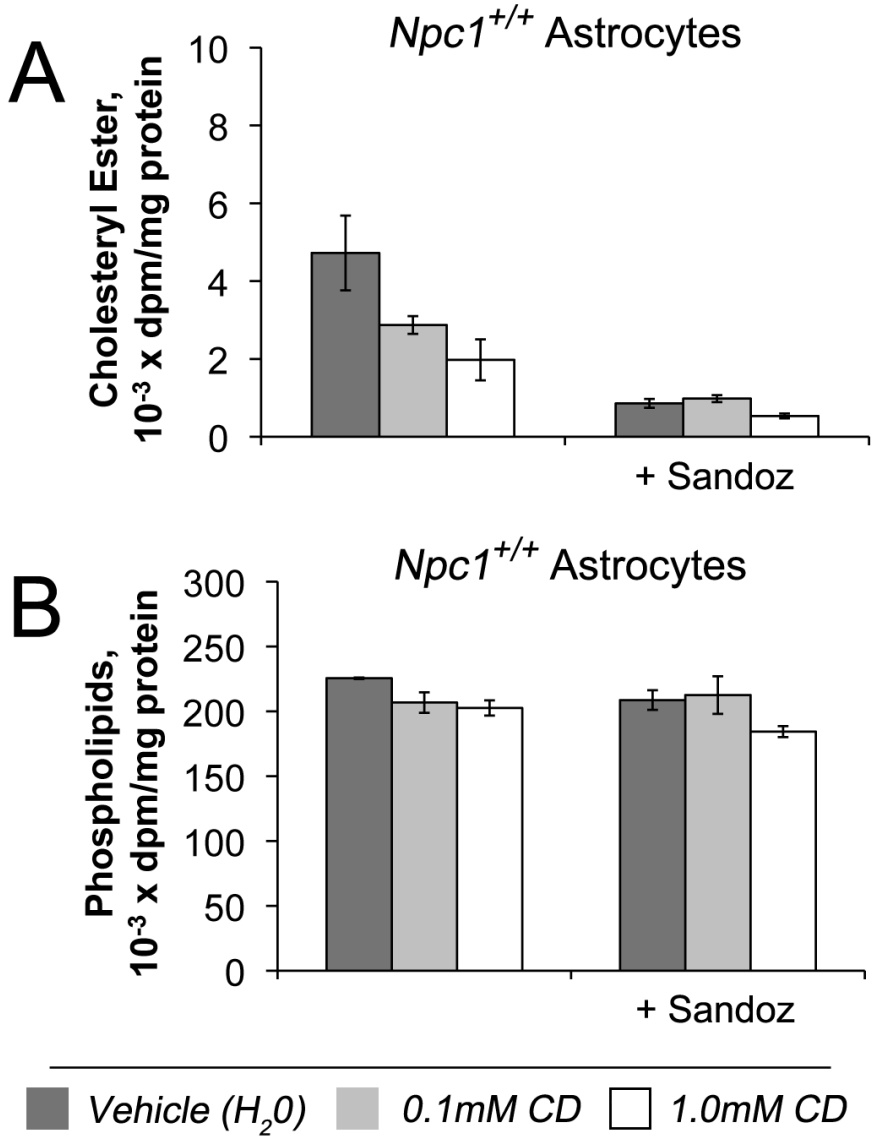


FIGURE 3.29 - **A low dose of HPCD does not increase the rate of cholesteryl ester formation in *Npc1*$^{+/+}$ astrocytes *in vitro*.** Incorporation of [$^{14}$C]oleate into newly formed cholesteryl esters (A) and phospholipids (B) in *Npc1*$^{+/+}$ astrocytes treated for 24 h with vehicle (dark grey bars), 0.1 mM HPCD (light grey bars), or 1.0 mM HPCD (white bars). Following the 24 h treatment, cells were incubated an additional 4 h with [$^{14}$C]oleate in the presence or absence of the ACAT inhibitor Sandoz 58-035, lipids were extracted, separated by thin layer chromatography, and radioactivity was measured in cholesteryl esters and phospholipids. Data are means from three independent cell preparations. Error bars represent standard error. Data were analyzed using the Student's *t* test.

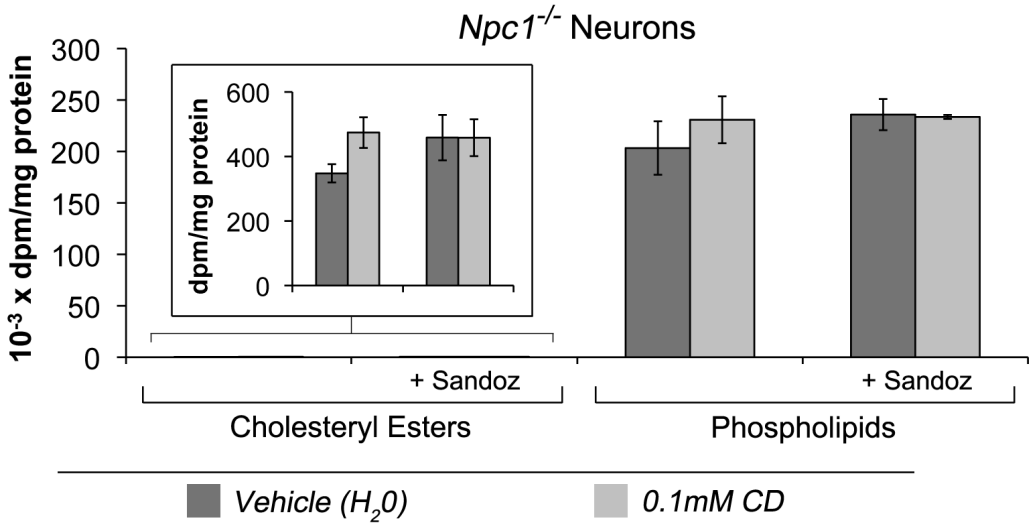


FIGURE 3.30 - **Rate of cholesteryl ester formation is very low in *Npc1*$^{-/-}$ neurons *in vitro*.** Incorporation of [$^{14}$C]oleate into newly formed cholesteryl esters and phospholipids in *Npc1*$^{-/-}$ cerebellar granule cells treated with vehicle (dark grey bars) or 0.1 mM HPCD (light grey bars). Cells were incubated 24 h with the indicated treatment and [$^{14}$C]oleate in the presence or absence of the ACAT inhibitor Sandoz 58-035, lipids were extracted, separated by thin layer chromatography, and radioactivity was measured in cholesteryl esters and phospholipids. Data are means from three independent cell preparations. Error bars represent standard error. Data were analyzed using the Student's *t* test.

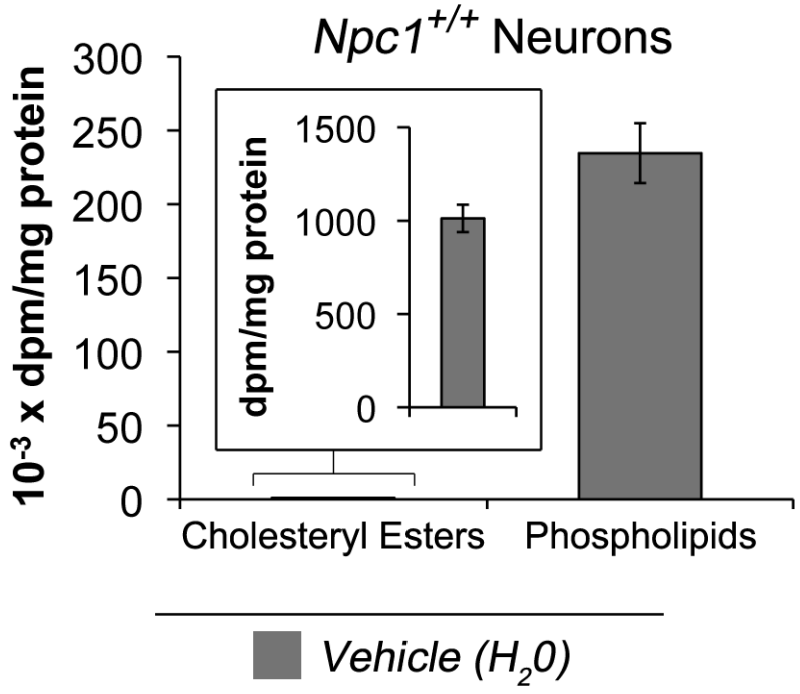


FIGURE 3.31 - **Rate of cholesteryl ester formation is very low in *Npc1*$^{+/+}$ neurons *in vitro*.** Incorporation of [$^{14}$C]oleate into newly formed cholesteryl esters and phospholipids in *Npc1*$^{+/+}$ cerebellar granule cells treated with vehicle (dark grey bars). Cells were incubated 24 h with the indicated treatment and [$^{14}$C]oleate, lipids were extracted, separated by thin layer chromatography, and radioactivity was measured in cholesteryl esters and phospholipids. Data are means from three independent cell preparations. Error bars represent standard error.

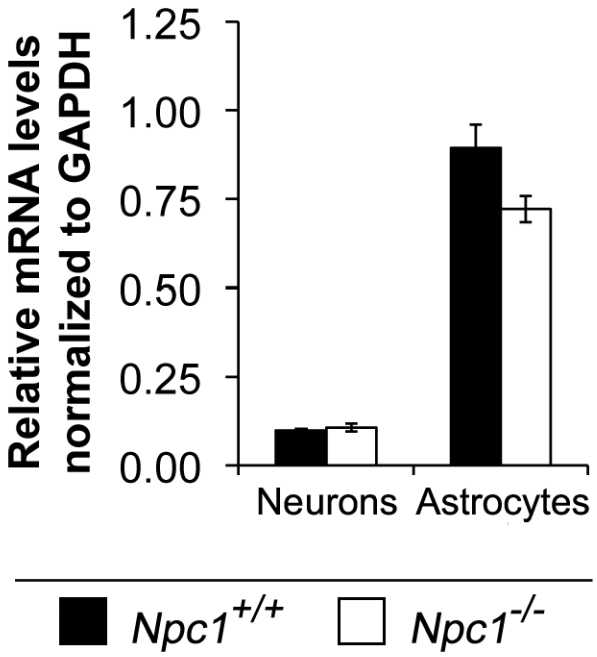


FIGURE 3.32 – **ACAT1 mRNA levels are lower in cultured *Npc1*$^{+/+}$ and *Npc1*$^{-/-}$ neurons than in *Npc1*$^{+/+}$ and *Npc1*$^{-/-}$ astrocytes.** Quantitative real-time PCR analysis of ACAT1 mRNA in *Npc1*$^{+/+}$ (black bars) and *Npc1*$^{-/-}$ (white bars) cerebellar granule cells and astrocytes treated for 24 h with vehicle. Data are means from three independent cell preparations analyzed in duplicate and normalized to GAPDH mRNA. Error bars represent standard error.

*3.B(v) A low dose of cyclodextrin decreases expression of genes involved in cholesterol synthesis in Npc1*$^{-/-}$ *neurons and increases expression of genes involved in cholesterol efflux in Npc1*$^{-/-}$ *astrocytes*

At the transcript level, cells differentially regulate the expression of a variety of genes in response to alterations in cellular cholesterol levels. For instance, when cholesterol levels increase, genes involved in cholesterol synthesis and uptake, including the transcription factor SREBP2 and its target genes HMGCR and LDLR, are normally

decreased, while genes involved in cholesterol efflux, such as the LXR target genes ABCA1 and ABCG1, are increased. Conversely, if cholesterol were depleted from cells, the opposite response would occur, with expression of genes involved in cholesterol synthesis and uptake being increased, while those involved in cholesterol efflux decreased. To investigate these changes in response to HPCD treatments in *Npc1*$^{-/-}$ CGC and astrocyte cultures, we used qPCR analysis. *Npc1*$^{-/-}$ CGCs treated with 0.1 mM HPCD had significantly lower levels of mRNAs encoding both SREBP2 and its target gene HMGCR compared to vehicle treated cultures (Fig. 3.33*A*). Treatment of *Npc1*$^{-/-}$ CGCs with 0.1 mM HPCD resulted in no changes in LDLR, ABCA1, or ABCG1 mRNA levels compared to vehicle treatment (Fig. 3.33*A*). When *Npc1*$^{-/-}$ CGCs were incubated with the higher dose of 1.0 mM HPCD, there was a large increase in SREBP2, HMGCR and LDLR mRNAs, while ABCA1 and ABCG1 mRNAs were significantly lower than for vehicle treatment (Fig. 3.33*A*). Importantly, 0.1 mM HPCD had no effect on genes involved in cholesterol synthesis, uptake, or efflux in *Npc1*$^{+/+}$ CGCs (Fig. 3.33*B*). Treatment of *Npc1*$^{+/+}$ CGCs with 1.0 mM HPCD had similar effects to those in *Npc1*$^{-/-}$ CGCs, so that SREBP2 mRNA, and mRNAs encoding its target genes, were dramatically increased while mRNAs encoding ABCA1 and ABCG1 were significantly decreased (Fig. 3.33*B*). These results correlate with the changes in incorporation of [$^{3}$H]acetate into cholesterol mediated by HPCD treatment (Fig. 3.26 and 3.27).

In contrast, treatment of *Npc1*$^{-/-}$ astrocytes with 0.1 mM HPCD did not change the amount of SREBP2 mRNA or its target genes, but did significantly increase mRNAs encoding both ABCA1 and ABCG1 compared to vehicle (Fig. 3.34*A*). Treatment of *Npc1*$^{-/-}$ astrocytes with 1.0 mM HPCD increased SREBP2 and HMGCR mRNAs, but had no effect on LDLR, ABCA1, or ABCG1 (Fig. 3.34*A*). *Npc1*$^{+/+}$ astrocytes treated with 0.1 mM HPCD showed no differences in levels of mRNAs encoding SREBP2, HMGCR, LDLR, ABCA1, or ABCG1 compared to vehicle treatment (Fig. 3.34*B*). While 1.0 mM HPCD treatment of *Npc1*$^{+/+}$ astrocytes had no effect on mRNA levels of SREBP2 or its targets, mRNAs encoding ABCA1 and ABCG1 were decreased compared to vehicle treatment (Fig. 3.34*B*). Taken together, these results suggest that *Npc1*$^{-/-}$ neurons may be responding to the liberated cholesterol by decreasing cholesterol synthesis, while *Npc1*$^{-/-}$ astrocytes appear to respond by increasing cholesterol efflux. Thus, the decrease in [$^{3}$H]acetate incorporation into cholesterol in 0.1 mM HPCD-treated *Npc1*$^{-/-}$ astrocytes may be a response to increased efflux rather than decreased cholesterol synthesis. Furthermore, 1.0 mM HPCD appears to be depleting neurons and astrocytes of cholesterol, presumably by extracting cholesterol from the plasma membrane, leading to increases in expression of genes involved in cholesterol synthesis and/or decreases in genes involved in cholesterol efflux.

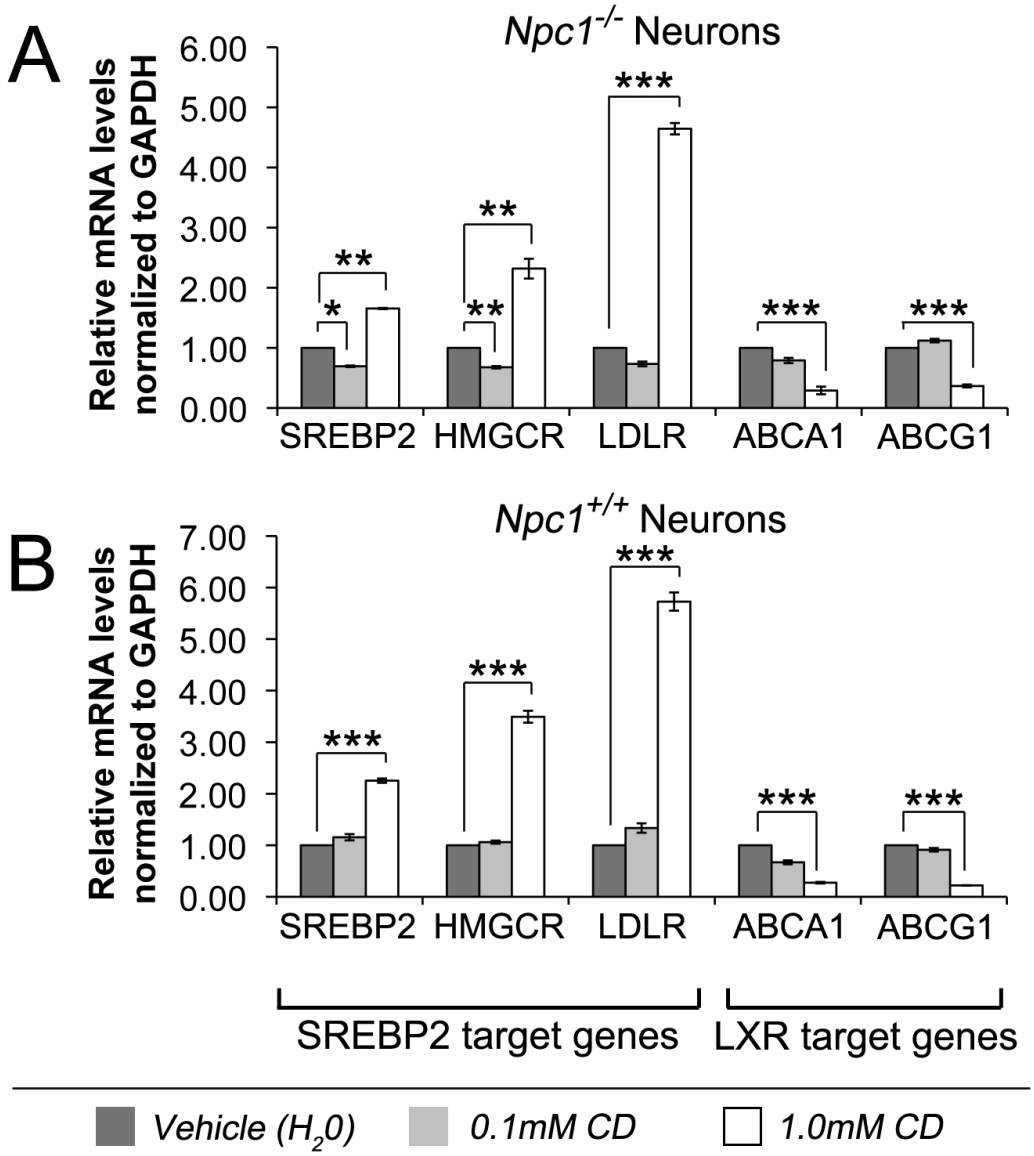


FIGURE 3.33 - **A low dose of HPCD decreases mRNAs encoded by genes involved in cholesterol synthesis in *Npc1*$^{-/-}$ neurons *in vitro*.** Quantitative real-time PCR analysis of genes involved in cholesterol metabolism in *Npc1*$^{-/-}$ cerebellar granule cells (A) and *Npc1*$^{+/+}$ cerebellar granule cells (B) treated for 24 h with vehicle (dark grey bars), 0.1 mM HPCD (light grey bars), or 1.0 mM HPCD (white bars). Results are normalized to levels of GAPDH mRNA. Data for 0.1 mM HPCD v. vehicle are means from three independent cell preparations performed in duplicate. Data for 1.0 mM HPCD v. vehicle in *Npc1*$^{-/-}$ cerebellar granule cells are means from two independent cell preparations analyzed in triplicate. Data for 1.0 mM HPCD v. vehicle in *Npc1*$^{+/+}$ cerebellar granule cells are means from three independent experiments analyzed in triplicate. Error bars represent standard error. Data were analyzed using the Student's *t* test (* $p<0.05$; ** $p<0.01$; ***$p<0.001$).

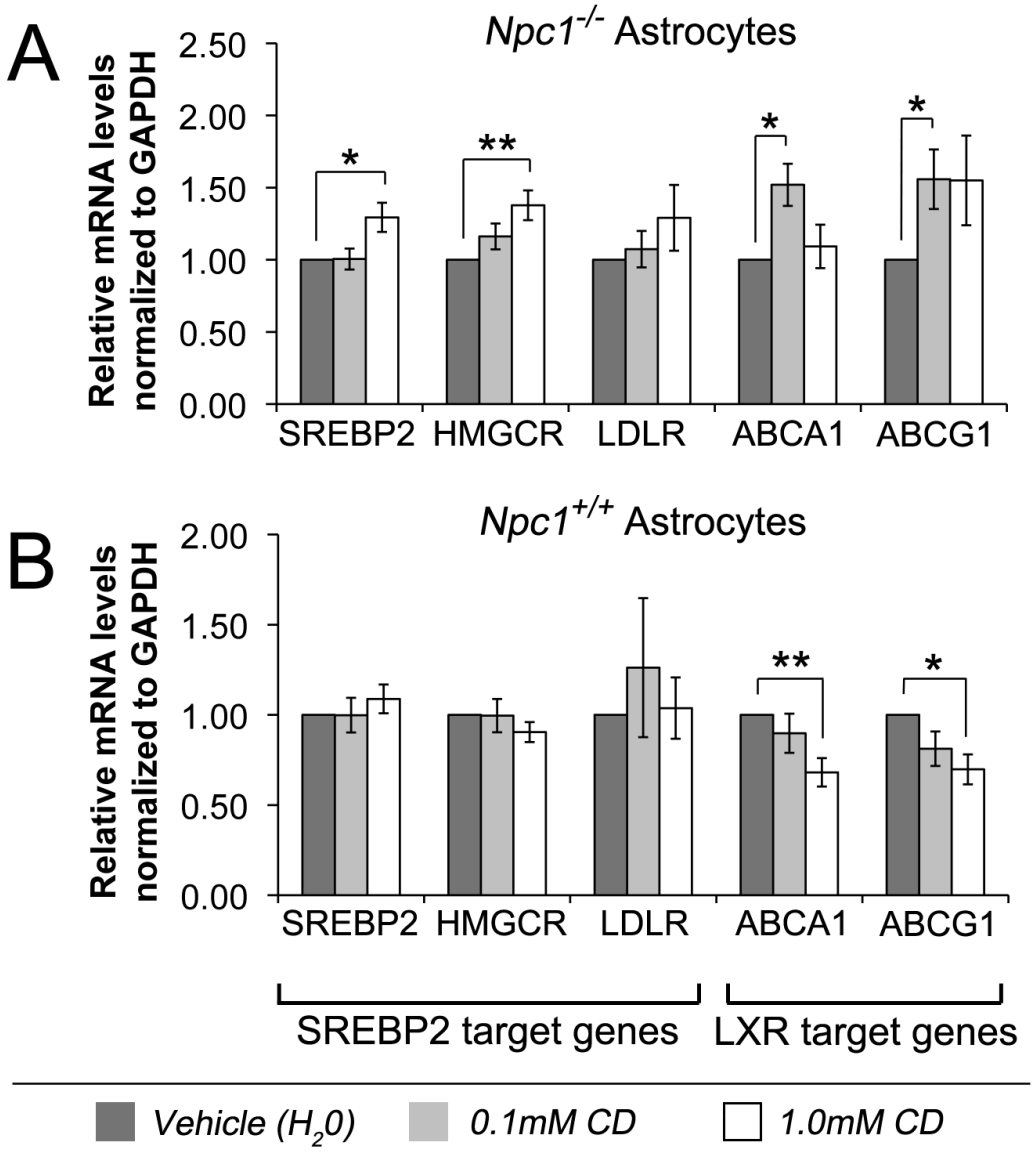


FIGURE 3.34 - **A low dose of HPCD increases mRNAs encoded by genes involved in cholesterol efflux in *Npc1*$^{-/-}$ astrocytes *in vitro*.** Quantitative real-time PCR analysis of genes involved in cholesterol metabolism in *Npc1*$^{-/-}$ astrocytes (A) and *Npc1*$^{+/+}$ astrocytes (B) treated for 24 h with vehicle (dark grey bars), 0.1 mM HPCD (light grey bars), or 1.0 mM HPCD (white bars). Results are normalized to levels of GAPDH mRNA. Data for 0.1 mM HPCD v. vehicle are means from three independent cell preparations analyzed in duplicate, whereas data for 1.0 mM HPCD v. vehicle are means from three independent experiments analyzed in triplicate. Error bars represent standard error. Data were analyzed using the Student's *t* test (* $p<0.05$; ** $p<0.01$).

# 4. DISCUSSION

## *4.A ROLE OF MICROGLIA IN NPC DISEASE*

Microglia are the resident immune cells of the CNS, which upon activation can secrete potentially neurotoxic molecules such as TNFα [181]. Inappropriate activation of microglia has been implicated in several neurodegenerative disorders including NPC disease [170, 174, 212]. However, it remains unclear whether *Npc1*$^{-/-}$ microglia initiate neuron death, or whether microglia are becoming activated in response to cell death and dysfunction in the NPC brain. Moreover, it is unclear whether the profound increase in active microglia in the *Npc1*$^{-/-}$ mouse brain actually contributes to neurodegeneration, or if it is a response to prevent the progressive neuron death seen in NPC disease. Consistent with the findings of other groups, our immunohistochemical analysis showed active microglia accumulate in the *Npc1*$^{-/-}$ mouse brain. To further investigate microglia in NPC disease, primary microglial cultures were prepared from the cerebral cortex of *Npc1*$^{-/-}$ mice. *Npc1*$^{-/-}$ microglia have an altered morphology, appearing to be slightly larger than *Npc1*$^{+/+}$ microglia. Filipin staining of unesterified cholesterol showed that NPC1-deficient microglia have an altered cholesterol distribution characteristic of NPC-deficient cells. Additionally, treatment of wild-type microglia with U18666A, a compound which mimics the cholesterol accumulation in NPC disease, caused microglia to assume an activated morphology. Taken together, these results suggest that cholesterol accumulation might activate

microglia, which in turn could lead to increased secretion of potentially toxic molecules such as TNFα. In support of this idea, immunocytochemical analysis of *Npc1*$^{-/-}$ microglia cultures revealed increased staining for TNFα and TNFR1. However, TNFα levels were not increased in the medium of *Npc1*$^{-/-}$ microglia cultures when compared to *Npc1*$^{+/+}$ controls. Moreover, qPCR analysis did not reveal any differences in pro-inflammatory or oxidative stress genes between *Npc1*$^{+/+}$ and *Npc1*$^{-/-}$ microglia, although *Npc1*$^{-/-}$ microglia did show a signifcant decrease in IL10 mRNA, an anti-inflammatory cytokine. To determine whether *Npc1*$^{-/-}$ microglia contribute to neuron death in NPC disease, microglia were cultured directly with CGCs. Surprisingly, there were no differences in the amount of neuronal death between neurons cultured with *Npc1*$^{+/+}$ or *Npc1*$^{-/-}$ microglia. Thus, *Npc1*$^{-/-}$ microglia have an altered phenotype compared to *Npc1*$^{+/+}$ microglia, but this does not lead to neuron death in the *in vitro* co-culture system.

*4.A(i) Accumulation of active microglia in the NPC1-deficient brain*

Although activated microglia accumulate extensively in both the *Npc1*$^{-/-}$ mouse cortex and cerebellum compared to *Npc1*$^{+/+}$ controls, it remains to be determined what is leading to this microglial response. In a healthy brain, microglia play a key role in maintaining tissue integrity, and upon detection of damage or dysfunction in the brain environment, can become highly activated [184-186]. It seems most likely that microglia are becoming activated due to cellular death and dysfunction in the *Npc1*$^{-/-}$

mouse brain. However, Baudry *et al.* found microglia with an active morphology in the *Npc1*$^{-/-}$ mouse brain prior to any detectable neurodegeneration, suggesting NPC1 deficiency in microglia might autonomously lead to microglial activation [170]. This activation may be due to accumulation of cholesterol and other lipids within the LE/L, or altered vesicular trafficking within *Npc1*$^{-/-}$ microglia. Along these lines, we found that primary *Npc1*$^{-/-}$ microglia had an altered cholesterol distribution and morphology, as well as increased immunostaining for TNFα. Conversely, *Npc1*$^{-/-}$ microglia did not have increased levels of mRNAs encoding pro-inflammatory cytokine or oxidative stress proteins, and were unable to induce neuron death in neuron-microglia co-cultures. Therefore, *Npc1*$^{-/-}$ microglia do show alterations that may lead to their activation in the *Npc1*$^{-/-}$ mouse brain, though it is also quite possible that microglia are being activated in the *Npc1*$^{-/-}$ mouse brain by neuron death that the methods employed by Baudry *et al.* were not sensitive enough to detect [170]. As well, there could be neuronal dysfunction, or damage, that is leading to activation of microglia in the young *Npc1*$^{-/-}$ mouse brain. Furthermore, microglia may be activated in response to dysfunction or death of other brain cells. For instance, degeneration of oligodendrocytes could lead to microglial activation, particularly since progressive demyelination is seen early during the course of NPC disease [143, 174].

Another possibility, though less likely, is that microglia are becoming active in the brain due to events occurring in the peripheral

tissues. For instance, some evidence suggests that inflammation in the liver can lead to activation of microglia in the CNS [266]. Furthermore, several studies have found that feeding rabbits a cholesterol-enriched diet leads to increased activation of microglia within the brain [267, 268]. Since peripheral cholesterol does not cross the BBB and enter into the CNS, this implies that changes peripheral to the brain are responsible for these effects. Pro-inflammatory cytokines including TNFα and IL1β have been shown to cross the BBB through a saturable mechanism [269, 270]. Although *in vitro* evidence suggests these cytokines could damage the BBB [271], experiments performed in mice found that under these conditions the BBB remained intact [269, 270]. Thus, inflammation in peripheral tissues may be able to effect microglia through cytokines that are transported from the circulation into the CNS. As NPC disease shows liver damage and altered cholesterol metabolism in peripheral tissues [138, 139], we cannot rule out the possibility that these effects in the periphery contribute to microglial activation seen in the *Npc1*$^{-/-}$ mouse brain.

Recent evidence suggests that macrophages and other immune cells may be able to cross the BBB, particularly in states of disease and inflammation. Initial studies proposing this phenomenon used chimeric mice that had received a bone marrow transplantation with labeled donor cells [272-275]. These results were confounded by the fact that whole body irradiation was used in order to generate the chimeric mice, a

process which could damage the BBB and alter the CNS. Thus, it was difficult to determine if the macrophages seen infiltrating the CNS of these chimeric mice would enter the brain in a healthy mouse, or if the influx of these macrophages into the CNS was due to the irradiation treatment. In studies using non-irradiated parabiotic mice, the number of macrophages detected in the brain was dramatically reduced compared to irradiated studies [276]. Moreover, it has been shown that whole body irradiation can drastically alter gene expression in the mouse CNS, leading to increased production of chemokines and cytokines such as TNFα [277]. In order to determine if macrophages could infiltrate the brain independently of irradiation of the CNS, Mildner *et al.* generated chimeric mice containing fluorescently labeled macrophages, using targeted irradiation that excluded the brain [277]. Not only did this procedure prevent chemokine and cytokine induction in the brain, it also eliminated the infiltration of donor-derived macrophages into the brain [277]. The authors performed similar experiments in mouse models which had CNS damage, but retained an intact BBB. In mice with cuprizone-induced demyelination in the corpus callosum, and in mice subjected to unilateral facial nerve axotomy, donor-derived macrophages were unable to infiltrate the brain, unless it had been irradiated [277]. Other studies suggest that macrophages are recruited into the CNS during periods of inflammation through a chemokine-dependent mechanism [266]. Macrophages that had infiltrated the CNS were identified based on CD45 expression using

flow cytometry, with macrophages being defined as $CD45^{high}$-expressing cells and microglia being defined as $CD45^{low}$-expressing cells [266]. This type of classification has been used by other groups [278-280]. However, controversy exists over the validity of this marker, as microglia are highly plastic cells from the monocytic lineage, and it remains a possibility that activating stimuli could lead to increased CD45 expression in activated microglia. Thus, there is still debate as to whether macrophages do indeed infiltrate the CNS during disease or inflammation. Even so, since Iba1 is expressed in both microglia and macrophages [281, 282], it remains a distinct possibility that the increase in Iba1-positive cells could be, at least in part, due to infiltrating macrophages.

*4.A(ii) Consequences of altered cholesterol metabolism in microglia*

Alterations in cholesterol metabolism have been found to impact microglia and macrophage function. Conflicting reports exist regarding the effects that statins (inhibitors of HMGCR) have on microglia function. The majority of reports indicate that inhibition of the cholesterol synthesis pathway attenuates the activation of cultured microglia in response to stimuli such as the bacterial endotoxin lipopolysaccharide (LPS), interferon-γ, and β-amyloid [283-285]. Furthermore, statins administered to rats decreased both age-related and LPS-induced microglial activation [286]. Interestingly, the inhibition of microglial activation did not appear to be due to decreases in cholesterol levels, as cholesterol supplementation was not sufficient to prevent these effects [283, 285]. Instead, it appears

that statins decrease microglial activation by decreasing the synthesis of non-steroid isoprenoids, which are synthesized from intermediates in the cholesterol biosynthetic pathway [283, 285]. Isoprenoids can be covalently linked to proteins in a process termed prenylation. This post-translational lipid modification effects protein function and localization [287]. Other evidence suggests statins may have negative effects on microglial function as well. For instance, statins have been shown to alter the actin cytoskeleton in microglia, and to abolish chemokine-induced microglia motility [288]. Such effects could impair microglial functions that are necessary for maintaining brain tissue integrity. Moreover, the administration of statins to hippocampal slice cultures isolated from rats increased microglial activation in a time- and concentration-dependent manner [289]. However, it is possible microglia are becoming activated due to the effect of statins on other cells present in the slice cultures, such as neurons and astrocytes, rather than direct effects of statins on microglia. Taken together, these results suggest that altering the cholesterol biosynthetic pathway can affect microglial function, particularly by altering protein prenylation.

As a consequence of cholesterol being trapped within LE/Ls and not reaching the ER where regulation of cholesterol homeostasis occurs, NPC1-deficient fibroblasts increase cholesterol biosynthesis [79]. The increase in cholesterol synthesis, and flux through the mevalonate pathway, could also increase isoprenoid synthesis. As decreased

isoprenoid synthesis has been implicated in attenuating microglial activation [283-285], it is possible that increased isoprenoid levels may render *Npc1*$^{-/-}$ microglia more susceptible to activating stimuli. Conversely, if the cell is depleted of cholesterol due to the impaired trafficking of cholesterol from LE/Ls, the cell may preferentially synthesize cholesterol and minimize the amount of cholesterol precursors being shunted out of the cholesterol biosynthetic pathway for isoprenoid synthesis. This could decrease microglia activation, but may also affect microglia motility and the ability of microglia to generate an appropriate inflammatory response [288]. Although *Npc1*$^{-/-}$ microglia show an altered cholesterol distribution, it is unclear how cholesterol synthesis is affected in *Npc1*$^{-/-}$ microglia. Despite the finding that other NPC1-deficient cells have increased cholesterol biosynthesis, the NPC1-deficient mouse brain shows similar levels of cholesterol synthesis to wild-type brains [246]. Moreover, our results demonstrate that cholesterol synthesis in *Npc1*$^{-/-}$ neurons and astrocytes is identical to that in *Npc1*$^{+/+}$ controls. Therefore, cholesterol synthesis in *Npc1*$^{-/-}$ microglia may not be altered, but still needs to be investigated.

In order to investigate the effects that altered cholesterol trafficking could have on microglia, we initially used the amphipathic amine U18666A in order to induce an NPC-like phenotype in microglia. Vehicle treated microglia predominantly displayed ameboid and ramified morphologies, while U18666A caused most cells to have a dramatic and rapid shift to a

spherical, active morphology. While it is tempting to conclude that accumulation of cholesterol within the LE/L results in activation of microglia, U18666A has additional effects alongside its ability to impair cholesterol trafficking out of the LE/L. Particularly, U18666A inhibits several enzymes in the cholesterol synthesis pathway [102, 103]. Thus, it is entirely possible that inhibition of cholesterol synthesis, rather than the impairment of cholesterol trafficking through the endosomal system, leads to alterations in microglia morphology. Interestingly, Kuipers *et al.* found that inhibition of cholesterol synthesis using simvastatin dramatically altered actin distribution, causing microglia cells to "round up" [288]. Moreover, when we cultured *Npc1*$^{-/-}$ microglia we did not see the same drastic change in morphology as we observed with U18666A treatment. Instead, primary *Npc1*$^{-/-}$ microglia appeared, for the most part, similar to *Npc1*$^{+/+}$ microglia. Thus, these results support the idea that U18666A alters microglia morphology by impairing the cholesterol biosynthetic pathway. Nonetheless, *Npc1*$^{-/-}$ microglia did appear to be larger than *Npc1*$^{+/+}$ microglia although the significance of this observation is not known. Furthermore, U18666A treatment of macrophages increases TNFα production and impairs phagosome maturation [290, 291]. Although these studies failed to determine if the effects were caused by cholesterol accumulation, such results suggest that alteration of endosomal cholesterol trafficking, as well as cholesterol metabolism, may lead to altered microglial function and behavior. Thus, to determine if NPC1

deficiency in microglia altered microglia function, we began to characterize further the properties of microglia isolated from *Npc1*$^{+/+}$ and *Npc1*$^{-/-}$ mice.

*4.A(iii) Increased TNFα in NPC1-deficient microglia*

Microglia are considered to be the major source of TNFα in the CNS [261]. We performed several different experiments to investigate TNFα in *Npc1*$^{-/-}$ microglia, since TNFα is often associated with inflammation-mediated death, and increased levels of mRNAs encoding TNFα (and other genes involved in the TNFα death pathway) have been detected in the *Npc1*$^{-/-}$ mouse brain [159]. Moreover, TNFα has been implicated in NPC liver disease, as apoptosis seen in NPC1-knockdown mouse livers was attenuated through elimination of TNFα by genetic manipulation, or through use of anti-TNFα antibodies [292]. TNFα is a pro-inflammatory cytokine that exists in a soluble, as well as a membrane-bound form, both of which are biologically active [293]. The actions of TNFα are complex, with TNFα being linked to beneficial, pro-survival effects, and also detrimental, cytotoxic consequences [294-296]. These actions depend on a number of factors including the stimulus inducing TNFα production, the concentration of TNFα, the length of TNFα exposure, as well as other molecules present during TNFα exposure [295, 296]. Moreover, TNFα exerts its effects through two different receptors, TNFR1 and TNFR2. TNFR2 preferably binds membrane-bound TNFα and is generally associated with pro-survival effects of TNFα [297]. On the other hand, TNFR1 preferentially binds soluble TNFα and is thought to be

primarily involved in TNFα-mediated death due to the presence of a death domain in its cytoplasmic tail [298, 299]. However, TNFR1 signaling is complex, and TNFα signaling through TNFR1 can also lead to anti-apoptotic effects [294, 300]. It has been proposed that these opposing outcomes may be regulated through compartmentalization of TNFR1 signaling [300, 301]. In this model, the initial binding of TNFα to TNFR1 results in the recruitment of TNFR-associated death domain, TNFR-associated factor-2, and receptor-interacting protein-1, which can lead to the activation of the survival transcription factor, nuclear factor-κB [300-304]. Within minutes of TNFα binding to TNFR1, the complex is internalized through clathrin-dependent endocytosis [300, 301]. This results in the termination of nuclear factor-κB signaling, and the recruitment of FAS-associated death domain protein and caspase-8, ultimately leading to apoptosis [300, 301]. Thus, while TNFα is often associated with inducing cell death, the actions of TNFα are complex and can be regulated through a variety of mechanisms.

We initially performed immunocytochemical staining for TNFα in primary microglia cultures and found TNFα staining was profoundly increased in *Npc1*$^{-/-}$ microglia compared to *Npc1*$^{+/+}$ microglia. Surprisingly, however, there were no differences in the amount of TNFα mRNA or in the amount of TNFα secreted by *Npc1*$^{-/-}$ microglia compared to *Npc1*$^{+/+}$ microglia. Other than mast cells, immune cells do not appear to store preformed TNFα [305, 306]. Instead, upon activation, cells such as

macrophages and microglia synthesize TNFα, which is initially in a membrane-bound form [307]. Membrane-bound TNFα is trafficked to the plasma membrane via the Golgi apparatus, where it can be cleaved by TNFα-converting enzyme (TACE), releasing mature, soluble TNFα from the cell [307-310]. Following activation, the majority of TNFα is located in the Golgi apparatus, and only transiently appears on the plasma membrane [311]. The amount of TNFα in the Golgi apparatus decreases at a rate that correlates with the release of cleaved TNFα from the cell, suggesting that TACE catalyzes a rate-limiting step in secretion of mature TNFα from the cell [311]. Recent evidence also suggests TNFα can be secreted from cells via secretory lysosomes [312], a special class of lysosome found in immune cells [313], and that have been implicated in the secretion of other cytokines such as IL1β [314].

What is leading to increased TNFα immunostaining in *Npc1*$^{-/-}$ microglia remains to be determined, although several possibilities exist. Most obviously, *Npc1*$^{-/-}$ microglia may be activated, and thus are producing more TNFα. This seems unlikely, as we do not see increased TNFα mRNA or secretion. Moreover, we did not see increases in the mRNA levels of other pro-inflammatory genes such as IL1β or any oxidative stress genes. Another possibility is that movement of TNFα out of *Npc1*$^{-/-}$ microglia is impaired. This is conceivable, as vesicular trafficking is impaired in NPC1-deficient cells [127, 128, 131], and as a result TNFα may become trapped within the endosomal compartment of *Npc1*$^{-/-}$

microglia. TNFα is trafficked from the Golgi apparatus to recycling endosomes, which subsequently fuse with the plasma membrane and release TNFα from the cell [308, 311]. Rab4 is a small GTPase that is involved in endocytic recycling to the plasma membrane, and has been shown to partially co-localize with the *trans*-Golgi network as well as with TNFα [312]. In NPC1-deficient cells, Rab4-mediated recycling of lipids and proteins is impaired [128]. Therefore, it is possible that vesicular trafficking of TNFα through this pathway is impaired in *Npc1*$^{-/-}$ microglia, resulting in accumulation of TNFα in the cell. Furthermore, accumulation of cholesterol in the LE/L of *Npc1*$^{-/-}$ microglia may inhibit the trafficking of secretory lysosomes to the cell surface where they would release TNFα. Other vesicle-mediated processes are also impaired in NPC1-deficient cells, including retrograde fusion of lysosomes and late endosomes, as well as the retrograde release of molecules such as sucrose and dextran [85, 131, 133]. Thus, impaired vesicular trafficking could prevent TNFα release via several mechanisms, ultimately leading to TNFα accumulation intracellularly.

A third possibility lies in the degradation of TNFα, which has been postulated to occur in the lysosomes. Several reports suggest excess membrane-bound TNFα can be endocytosed and either recycled back to the plasma membrane, or degraded within the cell, presumably by the lysosomes [309, 315]. One study estimated that approximately half of the TNFα that is produced in LPS-stimulated macrophages is degraded by the

lysosomes [316]. Thus, the lysosomal traffic jam seen in *Npc1*$^{-/-}$ cells could lead to the accumulation of TNFα that was sent to be degraded within lysosomes. Moreover, these studies also suggest that the rate-limiting step for processing of membrane-bound TNFα to the soluble form is catalyzed by TACE, and that non-processed, membrane-bound TNFα is cleared through lysosomal proteolysis [316]. TACE activity has been shown to be dependent on cholesterol levels, as depleting cellular cholesterol increased TACE activity [317-320]. As NPC1-deficient cells show alterations in cholesterol distribution in the cell, it remains a possibility that altered TACE function could have effects on TNFα secretion.

An additional explanation for increased TNFα immunostaining lies in deficiencies in lysosomal function. Some evidence has suggested that lysosomal enzymes such as cathepsin B and acid sphingomyelinase are required for the proper secretion of TNFα. Inhibition of cathepsin B in LPS-stimulated macrophages caused accumulation of membrane-bound TNFα in vesicles that failed to reach the plasma membrane [321]. In contrast, LPS-stimulated macrophages lacking acid sphingomyelinase secreted several-fold more TNFα than did wild-type macrophages [316]. Therefore, lipid accumulation in *Npc1*$^{-/-}$ LE/Ls could impair the functions of lysosomal enzymes and alter TNFα metabolism. Though these results imply that alterations of lysosomal enzymes could affect TNFα metabolism, these studies fail to conclusively establish that lysosomal

forms of these enzymes are necessary for the TNFα effects. As both cathepsin B and acid sphingomyelinase have been shown to function at sites outside of the lysosomes, such actions cannot be overlooked [321]. Several other lines of evidence also suggest that alterations of these lysosomal enzymes are insufficient to explain the increased TNFα immunostaining seen in *Npc1*$^{-/-}$ microglia. For instance, cathepsin B is increased in the *Npc1*$^{-/-}$ mouse brain, though it is possible that cathepsin B function is impaired [153]. Furthermore, even though acid sphingomyelinase activity is impaired in NPC1-deficient cells [123], increases in TNFα mRNA or secretion did not occur in our studies of *Npc1*$^{-/-}$ microglia.

All of these hypotheses fail to address what is initiating the increased amounts of TNFα in *Npc1*$^{-/-}$ microglia. In general, microglia and macrophages do not have an intracellular store of TNFα and instead synthesize TNFα upon stimulation [305, 306]. In the majority of experiments on TNFα production in these cells, microglia or macrophages are initially activated with LPS in order to stimulate TNFα production. However, we observed no increase in TNFα mRNA in NPC1-deficient microglia, suggesting our *Npc1*$^{-/-}$ microglia cultures are not actively synthesizing TNFα. There is a possibility that the levels of TNFα are not actually increased, but instead the increased TNFα immunostaining is due to alteration in the distribution of TNFα. However, as microglia do not store TNFα, it is unclear if microglia would have endogenous TNFα levels

that are sufficient to cause the increased staining seen in *Npc1*$^{-/-}$ microglia. Another explanation is that replating microglia during the isolation procedure caused them to become activated, so that the TNFα produced from this activation became trapped within the cell. Additionally, the TNFα could have accumulated through interactions with astrocytes in the initial mixed glia cultures prior to isolation of microglia. We also cannot eliminate the possibility that TNFα is produced at low levels within *Npc1*$^{-/-}$ microglia, and these basal amounts of TNFα gradually accumulate in the cell. In any case, TNFα is increased in *Npc1*$^{-/-}$ microglia, though the events leading to this remain to be more clearly defined.

The fact that pro-inflammatory cytokine and oxidative stress gene mRNAs are not increased suggests that our *Npc1*$^{-/-}$ microglia cultures are not activated. However, the increased TNFα immunostaining clearly shows that *Npc1*$^{-/-}$ microglia are altered in some way. The significance of this alteration may only become evident upon microglia activation. While we attempted to activate the microglia cultures with LPS, our results were inconsistent, often showing no indication that activation had actually occurred, particularly at the mRNA level. Nonetheless, increasing evidence suggests that microglia can become 'primed', which results in microglia being more easily activated upon stimulus and/or causes microglia to become more highly activated upon stimulation [322-324]. Often, priming occurs from an initial activating stimulus leaving microglia more readily activated upon any subsequent stimulation [322-324]. In the

case of *Npc1*$^{-/-}$ microglia, we suggest that the initial priming event is the cholesterol trafficking defect caused by lack of NPC1, and this may cause *Npc1*$^{-/-}$ microglia to become more readily or highly activated upon subsequent stimuli. Upon activation, *Npc1*$^{-/-}$ microglia may secrete excess amounts of TNFα, as *Npc1*$^{-/-}$ microglia show increased TNFα immunostaining. Whether this TNFα is available for secretion upon activation, or if it is simply trapped within the cells, remains to be determined.

As is the case with increased TNFα immunostaining in *Npc1*$^{-/-}$ microglia, it is equally unclear what is leading to increased TNFR1 immunostaining. Again, there is a possibility that the actual concentration of TNFR1 is unchanged and the increased signal detected by immunofluorescence in *Npc1*$^{-/-}$ microglia is due to an altered localization of TNFR1. This scenario seems more plausible for TNFR1 than TNFα, as extensive TNFR1 immunostaining was observed in *Npc1*$^{+/+}$ microglia. Other possibilities also exist that could lead to increased TNFR1 levels in *Npc1*$^{-/-}$ microglia. For instance, alterations in TACE function caused by the changes in cholesterol metabolism could be responsible for the increased amount of TNFR1 [317-320]. TACE not only cleaves TNFα, but also cleaves other substrates including TNFR1 [325], generating soluble TNFR1 that is thought to neutralize TNFα activity [326, 327]. Along these lines, decreased TACE activity could lead to increased TNFR1 that remained membrane-bound. Alternatively, TACE activity may be

unaltered, and instead TNFR1 is increased in an attempt to counteract the increased levels of TNFα accumulating in *Npc1*$^{-/-}$ microglia. Furthermore, TNFR1 may also be trapped within the endosomal pathway, as evidence suggests that upon TNFα binding, the complex is internalized by clathrin-dependent endocytosis and enters a Rab-regulated pathway [300, 301]. As Rab-mediated vesicular trafficking is impaired in NPC1-deficient cells, TNFR1 may not be able to efficiently exit from this compartment.

Increased TNFR1 levels could have both beneficial, as well as detrimental, effects. For instance, TNFR1 might be up-regulated to neutralize TNFα, especially since the increased TNFα in NPC1-deficient microglia might lead to a larger inflammatory response upon microglial activation. The induction of TNFR1 "shedding" has been shown to be neuroprotective *in vitro* and *in vivo* [328]. Furthermore, Parkinson disease patients have been shown to have soluble TNFR1, and high levels of soluble TNFR1 were associated with late disease onset suggesting soluble TNFR1 may have some neuroprotective effect [329]. Conversely, increased TNFR1 could also provoke a stronger pro-inflammatory reaction by activated *Npc1*$^{-/-}$ microglia, as evidence suggests that TNFα can activate microglia through TNFR1 via an autocrine pathway [330]. Upon TNFα exposure, microglia show increased synthesis of additional TNFα as well as other pro-inflammatory cytokine mRNAs [330]. The increased TNFR1 levels in *Npc1*$^{-/-}$ microglia could amplify this effect upon TNFα exposure.

*4.A(iv) Implications of decreased IL10 in NPC1-deficient microglia*

Although much emphasis has been placed on the potentially cytotoxic aspects of microglia, the role of microglia is ultimately to maintain brain health. IL10 is an anti-inflammatory cytokine that decreases the synthesis of pro-inflammatory cytokines such as TNFα, IL1β, and interleukin-6, as well as the production of reactive oxygen species, both *in vitro* and *in vivo* [331-334]. Following LPS-induced inflammation in the rat cerebral cortex, IL10 immunostaining was primarily detected in activated microglia [335]. When IL10 activity was abrogated using anti-IL10 antibodies, the amount of neurodegeneration increased, as did reactive oxygen species production and the levels of pro-inflammatory cytokines [335]. In a similar fashion, IL10 administration to rats reduced brain injury following focal stroke [336], and improved functional motor recovery in rats with traumatic spinal cord injury [337]. In addition to anti-inflammatory effects, IL10 also prevented excitotoxic death in murine neuron cultures, an effect that appeared to be mediated through inhibition of pro-apoptotic proteins such as caspase-3 [338, 339]. Thus, it could be hypothesized that decreased levels of IL10 contribute to increased neurodegeneration in NPC disease through several mechanisms. While an initial pro-inflammatory response appears to be beneficial and necessary for appropriate wound healing, the activation state of microglia must ultimately be shifted to a state that promotes cell survival and tissue repair [198]. As IL10 decreases pro-inflammatory cytokine production, the reduction in

IL10 mRNA levels in *Npc1*$^{-/-}$ microglia could prevent microglia from being able to properly regulate their activation status. As a consequence, microglia may become chronically activated, leading to prolonged production of pro-inflammatory cytokines and other potentially neurotoxic molecules that would eventually lead to neuron death. Furthermore, as IL10 appears to have pro-survival effects on neurons, decreased IL10 could decrease neuroprotection mediated by microglia. It remains to be confirmed, however, whether IL10 protein levels are also decreased in *Npc1*$^{-/-}$ microglia, and whether these changes would actually lead to increased inflammation and neurodegeneration in the NPC brain, or if other anti-inflammatory cytokines are able to compensate.

*4.A(v) Microglia-neuron co-cultures*

Surprisingly, we did not see any increase in neuron death caused by *Npc1*$^{-/-}$ microglia in our neuron-microglia co-cultures. While this suggests *Npc1*$^{-/-}$ microglia do not induce neuron death, we cannot rule out microglial contribution to the progressive neurodegeneration in NPC disease *in vivo*. Neuron-microglia co-culture systems are extremely simplified compared to the CNS, lacking the many cell types, and cell-connections, that are present in the brain. It is possible that microglia need to interact with other glial cells, such as astrocytes, in order to induce neuron death. Furthermore, microglia may induce neuron death through indirect functions such as alteration of astrocyte function, which in turn could be neurotoxic. In a similar fashion, microglia may be toxic to cells

other than neurons such as oligodendrocytes, thereby impairing myelination, and ultimately causing neuron dysfunction. Alternatively, the culture conditions we used for the CGCs *in vitro* may not be conducive for *Npc1*$^{-/-}$ microglia to elicit CGC death. Although *Npc1*$^{-/-}$ CGCs undergo death in *Npc1*$^{-/-}$ mouse brains [222], *in vitro* their viability appears to be identical to that of *Npc1*$^{+/+}$ CGCs, with no increase in apoptosis, despite having an altered cholesterol distribution. The lack of death of *Npc1*$^{-/-}$ CGCs *in vitro* could be due to absence of exogenous factors that contribute to CGC death in the brain, or could be due to the culture media and supplements promoting maximal survival of *Npc1*$^{-/-}$ CGCs *in vitro*. The neurotrophic media may prevent *Npc1*$^{-/-}$ microglia from inducing death in neuron-microglia cultures. In an attempt to address this possibility, we also examined co-cultures in which media supplements were removed and found *Npc1*$^{-/-}$ microglia still failed to induce neuron death. Nevertheless, the Neurobasal$^{TM}$ 'A' media may still contain components that prevent microglia-induced death, or removal of the supplements might have caused a shift from an overly protective culture condition to an overly toxic culture condition that might have masked any *Npc1*$^{-/-}$ microglia-induced death. Furthermore, it may be that *Npc1*$^{-/-}$ microglia only exacerbate neuron death *in vivo* as a response to neurodegeneration. Thus, since *Npc1*$^{-/-}$ and *Npc1*$^{+/+}$ CGCs show similar levels of apoptosis *in vitro*, this effect is not evident in our cultures.

It is also possible that the type of neurons we are using (CGCs) are not particularly sensitive to microglia-induced death, or that the microglia are not conducive to inducing neuron death. There is increasing evidence that microglia isolated from different brain regions express region-specific protein profiles that differ from microglia in other brain regions [340, 341]. Thus microglia from one brain region may behave differently from those from another brain region. Consequently, microglia from particular brain regions, such as the cerebellum, might be more neurotoxic than other types of microglia in NPC disease. In a similar fashion, the cell death in the NPC brain is restricted to particular subsets of neurons [150, 152]. Thus, perhaps only some of these neurons are susceptible to killing by microglia. Evidence suggests that the extensive Purkinje cell death in NPC disease is cell autonomous, as NPC1-deficiency restricted to Purkinje cells caused Purkinje cell death despite the presence of *Npc1*$^{+/+}$ cells, such as microglia, in the rest of the brain matter [154, 155]. However, microglia are still active in these brains, and may contribute to Purkinje cell death, even though the initial insult occurs in Purkinje cells [154, 155]. Likewise, CGCs degenerate and show axonal abnormalities in NPC disease [222, 342], but this may be occurring independently of microglia. Thus, while our co-culture experiments fail to show that *Npc1*$^{-/-}$ microglia contribute to neuron death, this does not eliminate the possibility of microglial involvement in the NPC brain, and may simply be due to the limitations of *in vitro* co-cultures.

*4.A(vi) Phagocytosis*

Microglia not only secrete a variety of different factors, but are also the resident phagocytic cells of the CNS. Phagocytosis is a complex process that can be mediated by a number of different receptors and pathways, and thus can elicit a variety of responses depending upon the material being phagocytosed [343]. For instance, phagocytosis of apoptotic cells typically leads to suppression of an inflammatory response [344, 345], while phagocytosis of invading pathogens can induce inflammation [346]. We measured the rate at which *Npc1*$^{-/-}$ and *Npc1*$^{+/+}$ microglia phagocytose carboxylate-modified beads, which are thought to mimic the surface charge of apoptotic cells [347]. Since *Npc1*$^{-/-}$ microglia show an accumulation of cholesterol and other lipids in the LE/L, we predicted that this buildup of material would impair the cell's ability to phagocytose particles. However, we found no difference in the rate of phagocytosis of beads between *Npc1*$^{-/-}$ and *Npc1*$^{+/+}$ microglia. This observation suggests that the ability of *Npc1*$^{-/-}$ microglia to effectively remove degenerating neurons in the NPC brain is not impaired. However, carboxylate-modified beads do not perfectly mimic apoptotic cells [348], which can initiate phagocytosis through several pathways including a phosphatidylserine-mediated mechanism that is absent from the beads [349, 350]. Likewise, these beads do not mimic smaller cellular debris that may need to be phagocytosed in the NPC brain. There is also the possibility that other aspects of phagocytosis that we did not investigate

are impaired in *Npc1*$^{-/-}$ microglia, despite the normal ability to uptake latex beads. For instance, we found IL10 mRNA is decreased in *Npc1*$^{-/-}$ microglia. Thus *Npc1*$^{-/-}$ microglia may be unable to inhibit inflammation when phagocytosing apoptotic cells, which is important for preventing the damage to surrounding cells. Microglia are extremely complex and have a large number of responses we are only beginning to understand. While experiments such as the phagocytosis assay and the co-culture studies suggest *Npc1*$^{-/-}$ microglia function similarly to *Npc1*$^{+/+}$ microglia, we have used ideal culture conditions, and it remains to be determined if the same response would occur under less than ideal conditions, or *in vivo*.

### *4.B CYCLODEXTRIN TREATMENT OF NPC1-DEFICIENT NEURONS AND ASTROCYTES*

HPCD has been shown to decrease neurodegeneration in *Npc1*$^{-/-}$ mice [106, 246-248, 252], however it is unclear whether HPCD has a direct effect on *Npc1*$^{-/-}$ neurons, or if the decreased neurodegeneration is secondary to HPCD effects on glial cells. Moreover, as different cells show varying sensitivities to HPCD [224], it is unclear what concentrations of HPCD can be tolerated by neurons. We have shown that a low dose of HPCD (0.1 mM) reduces intracellular cholesterol staining and incorporation of [$^{3}$H]acetate into newly synthesized cholesterol in both neurons and astrocytes isolated from *Npc1*$^{-/-}$ mice. ACAT-mediated cholesterol esterification is also increased by 0.1 mM HPCD treatment of *Npc1*$^{-/-}$ astrocytes, but this effect is not seen in neurons as they form very

little CE, even in the presence of functional NPC1. Interestingly, *Npc1*$^{-/-}$ neurons and astrocytes respond differently to 0.1 mM HPCD at the transcript level, with neurons decreasing genes involved in cholesterol synthesis, while astrocytes increase genes involved in cholesterol efflux. Although the mechanisms are different, both of these changes would be expected to decrease cholesterol within the cell. 0.1 mM HPCD had no effects on *Npc1*$^{+/+}$ neurons and astrocytes, except for causing a small increase in [$^{3}$H]acetate incorporation into cholesterol in *Npc1*$^{+/+}$ neurons, an effect contrary to that seen in *Npc1*$^{-/-}$ cells. Importantly, administration of a 10-fold higher dose of HPCD (1.0 mM) to *Npc1*$^{-/-}$ neurons and astrocytes results in effects that are mostly opposite from those seen with 0.1 mM HPCD treatment. Although 1.0 mM HPCD decreases intracellular cholesterol staining in *Npc1*$^{-/-}$ cells, incorporation of radiolabel into newly synthesized cholesterol is dramatically increased in both *Npc1*$^{-/-}$ and *Npc1*$^{+/+}$ neurons and astrocytes. *Npc1*$^{-/-}$ astrocytes treated with 1.0 mM HPCD also have a decrease in ACAT-mediated cholesterol esterification, while no effect is seen in *Npc1*$^{+/+}$ astrocytes. At the transcript level, 1.0 mM HPCD treatment of *Npc1*$^{-/-}$ and *Npc1*$^{+/+}$ neurons causes an increase in expression of genes involved in cholesterol synthesis and uptake, while genes involved in cholesterol efflux are significantly decreased. *Npc1*$^{-/-}$ astrocytes also show an increase in mRNA of genes involved in cholesterol synthesis, while *Npc1*$^{+/+}$ astrocytes have decreased expression of genes involved in cholesterol efflux. Taken together, these results

suggest 0.1 mM HPCD can liberate cholesterol sequestered in LE/Ls in *Npc1*$^{-/-}$ brain cells allowing cholesterol to reach the ER where it can regulate cholesterol metabolism. On the other hand, 1.0 mM HPCD depletes brain cells of cholesterol.

*4.B(i) Potential mechanisms of action of cyclodextrin in NPC1-deficient cells*

The effects seen with 0.1 mM HPCD are consistent with findings by several groups that suggest low doses of βCD are liberating cholesterol trapped within the LE/L compartment of *Npc1*$^{-/-}$ cells both *in vitro* and *in vivo* [246, 247, 249, 250, 252]. *Npc1*$^{-/-}$ cells respond to an increase in cellular cholesterol flowing from the LE/L by decreasing cholesterol synthesis, increasing cholesterol storage as CE, and increasing the efflux of cholesterol out of the cell. *Npc1*$^{+/+}$ cells lack this intracellular pool of cholesterol trapped in the LE/L, and as a result 0.1mM HPCD has little effect. If HPCD were simply removing cholesterol from the plasma membrane, one would expect the opposite effects on cholesterol homeostatic mechanisms. That is, the cell would sense a depletion of cholesterol, and in response would increase synthesis while decreasing cholesterol storage and efflux. Indeed, this is what we observed when we treated the cells with a higher concentration (1.0 mM) of HPCD. Although this dose of HPCD still reduces intracellular sequestration of cholesterol, it likely removes excess cholesterol from the plasma membrane as well, leading to an overall depletion of cellular cholesterol. Further evidence

indicating that βCD liberates LE/L cholesterol in NPC1-deficient cells comes from mice injected with radiolabeled HPCD [252]. Nearly all of the radiolabeled HPCD, but very little cholesterol, was recovered in the urine [252]. Instead, HPCD-treated *Npc1*$^{-/-}$ mice showed increased secretion of bile acids several days after HPCD administration, suggesting cholesterol was not being stripped from membranes and eliminated from the body, but instead was being metabolized by the cell and converted to bile acids for excretion [252].

Although several lines of evidence suggest low doses of HPCD lead to the release of cholesterol trapped in the LE/L of *Npc1*$^{-/-}$ cells, the mechanism through which this is occurring remains to be defined. It seems unlikely that extraction of cholesterol from the plasma membrane by HPCD would lead to flux of cholesterol out of the LE/L, and thus it has been proposed that βCD is brought into the endocytic pathway via bulk phase endocytosis [246]. In support of this theory, human *NPC1*$^{-/-}$ fibroblasts exposed to cholesterol-loaded MβCD for 1h and then cultured in FBS-containing medium lacking MβCD, initially showed increased cholesterol staining [250]. After 24h of culture, however, cholesterol staining was dramatically reduced, despite the lack of MβCD in the medium, implying that MβCD had been internalized into the cells [250]. Furthermore, MβCD linked to fluorescent dextran polymers was targeted to the LE/L and reduced cholesterol staining [250]. Other groups using CD as a carrier to deliver drugs and genes into cells provide additional

evidence that CD may be endocytosed. For instance, when cells were incubated with a fluorescent drug analog complexed with γCD, confocal microscopy revealed the drug colocalized with lysosomes, an effect not seen with drug in the absence of γCD [351]. Similarly, when plasmid DNA was complexed in labeled polycationic βCD, it entered into the cell through both clathrin-dependent and clathrin-independent endocytosis [352]. Thus, it appears as though CD may be able to enter into the endocytic compartment of cells.

Once inside the endocytic compartment, it is unclear how HPCD would liberate cholesterol trapped within the LE/L. One possibility is that HPCD might alter the LE/L membrane allowing cholesterol to escape, though destabilizing this membrane would likely lead to leakage of other lysosomal enzymes and apoptosis [353], an effect we did not see with HPCD treatment. Furthermore, HPCD treatment of *Npc1*$^{-/-}$ mice improved the NPC phenotype and delayed neuron death [246-248], observations that would not be consistent with decreased integrity of the lysosomal membrane. Another hypothesis is that HPCD could replace the function of NPC1. However, βCD shows beneficial effects in both *NPC2*$^{-/-}$ human fibroblasts and *Npc2*-hypomorph mice [248, 250], suggesting the beneficial effect of HPCD is independent of either NPC1 or NPC2. Although βCD is often used at high concentrations (5-10mM) to extract cholesterol from plasma membranes [227], βCD has also been shown to shuttle cholesterol between different membranes at the lower

concentrations used in our experiments [244, 245]. Thus, it is possible that HPCD is delivering cholesterol trapped in the LE/L across the glycocalyx in the lumen of the LE/L to the limiting membrane of the lysosome independently of NPC1 or NPC2. As cholesterol can rapidly flip across membranes [245], this cholesterol could then enter into the cytosolic pool via an unknown mechanism. Alternatively, excess cholesterol in *Npc1*$^{-/-}$ endosomes has been shown to alter Rab-mediated endosomal trafficking. In particular, Rab4 is required for appropriate endosome recycling back to the plasma membrane [128]. Even though Rab4 levels are increased in NPC1-deficient cells, excess cholesterol prevents it from being extracted from the endosomal membrane, a process required for proper Rab4 function [128]. Thus, it is possible that βCD that enters into the endocytic pathway can bind to excess cholesterol present in the LE/L. This could prevent excess cholesterol trapped in the LE/L from interfering with proteins such as Rab4, allowing proper endosomal trafficking to occur. Ultimately, this may allow cholesterol to exit the LE/Ls through NPC1/NPC2 independent mechanisms.

Although βCD preferentially binds cholesterol, it also has the capability to bind other lipids, albeit with a much lower affinity. For instance, evidence suggests βCD can bind phospholipids and sphingomyelin [232, 242]. Furthermore, 5mM MβCD has been shown to extract significant amounts of sphingomyelin and glycosphingolipids from rat CGC cultures [354]. In either case, βCD still bound cholesterol with a

much higher affinity than any of the other lipids, and the concentrations of βCD used in these experiments were significantly higher than the HPCD dose we used to liberate cholesterol from the LE/Ls of *Npc1*$^{-/-}$ cells. Nonetheless, while it seems most likely that the action of HPCD is due to its interaction with cholesterol, the possibility exists that HPCD is binding to other lipids trapped in the LE/L of NPC1-deficient cells, and the liberation of cholesterol from the LE/L occurs secondarily to HPCD interacting with these other lipids.

Research is beginning to elucidate the mechanisms through which cholesterol can exit the LE/L through an NPC1/NPC2-dependent mechanism [96], but it is still poorly understood how cholesterol actually crosses the LE/L membrane, and how cholesterol enters into the cytosolic pool. Due to its insolubility in water it is unlikely that cholesterol can move by diffusion from the limiting membrane of the lysosomes to other membranes in the cell. Several different mechanisms have been proposed that include both vesicular and non-vesicular mechanisms [355]. Due to the low solubility of cholesterol, non-vesicular transport of cholesterol would either require a carrier molecule which remains to be defined, or the cholesterol might be transferred by juxtaposition of the donor and acceptor membranes. Thus, there exists the possibility that HPCD could alter the transport of cholesterol from the LE/L membrane to other compartments of the cell. However, it is unclear how HPCD would be able to modify these processes. Moreover, even if one of these

transport mechanisms was altered by HPCD, it is unclear how these transport pathways could gain access to, and liberate, cholesterol that is trapped within the LE/L in NPC1-deficient cells.

Our findings show interesting differences between the effects of HPCD on *Npc1*$^{-/-}$ neurons and astrocytes. At low doses (0.1 mM), HPCD appears to liberate cholesterol from the LE/L of both *Npc1*$^{-/-}$ neurons and astrocytes, leading to decreased punctate filipin staining of cholesterol and decreased levels of radiolabel detected in newly synthesized cholesterol. The difference appears to depend on how the cell deals with this increased amount of cholesterol once it moves out of the LE/L. Neurons showed a decrease in expression of SREBP2 mRNA and genes involved in cholesterol synthesis, while astrocytes showed increased mRNA for ABCA1 and ABCG1, proteins involved in cholesterol efflux out of cells. Both changes would ultimately reduce cholesterol burden on the cell. These different approaches may reflect the different functions of neurons and astrocytes. Particularly, astrocytes are the major cells involved in secreting lipoproteins in the CNS [56, 57], and thus may respond to the cholesterol being liberated from the LE/L by increasing lipoprotein production. As neurons are not major producers of lipoproteins, these cells may instead rely upon decreasing cholesterol synthesis in order to deal with the liberated LE/L cholesterol. While we hypothesized that 0.1mM HPCD would decrease the expression of the LDLR in order to reduce the influx of cholesterol into the cell, we did not see any changes in

LDLR mRNA in *Npc1*$^{-/-}$ neurons or astrocytes. It is possible that the protein levels of the LDLR are being decreased, which may be mediated through PCSK9-mediated LDLR degradation [36, 37]. Furthermore, the CNS expresses several different lipoprotein receptors of the LDLR superfamily [52, 53, 56], and thus HPCD may decrease the expression of other lipoprotein receptors that were not investigated in this study.

*4.B(ii) Cyclodextrin and the blood-brain barrier*

The ability of βCD to cross the BBB poses a potential problem for the therapeutic use of this compound in NPC disease. Experiments performed *in vitro* using a BBB model and *in vivo* in mice both suggest that the BBB is relatively impermeable to βCD [356, 357]. However, it is important to note that in both of these studies, a small amount of βCD was still able to cross the BBB. This small amount of βCD could have an effect in the brain, and may explain why effects of HPCD administered to *Npc1*$^{-/-}$ mice are smaller in the brain than in other tissues. Experiments where CD was used as a delivery agent found that CD increased the uptake of several compounds into the CNS compared to administration of the compounds alone, providing further evidence CD may cross the BBB [358, 359]. These experiments, however, do not provide direct evidence that βCD crosses the BBB, and instead the increased flux of compound into the brain may have been due to βCD increasing the stability of these compounds in the circulation, rather than βCD carrying the compound into the CNS. Alternatively, it is possible that HPCD is able to enter the CNS

in young *Npc1*$^{-/-}$ mice due to the BBB not being fully formed. Experiments suggest the mouse BBB is not fully matured until two weeks after birth [360, 361]. Thus, HPCD administered at postnatal day 7 or 10 could gain access to the CNS through an immature BBB, which might explain why a single injection of HPCD at postnatal day 7 rescues a similar amount of Purkinje cells as do weekly injections starting at postnatal day 7 [246, 247]. However, a partially formed BBB would not explain the prolonged clearance of lipids from neurons of *Npc1*$^{-/-}$ mice receiving serial injections of HPCD, nor would it explain why *Npc1*$^{-/-}$ mice receiving serial injections of HPCD beginning at p21, after the formation of the BBB is presumably complete, still show reduced lipid storage [248]. The integrity of the BBB in NPC disease has not been fully investigated, so the possibility exists that the BBB is leaky in NPC1-deficient mice, thereby allowing HPCD to enter the CNS more rapidly. Additionally, HPCD itself could be damaging the BBB, although this would be predicted to have detrimental consequences, which opposes the therapeutic benefit seen when HPCD is administered to *Npc1*$^{-/-}$ mice. Clearly, it is difficult to rationalize how HPCD could be having these dramatic effects on the CNS without crossing the BBB. Thus, it appears as though a small portion of HPCD administered peripherally to *Npc1*$^{-/-}$ mice must be able to cross the BBB and enter the brain. Further experiments will need to be conducted to determine how much HPCD, if any, is actually entering into the brain.

*4.B(iii) Cyclodextrin is potentially toxic to neurons and astrocytes*

HPCD has shown much promise for therapeutic use in NPC disease. Our findings illustrate the importance of determining the appropriate concentration of HPCD for therapeutic use in the CNS. Studies in humans have already been initiated as the Food and Drug Administration has approved HPCD for compassionate use. While low concentrations of 0.1 mM HPCD release LE/L cholesterol in both *Npc1*$^{-/-}$ neurons and astrocytes *in vitro*, 1.0 mM HPCD appeared to deplete these cells of cholesterol, an effect that would have detrimental consequences over a prolonged period of time. Furthermore, when 10 mM HPCD was administered to cultures, it completely killed the neurons and drastically altered the morphology of the astrocytes. As these experiments were performed *in vitro*, in the absence of serum, the effects of these doses may not translate directly to those *in vivo*. Additionally, the rapid clearance of HPCD from the circulation in mice [246], as well as humans [243], may render higher doses of HPCD more tolerable, as the time cells are actually exposed to HPCD would be relatively short compared to our 24 h incubations *in vitro*. Nonetheless, the doses being administered to *Npc1*$^{-/-}$ mice are several-fold higher than doses that have been shown to be generally non-toxic in animal models and humans [243]. High doses of HPCD can lead to adverse signs and even premature deaths in rats [243]. Similar to other studies, repeated HPCD administration to *Npc1*$^{-/-}$ mice leads to some kidney abnormalities [243, 247]. Moreover, when the same

dose of HPCD given to *Npc1*$^{-/-}$ mice was administered to *Npc1*$^{-/-}$ cats, these cats showed an impairment in hearing [362]. While this hearing loss was not seen with a single injection, effects were detectable following several weeks of injections [362]. This suggests that frequent exposure of cells to HPCD could eventually be toxic, or that repeated administration of HPCD could eventually lead to a toxic buildup of HPCD in tissues such as the CNS. Since neurons appear to be particularly sensitive to HPCD, it will be important to determine what concentration of HPCD is able to cross the BBB and enter into the CNS. Although HPCD shows very promising effects, the properties of HPCD also make it a potentially dangerous molecule for treatment of humans due to its abilities to alter membranes, and great care should be exercised in choosing an appropriate dose for treatment. Nonetheless, the severity of NPC disease symptoms may ultimately outweigh the negative effects mediated by HPCD.

### *4.C CONCLUSIONS*

The progression of NPC disease in the CNS is complex, and the mechanisms leading to the progressive and selective neurodegeneration remain largely unknown. Several different studies have implicated microglia as contributors to the phenotype of NPC disease, although their exact role is undefined. We have shown that NPC1-deficient microglia are altered in a fashion that could contribute to neurodegeneration in NPC disease. For instance, *Npc1*$^{-/-}$ microglia show increased TNFα and TNFR1 immunostaining, both of which could lead to a more severe

inflammatory response. Furthermore, when compared to *Npc1*$^{+/+}$ microglia, *Npc1*$^{-/-}$ microglia have lower levels of IL10 mRNA, an anti-inflammatory cytokine that can suppress inflammation. Despite these changes, *Npc1*$^{-/-}$ microglia did not induce neuron death in several different neuron-microglia co-culture systems. However, the changes we observed may only induce detrimental consequences when these microglia are activated. Indeed, *Npc1*$^{-/-}$ microglia did not show increased levels of activation compared to *Npc1*$^{+/+}$ microglia based upon TNFα secretion, as well as mRNA expression of pro-inflammatory cytokines and oxidative stress genes. Further experiments need to be conducted in which *Npc1*$^{-/-}$ and *Npc1*$^{+/+}$ microglia are compared under conditions of activation, such as stimulation with LPS. Ultimately, *in vivo* experiments will be required to determine the exact role microglia play in NPC disease progression. The massive accumulation of active microglia in the NPC1-deficient brain strongly suggests that microglia exacerbate the neurodegeneration in NPC disease. In support of this conclusion, anti-inflammatory treatments have been shown to significantly delay the onset of symptoms and prolong the lifespan of *Npc1*$^{-/-}$ mice [363]. Ultimately, generation of mice with microglia-specific elimination of NPC1 would shed much light on whether microglia are capable of inducing neurodegeneration autonomously, or whether microglia contribute to neurodegeneration in response to cell death in the NPC1-deficient brain.

Although treatment options for NPC disease have been limited, the recent experiments using HPCD to treat NPC1-deficient mice have shown much promise, reversing many aspects of NPC disease and dramatically increasing the lifespan. Our findings expand on the observation that HPCD reduces neurodegeneration in *Npc1*$^{-/-}$ mice. We have shown HPCD is capable of liberating cholesterol trapped in the LE/L of both *Npc1*$^{-/-}$ neurons and astrocytes, making the cholesterol available to regulate cholesterol metabolism at the ER. Our results suggest that treatment of *Npc1*$^{-/-}$ neurons with 0.1 mM HPCD decreases cholesterol synthesis, while treatment of *Npc1*$^{-/-}$ astrocytes with 0.1 mM HPCD increases cholesterol efflux. Measurement of the amounts of cholesterol released into the medium of astrocytes in response to HPCD treatment will help to determine if this is indeed the case. Furthermore, changes in expression of genes involved in cholesterol metabolism at the mRNA level need to be confirmed at the protein level, as changes in mRNA do not always translate to changes at the protein level. This is particularly important with genes such as SREBP2, which is primarily regulated by post-translational modifications. Experiments using radiolabeled HPCD and subcellular fractionation would confirm that HPCD does indeed enter the endosomal system, although more elaborate experiments will need to be designed to determine the mechanism through which HPCD bypasses NPC1 and NPC2 defects.

We have also shown that the effects of HPCD are concentration dependent, which is particularly important when considering HPCD for therapeutic use in NPC disease. While a low dose (0.1 mM) of HPCD liberates LE/L cholesterol, a ten-fold higher dose (1.0 mM) depleted cells of cholesterol and would ultimately be predicted to de detrimental. Although HPCD does not appear to readily cross the BBB, it is likely that a small amount does enter the CNS since it is difficult to explain the neuroprotective effects of HPCD if it does not enter the brain. Thus, further experiments need to be conducted to determine the amount of HPCD that enters the CNS from the circulation. Since HPCD has the ability to dramatically alter membranes, and some cells such as neurons appear to be exquisitely sensitive to HPCD, care must be taken to ensure the appropriate dose is selected when considering the use of HPCD as a therapy for NPC disease patients. The fact that HPCD can liberate cholesterol from the LE/L of neurons suggests HPCD may be decreasing neurodegeneration by acting directly on neurons, an observation that further strengthens the use of HPCD for treatment of NPC disease. As HPCD has already been approved by the Food and Drug Administration for compassionate treatment in humans, it becomes even more important to determine the appropriate dose of HPCD and the potential side effects, particularly in the brain.

## 5. REFERENCES


1. Brown, D.A. and E. London, *Functions of lipid rafts in biological membranes*. Annual Review of Cell and Developmental Biology, 1998. **14**: p. 111-136.

2. Simons, K. and E. Ikonen, *Functional rafts in cell membranes.* Nature, 1997. **387**(6633): p. 569-572.

3. Witztum, J.L. and D. Steinberg, *Role of oxidized low density lipoprotein in atherogenesis.* Journal of Clinical Investigation, 1991. **88**(6): p. 1785-1792.

4. Bloch, K., *The biological synthesis of cholesterol.* Science, 1965. **150**(3692): p. 19-28.

5. Dietschy, J.M., S.D. Turley, and D.K. Spady, *Role of liver in the maintenance of cholesterol and low density lipoprotein homeostasis in different animal species, including humans.* J Lipid Res, 1993. **34**(10): p. 1637-1659.

6. Brown, M.S. and J.L. Goldstein, *A receptor-mediated pathway for cholesterol homeostasis.* Science, 1986. **232**(4746): p. 34-47.

7. Liu, B., et al., *Receptor-mediated and bulk-phase endocytosis cause macrophage and cholesterol accumulation in Niemann-Pick C disease.* J Lipid Res, 2007. **48**(8): p. 1710-23.

8. Anderson, R.A. and G.N. Sando, *Cloning and expression of cDNA encoding human lysosomal acid lipase/cholesteryl ester hydrolase. Similarities to gastric and lingual lipases.* Journal of Biological Chemistry, 1991. **266**(33): p. 22479-22484.

9. Goldstein, J.L., S.E. Dana, and J.R. Faust, *Role of lysosomal acid lipase in the metabolism of plasma low density lipoprotein. Observations in cultured fibroblasts from a patient with cholesteryl ester storage disease.* Journal of Biological Chemistry, 1975. **250**(21): p. 8487-8495.

10. Brown, M.S. and J.L. Goldstein, *The SREBP pathway: regulation of cholesterol metabolism by proteolysis of a membrane-bound transcription factor.* Cell, 1997. **89**(3): p. 331-40.

11. Brown, M.S., S.E. Dana, and J.L. Goldstein, *Cholesterol ester formation in cultured human fibroblasts. Stimulation by oxygenated sterols.* Journal of Biological Chemistry, 1975. **250**(10): p. 4025-4027.

12. Oram, J.F., et al., *ABCA1 is the cAMP-inducible apolipoprotein receptor that mediates cholesterol secretion from macrophages.* Journal of Biological Chemistry, 2000. **275**(44): p. 34508-34511.

13. Wang, N., et al., *ATP-binding cassette transporters G1 and G4 mediate cellular cholesterol efflux to high-density lipoproteins.* Proc Natl Acad Sci U S A, 2004. **101**(26): p. 9774-9779.

14. Ji, Y., et al., *Scavenger receptor BI promotes high density lipoprotein-mediated cellular cholesterol efflux.* Journal of Biological Chemistry, 1997. **272**(34): p. 20982-20985.

15. Rigotti, A., et al., *A targeted mutation in the murine gene encoding the high density lipoprotein (HDL) receptor scavenger receptor class B type I reveals its key role in HDL metabolism.* Proc Natl Acad Sci U S A, 1997. **94**(23): p. 12610-12615.

16. Xie, C., S.D. Turley, and J.M. Dietschy, *ABCA1 plays no role in the centripetal movement of cholesterol from peripheral tissues to the liver and intestine in the mouse.* J Lipid Res, 2009. **50**(7): p. 1316-1329.

17. Sakai, J., et al., *Sterol-regulated release of SREBP-2 from cell membranes requires two sequential cleavages, one within a transmembrane segment.* Cell, 1996. **85**(7): p. 1037-1046.

18. Brown, M.S., S.E. Dana, and J.L. Goldstein, *Regulation of 3 hydroxy 3 methylglutaryl coenzyme A reductase activity in human fibroblasts by lipoproteins.* Proc Natl Acad Sci U S A, 1973. **70**(7): p. 2162-2166.

19. Nohturfft, A., M.S. Brown, and J.L. Goldstein, *Topology of SREBP cleavage-activating protein, a polytopic membrane protein with a sterol-sensing domain.* Journal of Biological Chemistry, 1998. **273**(27): p. 17243-17250.

20. Sakai, J., et al., *Identification of complexes between the COOH-terminal domains of sterol regulatory element-binding proteins (SREBPS) and SREBP cleavage-activating protein.* Journal of Biological Chemistry, 1997. **272**(32): p. 20213-20221.

21. Sakai, J., et al., *Cleavage of sterol regulatory element-binding proteins (SREBPs) at site- 1 requires interaction with SREBP cleavage-activating protein. Evidence from in vivo competition studies.* Journal of Biological Chemistry, 1998. **273**(10): p. 5785-5793.

22. Nohturfft, A., et al., *Regulated step in cholesterol feedback localized to budding of SCAP from ER membranes.* Cell, 2000. **102**(3): p. 315-323.

23. Yang, T., et al., *Crucial step in cholesterol homeostasis: Sterols promote binding of SCAP to INSIG-1, a membrane protein that facilitates retention of SREBPs in ER.* Cell, 2002. **110**(4): p. 489-500.

24. Adams, C.M., et al., *Cholesterol and 25-hydroxycholesterol inhibit activation of SREBPs by different mechanisms, both involving SCAP and insigs.* Journal of Biological Chemistry, 2004. **279**(50): p. 52772-52780.

25. Brown, A.J., et al., *Cholesterol addition to ER membranes alters conformation of SCAP, the SREBP escort protein that regulates cholesterol metabolism.* Molecular Cell, 2002. **10**(2): p. 237-245.

26. Radhakrishnan, A., et al., *Sterol-regulated transport of SREBPs from endoplasmic reticulum to Golgi: Oxysterols block transport by binding to Insig.* Proc Natl Acad Sci U S A, 2007. **104**(16): p. 6511-6518.

27. Radhakrishnan, A., et al., *Direct binding of cholesterol to the purified membrane region of SCAP: Mechanism for a sterol-sensing domain.* Molecular Cell, 2004. **15**(2): p. 259-268.

28. Sun, L.P., et al., *Insig required for sterol-mediated inhibition of Scap/SREBP binding to COPII proteins in vitro.* Journal of Biological Chemistry, 2005. **280**(28): p. 26483-26490.

29. Espenshade, P.J., W.P. Li, and D. Yabe, *Sterols block binding of COPII proteins to SCAP, thereby controlling SCAP sorting in ER.* Proc Natl Acad Sci U S A, 2002. **99**(18): p. 11694-11699.

30. Sun, L.P., et al., *Sterol-regulated transport of SREBPs from endoplasmic reticulum to Golgi: Insig renders sorting signal in Scap inaccessible to COPII proteins.* Proc Natl Acad Sci U S A, 2007. **104**(16): p. 6519-6526.

31. Gil, G., J.R. Faust, and D.J. Chin, *Membrane-bound domain of HMG CoA reductase is required for sterol-enhanced degradation of the enzyme.* Cell, 1985. **41**(1): p. 249-258.

32. Nakanishi, M., J.L. Goldstein, and M.S. Brown, *Multivalent control of 3-hydroxy-3-methylglutaryl coenzyme A reductase. Mevalonate-derived product inhibits translation of mRNA and accelerates degradation of enzyme.* Journal of Biological Chemistry, 1988. **263**(18): p. 8929-8937.

33. Sever, N., et al., *Insig-dependent Ubiquitination and Degradation of Mammalian 3-Hydroxy-3-methylglutaryl-CoA Reductase Stimulated by Sterols and Geranylgeraniol.* Journal of Biological Chemistry, 2003. **278**(52): p. 52479-52490.

34. Sever, N., et al., *Accelerated degradation of HMG CoA reductase mediated by binding of insig-1 to its sterol-sensing domain.* Molecular Cell, 2003. **11**(1): p. 25-33.

35. Bottomley, M.J., et al., *Structural and biochemical characterization of the wild type PCSK9-EGF(AB) complex and natural familial hypercholesterolemia mutants.* Journal of Biological Chemistry, 2009. **284**(2): p. 1313-1323.

36. Zhang, D.W., et al., *Structural requirements for PCSK9-mediated degradation of the low-density lipoprotein receptor.* Proc Natl Acad Sci U S A, 2008. **105**(35): p. 13045-13050.

37. Zhang, D.W., et al., *Binding of proprotein convertase subtilisin/kexin type 9 to epidermal growth factor-like repeat A of low density lipoprotein receptor decreases receptor recycling and increases degradation.* Journal of Biological Chemistry, 2007. **282**(25): p. 18602-18612.

38. Costet, P., et al., *Sterol-dependent transactivation of the ABC1 promoter by the liver X receptor/retinoid X receptor.* Journal of Biological Chemistry, 2000. **275**(36): p. 28240-28245.

39. Janowski, B.A., et al., *An oxysterol signalling pathway mediated by the nuclear receptor LXRalpha.* Nature, 1996. **383**(6602): p. 728-731.

40. Peet, D.J., et al., *Cholesterol and bile acid metabolism are impaired in mice lacking the nuclear oxysterol receptor LXRalpha.* Cell, 1998. **93**(5): p. 693-704.

41. Venkateswaran, A., et al., *Control of cellular cholesterol efflux by the nuclear oxysterol receptor LXRalpha.* Proc Natl Acad Sci U S A, 2000. **97**(22): p. 12097-12102.

42. Naik, S.U., et al., *Pharmacological activation of liver X receptors promotes reverse cholesterol transport in vivo.* Circulation, 2006. **113**(1): p. 90-97.

43. Repa, J.J., et al., *Regulation of absorption and ABC1-mediated efflux of cholesterol by RXR heterodimers.* Science, 2000. **289**(5484): p. 1524-1529.

44. Turley, S.D., et al., *Brain does not utilize low density lipoprotein-cholesterol during fetal and neonatal development in the sheep.* J Lipid Res, 1996. **37**(9): p. 1953-61.

45. Quan, G., et al., *Ontogenesis and regulation of cholesterol metabolism in the central nervous system of the mouse.* Brain Res Dev Brain Res, 2003. **146**(1-2): p. 87-98.

46. Pitas, R.E., et al., *Lipoproteins and their receptors in the central nervous system. Characterization of the lipoproteins in cerebrospinal fluid and identification of apolipoprotein B,E(LDL) receptors in the brain.* Journal of Biological Chemistry, 1987. **262**(29): p. 14352-14360.

47. Ladu, M.J., et al., *Lipoproteins in the central nervous system*. Annals of the New York Academy of Sciences, 2000. **903**: p. 167-175.

48. Hirsch-Reinshagen, V., et al., *Deficiency of ABCA1 impairs apolipoprotein E metabolism in brain.* Journal of Biological Chemistry, 2004. **279**(39): p. 41197-41207.

49. Karten, B., et al., *Expression of ABCG1, but not ABCA1, correlates with cholesterol release by cerebellar astroglia.* Journal of Biological Chemistry, 2006. **281**(7): p. 4049-4057.

50. Karten, B., et al., *Generation and function of astroglial lipoproteins from Niemann-Pick type C1-deficient mice.* Biochem J, 2005. **387**(Pt 3): p. 779-88.

51. Nakamura, K., et al., *Expression and regulation of multiple murine ATP-binding cassette transporter G1 mRNAs/isoforms that stimulate cellular cholesterol efflux to high density lipoprotein.* Journal of Biological Chemistry, 2004. **279**(44): p. 45980-45989.

52. Beffert, U., et al., *The neurobiology of apolipoproteins and their receptors in the CNS and Alzheimer's disease.* Brain Research Reviews, 1998. **27**(2): p. 119-142.

53. Fagan, A.M., et al., *Apolipoprotein E-containing high density lipoprotein promotes neurite outgrowth and is a ligand for the low density lipoprotein receptor-related protein.* Journal of Biological Chemistry, 1996. **271**(47): p. 30121-30125.

54. DeMattos, R.B., et al., *Purification and characterization of astrocyte-secreted apolipoprotein E and J-containing lipoproteins from wild-type and human apoE transgenic mice.* Neurochemistry International, 2001. **39**(5-6): p. 415-425.

55. Boyles, J.K., R.E. Pitas, and E. Wilson, *Apolipoprotein E associated with astrocytic glia of the central nervous system and with nonmyelinating glia of the peripheral nervous system.* Journal of Clinical Investigation, 1985. **76**(4): p. 1501-1513.

56. Pitas, R.E., J.K. Boyles, and S.H. Lee, *Astrocytes synthesize apolipoprotein E and metabolize apolipoprotein E-containing lipoproteins.* Biochim Biophys Acta, 1987. **917**(1): p. 148-161.

57. Nieweg, K., H. Schaller, and F.W. Pfrieger, *Marked differences in cholesterol synthesis between neurons and glial cells from postnatal rats.* J Neurochem, 2009. **109**(1): p. 125-34.

58. Vance, J.E. and H. Hayashi, *Formation and function of apolipoprotein E-containing lipoproteins in the nervous system.* Biochim Biophys Acta, 2010. **1801**(8): p.806-18.

59. Hayashi, H., et al., *Glial Lipoproteins Stimulate Axon Growth of Central Nervous System Neurons in Compartmented Cultures.* Journal of Biological Chemistry, 2004. **279**(14): p. 14009-14015.

60. Matsuo, M., et al., *Involvement of low density lipoprotein receptor-related protein and ABCG1 in stimulation of axonal extension by Apo E-containing lipoproteins.* Biochim Biophys Acta, 2010(In Press).

61. Mauch, D.H., et al., *CNS synaptogenesis promoted by glia-derived cholesterol.* Science, 2001. **294**(5545): p. 1354-1357.

62. Karten, B., K.B. Peake, and J.E. Vance, *Mechanisms and consequences of impaired lipid trafficking in Niemann-Pick type C1-deficient mammalian cells.* Biochim Biophys Acta, 2009. **1791**(7): p. 659-70.

63. Karten, B., et al., *Cholesterol accumulates in cell bodies, but is decreased in distal axons, of Niemann-Pick C1-deficient neurons.* J Neurochem, 2002. **83**(5): p. 1154-63.

64. Korade, Z., et al., *Expression and p75 neurotrophin receptor dependence of cholesterol synthetic enzymes in adult mouse brain.* Neurobiology of Aging, 2007. **28**(10): p. 1522-1531.

65. Valdez, C.M., et al., *Cholesterol homeostasis markers are localized to mouse hippocampal pyramidal and granule layers.* Hippocampus, 2010. **20**(8): p. 902-905.

66. Nieweg, K., H. Schaller, and F.W. Pfrieger, *Marked differences in cholesterol synthesis between neurons and glial cells from postnatal rats.* J Neurochem, 2009. **109**(1): p. 125-134.

67. Funfschilling, U., et al., *Survival of adult neurons lacking cholesterol synthesis in vivo.* BMC Neuroscience, 2007. **8**.

68. Dietschy, J.M., T. Kita, and K.E. Suckling, *Cholesterol synthesis in vivo and in vitro in the WHHL rabbit, an animal with defective low density lipoprotein receptors.* J Lipid Res, 1983. **24**(4): p. 469-480.

69. Spady, D.K. and J.M. Dietschy, *Sterol synthesis in vivo in 18 tissues of the squirrel monkey, guinea pig, rabbit, hamster, and rat.* J Lipid Res, 1983. **24**(3): p. 303-315.

70. Bjorkhem, I., et al., *Importance of a novel oxidative mechanism for elimination of brain cholesterol. Turnover of cholesterol and 24(S)-hydroxycholesterol in rat brain as measured with 18O2 techniques in vivo and in vitro.* Journal of Biological Chemistry, 1997. **272**(48): p. 30178-30184.

71. Bjorkhem, I., et al., *Cholesterol homeostasis in human brain: Turnover of 24S- hydroxycholesterol and evidence for a cerebral origin of most of this oxysterol in the circulation.* J Lipid Res, 1998. **39**(8): p. 1594-1600.

72. Lutjohann, D., et al., *Cholesterol homeostasis in human brain: Evidence for an age-dependent flux of 24S-hydroxycholesterol from the brain into the circulation.* Proc Natl Acad Sci U S A, 1996. **93**(18): p. 9799-9804.

73. Lund, E.G., J.M. Guileyardo, and D.W. Russell, *cDNA cloning of cholesterol 24-hydroxylase, a mediator of cholesterol homeostasis in the brain.* Proc Natl Acad Sci U S A, 1999. **96**(13): p. 7238-7243.

74. Lund, E.G., et al., *Knockout of the cholesterol 24-hydroxylase gene in mice reveals a brain-specific mechanism of cholesterol turnover.* Journal of Biological Chemistry, 2003. **278**(25): p. 22980-22988.

75. Repa, J.J., et al., *Liver X receptor activation enhances cholesterol loss from the brain, decreases neuroinflammation, and increases survival of the NPC1 mouse.* J Neurosci, 2007. **27**(52): p. 14470-80.

76. Vanier, M.T. and G. Millat, *Niemann-Pick disease type C.* Clin Genet, 2003. **64**(4): p. 269-81.

77. Wraith, J.E., et al., *Natural history of Niemann-Pick disease type C in a multicentre observational retrospective cohort study.* Mol Genet Metab, 2009. **98**(3): p. 250-4.

78. Pentchev, P.G., et al., *A defect in cholesterol esterification in Niemann-Pick disease (type C) patients.* Proc Natl Acad Sci U S A, 1985. **82**(23): p. 8247-51.

79. Liscum, L. and J.R. Faust, *Low density lipoprotein (LDL)-mediated suppression of cholesterol synthesis and LDL uptake is defective in Niemann-Pick type C fibroblasts.* J Biol Chem, 1987. **262**(35): p. 17002-8.

80. Blanchette-Mackie, E.J., et al., *Type-C Niemann-Pick disease: low density lipoprotein uptake is associated with premature cholesterol accumulation in the Golgi complex and excessive cholesterol storage in lysosomes.* Proc Natl Acad Sci U S A, 1988. **85**(21): p. 8022-6.

81. Carstea, E.D., et al., *Niemann-Pick C1 disease gene: homology to mediators of cholesterol homeostasis.* Science, 1997. **277**(5323): p. 228-31.

82. Loftus, S.K., et al., *Murine model of Niemann-Pick C disease: mutation in a cholesterol homeostasis gene.* Science, 1997. **277**(5323): p. 232-5.

83. Huang, X., et al., *A Drosophila model of the Niemann-Pick type C lysosome storage disease: dnpc1a is required for molting and sterol homeostasis.* Development, 2005. **132**(22): p. 5115-24.

84. Higgins, M.E., et al., *Niemann-Pick C1 is a late endosome-resident protein that transiently associates with lysosomes and the trans-Golgi network.* Mol Genet Metab, 1999. **68**(1): p. 1-13.

85. Neufeld, E.B., et al., *The Niemann-Pick C1 protein resides in a vesicular compartment linked to retrograde transport of multiple lysosomal cargo.* J Biol Chem, 1999. **274**(14): p. 9627-35.

86. Davies, J.P. and Y.A. Ioannou, *Topological analysis of Niemann-Pick C1 protein reveals that the membrane orientation of the putative sterol-sensing domain is identical to those of 3-hydroxy-3-methylglutaryl-CoA reductase and sterol regulatory element binding protein cleavage-activating protein.* J Biol Chem, 2000. **275**(32): p. 24367-74.

87. Naureckiene, S., et al., *Identification of HE1 as the second gene of Niemann-Pick C disease.* Science, 2000. **290**(5500): p. 2298-301.

88. Okamura, N., et al., *A porcine homolog of the major secretory protein of human epididymis, HE1, specifically binds cholesterol.* Biochim Biophys Acta, 1999. **1438**(3): p. 377-87.

89. Cheruku, S.R., et al., *Mechanism of cholesterol transfer from the Niemann-Pick type C2 protein to model membranes supports a role in lysosomal cholesterol transport.* J Biol Chem, 2006. **281**(42): p. 31594-604.

90. Vanier, M.T., et al., *Genetic heterogeneity in Niemann-Pick C disease: a study using somatic cell hybridization and linkage analysis.* Am J Hum Genet, 1996. **58**(1): p. 118-25.

91. Sleat, D.E., et al., *Genetic evidence for nonredundant functional cooperativity between NPC1 and NPC2 in lipid transport.* Proc Natl Acad Sci U S A, 2004. **101**(16): p. 5886-91.

92. Infante, R.E., et al., *Purified NPC1 protein: II. Localization of sterol binding to a 240-amino acid soluble luminal loop.* J Biol Chem, 2008. **283**(2): p. 1064-75.

93. Xu, S., et al., *Structural basis of sterol binding by NPC2, a lysosomal protein deficient in Niemann-Pick type C2 disease.* J Biol Chem, 2007. **282**(32): p. 23525-31.

94. Infante, R.E., et al., *Purified NPC1 protein. I. Binding of cholesterol and oxysterols to a 1278-amino acid membrane protein.* J Biol Chem, 2008. **283**(2): p. 1052-63.

95. Liu, R., et al., *Characterization of fluorescent sterol binding to purified human NPC1.* J Biol Chem, 2009. **284**(3): p. 1840-52.

96. Kwon, H.J., et al., *Structure of N-terminal domain of NPC1 reveals distinct subdomains for binding and transfer of cholesterol.* Cell, 2009. **137**(7): p. 1213-24.

97. Infante, R.E., et al., *NPC2 facilitates bidirectional transfer of cholesterol between NPC1 and lipid bilayers, a step in cholesterol egress from lysosomes.* Proc Natl Acad Sci U S A, 2008. **105**(40): p. 15287-92.

98. Ohgami, N., et al., *Binding between the Niemann-Pick C1 protein and a photoactivatable cholesterol analog requires a functional sterol-sensing domain.* Proc Natl Acad Sci U S A, 2004. **101**(34): p. 12473-8.

99. Davies, J.P., F.W. Chen, and Y.A. Ioannou, *Transmembrane molecular pump activity of Niemann-Pick C1 protein.* Science, 2000. **290**(5500): p. 2295-8.

100. Passeggio, J. and L. Liscum, *Flux of fatty acids through NPC1 lysosomes.* J Biol Chem, 2005. **280**(11): p. 10333-9.

101. Liscum, L. and J.R. Faust, *The intracellular transport of low density lipoprotein-derived cholesterol is inhibited in Chinese hamster ovary cells cultured with 3 beta-[2-(diethylamino)ethoxy]androst-5-en-17-one.* Journal of Biological Chemistry, 1989. **264**(20): p. 11796-11806.

102. Harmala, A.S., et al., *Cholesterol transport from plasma membranes to intracellular membranes is inhibited by 3 beta-[2-(diethylamino)ethoxy]androst-5-en-17-one.* Biochim Biophys Acta, 1994. **1211**(3): p. 317-25.

103. Sexton, R.C., et al., *Effects of 3 beta-[2-(diethylamino)ethoxy]androst-5-en-17-one on the synthesis of cholesterol and ubiquinone in rat intestinal epithelial cell cultures.* Biochemistry, 1983. **22**(25): p. 5687-92.

104. Morris, M.D., et al., *Lysosome lipid storage disorder in NCTR-BALB/c mice. I. Description of the disease and genetics.* American Journal of Pathology, 1982. **108**(2): p. 140-149.

105. Shio, H., et al., *Lysosome lipid storage disorder in NCTR-BALB/c mice. II. Morphologic and cytochemical studies.* American Journal of Pathology, 1982. **108**(2): p. 150-159.

106. Liu, B., et al., *Genetic variations and treatments that affect the lifespan of the NPC1 mouse.* J Lipid Res, 2008. **49**(3): p. 663-9.

107. March, P.A., et al., *GABAergic neuroaxonal dystrophy and other cytopathological alterations in feline Niemann-Pick disease type C.* Acta Neuropathol, 1997. **94**(2): p. 164-172.

108. Somers, K.L., et al., *Complementation studies in human and feline Niemann-Pick type C disease.* Mol Genet Metab, 1999. **66**(2): p. 117-121.

109. Vite, C.H., et al., *Clinical, electrophysiological, and serum biochemical measures of progressive neurological and hepatic dysfunction in feline niemann-pick type C disease.* Pediatric Research, 2008. **64**(5): p. 544-549.

110. Malathi, K., et al., *Mutagenesis of the putative sterol-sensing domain of yeast Niemann Pick C-related protein reveals a primordial role in subcellular sphingolipid distribution.* Journal of Cell Biology, 2004. **164**(4): p. 547-556.

111. Zhang, S., et al., *Ncr1p, the yeast ortholog of mammalian Niemann Pick C1 protein, is dispensable for endocytic transport.* Traffic, 2004. **5**(12): p. 1017-1030.

112. Urano, Y., et al., *Transport of LDL-derived cholesterol from the NPC1 compartment to the ER involves the trans-Golgi network and the SNARE protein complex.* Proc Natl Acad Sci U S A, 2008. **105**(43): p. 16513-8.

113. Cruz, J.C. and T.Y. Chang, *Fate of endogenously synthesized cholesterol in Niemann-Pick type C1 cells.* J Biol Chem, 2000. **275**(52): p. 41309-16.

114. Wojtanik, K.M. and L. Liscum, *The transport of low density lipoprotein-derived cholesterol to the plasma membrane is defective in NPC1 cells.* J Biol Chem, 2003. **278**(17): p. 14850-6.

115. Shamburek, R.D., et al., *Intracellular trafficking of the free cholesterol derived from LDL cholesteryl ester is defective in vivo in Niemann-Pick C disease: insights on normal metabolism of HDL and LDL gained from the NP-C mutation.* J Lipid Res, 1997. **38**(12): p. 2422-35.

116. Lloyd-Evans, E., et al., *Niemann-Pick disease type C1 is a sphingosine storage disease that causes deregulation of lysosomal calcium.* Nat Med, 2008. **14**(11): p. 1247-55.

117. Li, H., et al., *GM2/GD2 and GM3 gangliosides have no effect on cellular cholesterol pools or turnover in normal or NPC1 mice.* J Lipid Res, 2008. **49**(8): p. 1816-28.

118. Liu, Y., et al., *Alleviation of neuronal ganglioside storage does not improve the clinical course of the Niemann-Pick C disease mouse.* Hum Mol Genet, 2000. **9**(7): p. 1087-92.

119. Gondre-Lewis, M.C., R. McGlynn, and S.U. Walkley, *Cholesterol accumulation in NPC1-deficient neurons is ganglioside dependent.* Curr Biol, 2003. **13**(15): p. 1324-9.

120. Puri, V., et al., *Cholesterol modulates membrane traffic along the endocytic pathway in sphingolipid-storage diseases.* Nat Cell Biol, 1999. **1**(6): p. 386-8.

121. Puri, V., et al., *Sphingolipid storage induces accumulation of intracellular cholesterol by stimulating SREBP-1 cleavage.* J Biol Chem, 2003. **278**(23): p. 20961-70.

122. Zervas, M., et al., *Critical role for glycosphingolipids in Niemann-Pick disease type C.* Curr Biol, 2001. **11**(16): p. 1283-7.

123. Devlin, C., et al., *Improvement in Lipid and Protein Trafficking in NPC1 Cells by Correction of a Secondary Enzyme Defect.* Traffic, 2010. **11**(5): p. 601-15.

124. Patterson, M.C., et al., *Long-Term Miglustat Therapy in Children With Niemann-Pick Disease Type C.* J Child Neurol, 2010. **25**(3): p. 300-5.

125. Pineda, M., et al., *Miglustat in patients with Niemann-Pick disease Type C (NP-C): a multicenter observational retrospective cohort study.* Mol Genet Metab, 2009. **98**(3): p. 243-9.

126. Somsel Rodman, J. and A. Wandinger-Ness, *Rab GTPases coordinate endocytosis.* J Cell Sci, 2000. **113**(Pt 2): p. 183-92.

127. Choudhury, A., et al., *Rab proteins mediate Golgi transport of caveola-internalized glycosphingolipids and correct lipid trafficking in Niemann-Pick C cells.* J Clin Invest, 2002. **109**(12): p. 1541-50.

128. Choudhury, A., et al., *Elevated endosomal cholesterol levels in Niemann-Pick cells inhibit rab4 and perturb membrane recycling.* Mol Biol Cell, 2004. **15**(10): p. 4500-11.

129. Kaptzan, T., et al., *Development of a Rab9 transgenic mouse and its ability to increase the lifespan of a murine model of Niemann-Pick type C disease.* Am J Pathol, 2009. **174**(1): p. 14-20.

130. Schweitzer, J.K., S.D. Pietrini, and C. D'Souza-Schorey, *ARF6-mediated endosome recycling reverses lipid accumulation defects in Niemann-Pick Type C disease.* PLoS One, 2009. **4**(4): p. e5193.

131. Goldman, S.D. and J.P. Krise, *Niemann-Pick C1 Functions Independently of Niemann-Pick C2 in the Initial Stage of Retrograde Transport of Membrane-impermeable Lysosomal Cargo.* J Biol Chem, 2010. **285**(7): p. 4983-94.

132. Goldman, S.D. and J.P. Krise, *Niemann-Pick C1 Functions Independently of Niemann-Pick C2 in the Initial Stage of Retrograde Transport of Membrane-impermeable Lysosomal Cargo.* J Biol Chem, 2010. **285**(7): p. 4983-94.

133. Gong, Y., et al., *Niemann-Pick C1 protein facilitates the efflux of the anticancer drug daunorubicin from cells according to a novel vesicle-mediated pathway.* J Pharmacol Exp Ther, 2006. **316**(1): p. 242-7.

134. Charman, M., et al., *MLN64 mediates egress of cholesterol from endosomes to mitochondria in the absence of functional Niemann-Pick Type C1 protein.* J Lipid Res, 2010. **51**(5): p. 1023-34.

135. Fernandez, A., et al., *Mitochondrial cholesterol loading exacerbates amyloid beta peptide-induced inflammation and neurotoxicity.* J Neurosci, 2009. **29**(20): p. 6394-405.

136. Mari, M., et al., *Mitochondrial free cholesterol loading sensitizes to TNF- and Fas-mediated steatohepatitis.* Cell Metab, 2006. **4**(3): p. 185-98.

137. Yu, W., et al., *Altered cholesterol metabolism in Niemann-Pick type C1 mouse brains affects mitochondrial function.* J Biol Chem, 2005. **280**(12): p. 11731-9.

138. Xie, C., S.D. Turley, and J.M. Dietschy, *Cholesterol accumulation in tissues of the Niemann-pick type C mouse is determined by the rate of lipoprotein-cholesterol uptake through the coated-pit pathway in each organ.* Proc Natl Acad Sci U S A, 1999. **96**(21): p. 11992-7.

139. Beltroy, E.P., et al., *Cholesterol accumulation and liver cell death in mice with Niemann-Pick type C disease.* Hepatology, 2005. **42**(4): p. 886-93.

140. Kelly, D.A., et al., *Niemann-Pick disease type C: diagnosis and outcome in children, with particular reference to liver disease.* J Pediatr, 1993. **123**(2): p. 242-7.

141. Kulinski, A. and J.E. Vance, *Lipid homeostasis and lipoprotein secretion in Niemann-Pick C1-deficient hepatocytes.* J Biol Chem, 2007. **282**(3): p. 1627-37.

142. Wang, M.D., et al., *Differential regulation of ATP binding cassette protein A1 expression and ApoA-I lipidation by Niemann-Pick type C1 in murine hepatocytes and macrophages.* J Biol Chem, 2007. **282**(31): p. 22525-33.

143. Xie, C., et al., *Cholesterol is sequestered in the brains of mice with Niemann-Pick type C disease but turnover is increased.* J Neuropathol Exp Neurol, 2000. **59**(12): p. 1106-17.

144. Reid, P.C., et al., *A novel cholesterol stain reveals early neuronal cholesterol accumulation in the Niemann-Pick type C1 mouse brain.* J Lipid Res, 2004. **45**(3): p. 582-91.

145. German, D.C., et al., *Degeneration of neurons and glia in the Niemann-Pick C mouse is unrelated to the low-density lipoprotein receptor.* Neuroscience, 2001. **105**(4): p. 999-1005.

146. Erickson, R.P., et al., *Pharmacological and genetic modifications of somatic cholesterol do not substantially alter the course of CNS disease in Niemann-Pick C mice.* J Inherit Metab Dis, 2000. **23**(1): p. 54-62.

147. Reid, P.C., et al., *Partial blockage of sterol biosynthesis with a squalene synthase inhibitor in early postnatal Niemann-Pick type C npcnih null mice brains reduces neuronal cholesterol accumulation, abrogates astrogliosis, but may inhibit myelin maturation.* J Neurosci Methods, 2008. **168**(1): p. 15-25.

148. Li, H., et al., *Molecular, anatomical, and biochemical events associated with neurodegeneration in mice with Niemann-Pick type C disease.* J Neuropathol Exp Neurol, 2005. **64**(4): p. 323-33.

149. Sarna, J.R., et al., *Patterned Purkinje cell degeneration in mouse models of Niemann-Pick type C disease.* J Comp Neurol, 2003. **456**(3): p. 279-91.

150. German, D.C., et al., *Selective neurodegeneration, without neurofibrillary tangles, in a mouse model of Niemann-Pick C disease.* J Comp Neurol, 2001. **433**(3): p. 415-25.

151. Luan, Z., et al., *Brainstem neuropathology in a mouse model of Niemann-Pick disease type C.* J Neurol Sci, 2008. **268**(1-2): p. 108-16.

152. Ong, W.Y., et al., *Neurodegeneration in Niemann-Pick type C disease mice.* Exp Brain Res, 2001. **141**(2): p. 218-31.

153. Amritraj, A., et al., *Increased activity and altered subcellular distribution of lysosomal enzymes determine neuronal vulnerability in Niemann-Pick type C1-deficient mice.* Am J Pathol, 2009. **175**(6): p. 2540-56.

154. Ko, D.C., et al., *Cell-autonomous death of cerebellar purkinje neurons with autophagy in Niemann-Pick type C disease.* PLoS Genet, 2005. **1**(1): p. 81-95.

155. Elrick, M.J., et al., *Conditional Niemann-Pick C mice demonstrate cell autonomous Purkinje cell neurodegeneration.* Hum Mol Genet, 2010. **19**(5): p. 837-47.

156. Liao, G., et al., *Cholesterol accumulation is associated with lysosomal dysfunction and autophagic stress in Npc1 -/- mouse brain.* Am J Pathol, 2007. **171**(3): p. 962-75.

157. Pacheco, C.D., R. Kunkel, and A.P. Lieberman, *Autophagy in Niemann-Pick C disease is dependent upon Beclin-1 and responsive to lipid trafficking defects.* Hum Mol Genet, 2007. **16**(12): p. 1495-503.

158. Klionsky, D.J. and S.D. Emr, *Autophagy as a regulated pathway of cellular degradation.* Science, 2000. **290**(5497): p. 1717-1721.

159. Wu, Y.P., et al., *Apoptosis accompanied by up-regulation of TNF-alpha death pathway genes in the brain of Niemann-Pick type C disease.* Mol Genet Metab, 2005. **84**(1): p. 9-17.

160. Alvarez, A.R., et al., *Imatinib therapy blocks cerebellar apoptosis and improves neurological symptoms in a mouse model of Niemann-Pick type C disease.* Faseb J, 2008. **22**(10): p. 3617-27.

161. Karten, B., et al., *Trafficking of cholesterol from cell bodies to distal axons in Niemann Pick C1-deficient neurons.* J Biol Chem, 2003. **278**(6): p. 4168-75.

162. Karten, B., et al., *The Niemann-Pick C1 protein in recycling endosomes of presynaptic nerve terminals.* J Lipid Res, 2006. **47**(3): p. 504-14.

163. Wasser, C.R., et al., *Cholesterol-dependent balance between evoked and spontaneous synaptic vesicle recycling.* J Physiol, 2007. **579**(Pt 2): p. 413-29.

164. Xu, S., et al., *Defects of synaptic vesicle turnover at excitatory and inhibitory synapses in Niemann-Pick C1-deficient neurons.* Neuroscience, 2010. **167**(3): p. 608-20.

165. Zervas, M., K. Dobrenis, and S.U. Walkley, *Neurons in Niemann-Pick disease type C accumulate gangliosides as well as unesterified cholesterol and undergo dendritic and axonal alterations.* J Neuropathol Exp Neurol, 2001. **60**(1): p. 49-64.

166. Bu, B., et al., *Niemann-Pick disease type C yields possible clue for why cerebellar neurons do not form neurofibrillary tangles.* Neurobiol Dis, 2002. **11**(2): p. 285-97.

167. Suzuki, K., et al., *Neurofibrillary tangles in Niemann-Pick disease type C.* Acta Neuropathol, 1995. **89**(3): p. 227-38.

168. Bu, B., et al., *Deregulation of cdk5, hyperphosphorylation, and cytoskeletal pathology in the Niemann-Pick type C murine model.* J Neurosci, 2002. **22**(15): p. 6515-25.

169. Volterra, A. and J. Meldolesi, *Astrocytes, from brain glue to communication elements: The revolution continues.* Nature Reviews Neuroscience, 2005. **6**(8): p. 626-640.

170. Baudry, M., et al., *Postnatal development of inflammation in a murine model of Niemann-Pick type C disease: immunohistochemical observations of microglia and astroglia.* Exp Neurol, 2003. **184**(2): p. 887-903.

171. Patel, S.C., et al., *Localization of Niemann-Pick C1 protein in astrocytes: implications for neuronal degeneration in Niemann- Pick type C disease.* Proc Natl Acad Sci U S A, 1999. **96**(4): p. 1657-62.

172. Chen, G., et al., *Decreased estradiol release from astrocytes contributes to the neurodegeneration in a mouse model of Niemann-Pick disease type C.* Glia, 2007. **55**(15): p. 1509-18.

173. Zhang, M., et al., *Astrocyte-only Npc1 reduces neuronal cholesterol and triples life span of Npc1-/- mice.* J Neurosci Res, 2008. **86**(13): p. 2848-56.

174. German, D.C., et al., *Neurodegeneration in the Niemann-Pick C mouse: glial involvement.* Neuroscience, 2002. **109**(3): p. 437-50.

175. Takikita, S., et al., *Perturbed myelination process of premyelinating oligodendrocyte in Niemann-Pick type C mouse.* J Neuropathol Exp Neurol, 2004. **63**(6): p. 660-73.

176. Suzuki, H., et al., *Pathologic changes of glial cells in murine model of Niemann-Pick disease type C: immunohistochemical, lectin-histochemical and ultrastructural observations.* Pediatr Int, 2003. **45**(1): p. 1-4.

177. Watabe, K., et al., *Establishment and characterization of immortalized Schwann cells from murine model of Niemann-Pick disease type C (spm/spm).* J Peripher Nerv Syst, 2001. **6**(2): p. 85-94.

178. Higashi, Y., et al., *Peripheral nerve pathology in Niemann-Pick type C mouse.* Acta Neuropathol, 1995. **90**(2): p. 158-63.

179. Goodrum, J.F. and P.G. Pentchev, *Cholesterol reutilization during myelination of regenerating PNS axons is impaired in Niemann-Pick disease type C mice.* J Neurosci Res, 1997. **49**(3): p. 389-92.

180. Goodrum, J.F., et al., *Axonal regeneration, but not myelination, is partially dependent on local cholesterol reutilization in regenerating nerve.* J Neuropathol Exp Neurol, 2000. **59**(11): p. 1002-10.

181. Kreutzberg, G.W., *Microglia: a sensor for pathological events in the CNS.* Trends Neurosci, 1996. **19**(8): p. 312-8.

182. Ling, E.A. and W.C. Wong, *The origin and nature of ramified and amoeboid microglia: a historical review and current concepts.* Glia, 1993. **7**(1): p. 9-18.

183. Del Rio Hortega, P., Cytology and Cellular Pathology of the Central Nervous System. (**Hoeber, 1932**) p. 481-534.

184. Nimmerjahn, A., F. Kirchhoff, and F. Helmchen, *Resting microglial cells are highly dynamic surveillants of brain parenchyma in vivo.* Science, 2005. **308**(5726): p. 1314-8.

185. Stence, N., M. Waite, and M.E. Dailey, *Dynamics of microglial activation: a confocal time-lapse analysis in hippocampal slices.* Glia, 2001. **33**(3): p. 256-66.

186. Tanga, F.Y., V. Raghavendra, and J.A. DeLeo, *Quantitative real-time RT-PCR assessment of spinal microglial and astrocytic activation markers in a rat model of neuropathic pain.* Neurochem Int, 2004. **45**(2-3): p. 397-407.

187. McGlade-McCulloh, E., et al., *Individual microglia move rapidly and directly to nerve lesions in the leech central nervous system.* Proc Natl Acad Sci U S A, 1989. **86**(3): p. 1093-7.

188. Graeber, M.B., W.J. Streit, and G.W. Kreutzberg, *Axotomy of the rat facial nerve leads to increased CR3 complement receptor expression by activated microglial cells.* J Neurosci Res, 1988. **21**(1): p. 18-24.

189. Giulian, D., et al., *The role of mononuclear phagocytes in wound healing after traumatic injury to adult mammalian brain.* J Neurosci, 1989. **9**(12): p. 4416-29.

190. Buttini, M., et al., *Expression of tumor necrosis factor alpha after focal cerebral ischaemia in the rat.* Neuroscience, 1996. **71**(1): p. 1-16.

191. Nakamura, Y., Q.S. Si, and K. Kataoka, *Lipopolysaccharide-induced microglial activation in culture: temporal profiles of morphological change and release of cytokines and nitric oxide.* Neurosci Res, 1999. **35**(2): p. 95-100.

192. Patrizio, M. and G. Levi, *Glutamate production by cultured microglia: differences between rat and mouse, enhancement by lipopolysaccharide and lack effect of HIV coat protein gp120 and depolarizing agents.* Neurosci Lett, 1994. **178**(2): p. 184-9.

193. Colton, C.A. and D.L. Gilbert, *Production of superoxide anions by a CNS macrophage, the microglia.* FEBS Lett, 1987. **223**(2): p. 284-8.

194. Chao, C.C., et al., *Activated microglia mediate neuronal cell injury via a nitric oxide mechanism.* J Immunol, 1992. **149**(8): p. 2736-41.

195. Lindholm, D., et al., *Transforming growth factor-beta 1 in the rat brain: increase after injury and inhibition of astrocyte proliferation.* J Cell Biol, 1992. **117**(2): p. 395-400.

196. Mizuno, T., et al., *Production of interleukin-10 by mouse glial cells in culture.* Biochem Biophys Res Commun, 1994. **205**(3): p. 1907-15.

197. Nakajima, K., et al., *Neurotrophin secretion from cultured microglia.* J Neurosci Res, 2001. **65**(4): p. 322-31.

198. Colton, C.A., *Heterogeneity of microglial activation in the innate immune response in the brain.* Journal of Neuroimmune Pharmacology, 2009. **4**(4): p. 399-418.

199. Kawamata, T., et al., *Immunologic reactions in amyotrophic lateral sclerosis brain and spinal cord tissue.* Am J Pathol, 1992. **140**(3): p. 691-707.

200. McGeer, P.L., et al., *Reactive microglia are positive for HLA-DR in the substantia nigra of Parkinson's and Alzheimer's disease brains.* Neurology, 1988. **38**(8): p. 1285-91.

201. McGeer, P.L., M. Schulzer, and E.G. McGeer, *Arthritis and anti-inflammatory agents as possible protective factors for Alzheimer's disease: a review of 17 epidemiologic studies.* Neurology, 1996. **47**(2): p. 425-32.

202. Wada, R., C.J. Tifft, and R.L. Proia, *Microglial activation precedes acute neurodegeneration in Sandhoff disease and is suppressed by bone marrow transplantation.* Proc Natl Acad Sci U S A, 2000. **97**(20): p. 10954-9.

203. Blum-Degen, D., et al., *Interleukin-1 beta and interleukin-6 are elevated in the cerebrospinal fluid of Alzheimer's and de novo Parkinson's disease patients.* Neurosci Lett, 1995. **202**(1-2): p. 17-20.

204. Hensley, K., et al., *Message and protein-level elevation of tumor necrosis factor alpha (TNF alpha) and TNF alpha-modulating cytokines in spinal cords of the G93A-SOD1 mouse model for amyotrophic lateral sclerosis.* Neurobiol Dis, 2003. **14**(1): p. 74-80.

205. Lim, G.P., et al., *Ibuprofen suppresses plaque pathology and inflammation in a mouse model for Alzheimer's disease.* J Neurosci, 2000. **20**(15): p. 5709-14.

206. Yrjanheikki, J., et al., *Tetracyclines inhibit microglial activation and are neuroprotective in global brain ischemia.* Proc Natl Acad Sci U S A, 1998. **95**(26): p. 15769-74.

207. Du, Y., et al., *Minocycline prevents nigrostriatal dopaminergic neurodegeneration in the MPTP model of Parkinson's disease.* Proc Natl Acad Sci U S A, 2001. **98**(25): p. 14669-74.

208. Beers, D.R., et al., *Wild-type microglia extend survival in PU.1 knockout mice with familial amyotrophic lateral sclerosis.* Proc Natl Acad Sci U S A, 2006. **103**(43): p. 16021-6.

209. Meda, L., et al., *Activation of microglial cells by beta-amyloid protein and interferon-gamma.* Nature, 1995. **374**(6523): p. 647-50.

210. Peyrin, J.M., et al., *Microglial cells respond to amyloidogenic PrP peptide by the production of inflammatory cytokines.* Neuroreport, 1999. **10**(4): p. 723-9.

211. Yates, S.L., et al., *Amyloid beta and amylin fibrils induce increases in proinflammatory cytokine and chemokine production by THP-1 cells and murine microglia.* J Neurochem, 2000. **74**(3): p. 1017-25.

212. Bae, J.S., et al., *Neuroglial activation in Niemann-Pick Type C mice is suppressed by intracerebral transplantation of bone marrow-derived mesenchymal stem cells.* Neurosci Lett, 2005. **381**(3): p. 234-6.

213. Suzuki, M., et al., *Endosomal accumulation of Toll-like receptor 4 causes constitutive secretion of cytokines and activation of signal transducers and activators of transcription in Niemann-Pick disease type C (NPC) fibroblasts: a potential basis for glial cell activation in the NPC brain.* J Neurosci, 2007. **27**(8): p. 1879-91.

214. Ahmad, I., et al., *Allopregnanolone treatment, both as a single injection or repetitively, delays demyelination and enhances survival of Niemann-Pick C mice.* J Neurosci Res, 2005. **82**(6): p. 811-21.

215. Langmade, S.J., et al., *Pregnane X receptor (PXR) activation: a mechanism for neuroprotection in a mouse model of Niemann-Pick C disease.* Proc Natl Acad Sci U S A, 2006. **103**(37): p. 13807-12.

216. Erickson, R.P. and O. Bernard, *Studies on neuronal death in the mouse model of Niemann-Pick C disease.* J Neurosci Res, 2002. **68**(6): p. 738-44.

217. Loftus, S.K., et al., *Rescue of neurodegeneration in Niemann-Pick C mice by a prion-promoter-driven Npc1 cDNA transgene.* Hum Mol Genet, 2002. **11**(24): p. 3107-14.

218. Borchelt, D.R., et al., *A vector for expressing foreign genes in the brains and hearts of transgenic mice.* Genet Anal, 1996. **13**(6): p. 159-63.

219. Fischer, M., et al., *Prion protein (PrP) with amino-proximal deletions restoring susceptibility of PrP knockout mice to scrapie.* Embo J, 1996. **15**(6): p. 1255-64.

220. Garden, G.A., et al., *Polyglutamine-expanded ataxin-7 promotes non-cell-autonomous purkinje cell degeneration and displays proteolytic cleavage in ataxic transgenic mice.* J Neurosci, 2002. **22**(12): p. 4897-905.

221. Cox, T., et al., *Novel oral treatment of Gaucher's disease with N-butyldeoxynojirimycin (OGT 918) to decrease substrate biosynthesis.* Lancet, 2000. **355**(9214): p. 1481-5.

222. Griffin, L.D., et al., *Niemann-Pick type C disease involves disrupted neurosteroidogenesis and responds to allopregnanolone.* Nat Med, 2004. **10**(7): p. 704-11.

223. Liao, G., et al., *Allopregnanolone treatment delays cholesterol accumulation and reduces autophagic/lysosomal dysfunction and inflammation in Npc1-/- mouse brain.* Brain Res, 2009. **1270**: p. 140-51.

224. Zidovetzki, R. and I. Levitan, *Use of cyclodextrins to manipulate plasma membrane cholesterol content: Evidence, misconceptions and control strategies.* Biochimica et Biophysica Acta - Biomembranes, 2007. **1768**(6): p. 1311-1324.

225. Uekama, K., F. Hirayama, and T. Irie, *Cyclodextrin drug carrier systems.* Chemical Reviews, 1998. **98**(5): p. 2045-2076.

226. Szente, L. and J. Szejtli, *Cyclodextrins as food ingredients.* Trends in Food Science and Technology, 2004. **15**(3-4): p. 137-142.

227. Christian, A.E., et al., *Use of cyclodextrins for manipulating cellular cholesterol content.* J Lipid Res, 1997. **38**(11): p. 2264-2272.

228. Diaz-Moscoso, A., et al., *Polycationic amphiphilic cyclodextrins for gene delivery: synthesis and effect of structural modifications on plasmid DNA complex stability, cytotoxicity, and gene expression.* Chemistry - A European Journal, 2009. **15**(46): p. 12871-12888.

229. Diaz-Moscoso, A., et al., *Insights in cellular uptake mechanisms of pDNA-polycationic amphiphilic cyclodextrin nanoparticles (CDplexes).* Journal of Controlled Release, 2010. **143**(3): p. 318-325.

230. Davis, M.E. and M.E. Brewster, *Cyclodextrin-based pharmaceutics: Past, present and future.* Nature Reviews Drug Discovery, 2004. **3**(12): p. 1023-1035.

231. Ohtani, Y., et al., *Differential effects of α, β- and γ-cyclodextrins on human erythrocytes.* European Journal of Biochemistry, 1989. **186**(1-2): p. 17-22.

232. Irie, T., K. Fukunaga, and J. Pitha, *Hydroxypropylcyclodextrins in parenteral use. I: Lipid dissolution and effects on lipid transfers in vitro.* Journal of Pharmaceutical Sciences, 1992. **81**(6): p. 521-523.

233. Ohvo, H. and J.P. Slotte, *Cyclodextrin-mediated removal of sterols from monolayers: Effects of sterol structure and phospholipids on desorption rate.* Biochemistry, 1996. **35**(24): p. 8018-8024.

234. Coleman, A.W., et al., *Aggregation of cyclodextrins: An explanation of the abnormal solubility of β-cyclodextrin.* Journal of Inclusion Phenomena and Molecular Recognition in Chemistry, 1992. **13**(2): p. 139-143.

235. Frank, D.W., J.E. Gray, and R.N. Weaver, *Cyclodextrin nephrosis in the rat.* American Journal of Pathology, 1976. **83**(2): p. 367-382.

236. Perrin, J.H., F.P. Field, and D.A. Hansen, *β-cyclodextrin as an aid to peritoneal dialysis. Renal toxicity of β-cyclodextrin in the rat.* Research Communications in Chemical Pathology and Pharmacology, 1978. **19**(2): p. 373-376.

237. Muller, B.W. and U. Brauns, *Solubilization of drugs by modified [beta]-cyclodextrins.* International Journal of Pharmaceutics, 1985. **26**(1-2): p. 77-88.

238. Kilsdonk, E.P.C., et al., *Cellular cholesterol efflux mediated by cyclodextrins.* Journal of Biological Chemistry, 1995. **270**(29): p. 17250-17256.

239. Irie, T. and K. Uekama, *Pharmaceutical applications of cyclodextrins. III. Toxicological issues and safety evaluation.* Journal of Pharmaceutical Sciences, 1997. **86**(2): p. 147-162.

240. Kiss, T., et al., *Evaluation of the cytotoxicity of β-cyclodextrin derivatives: Evidence for the role of cholesterol extraction.* European Journal of Pharmaceutical Sciences, 2010. **40**(4): p. 376-380.

241. Pitha, J., J. Milecki, and H. Fales, *Hydroxypropyl-β-cyclodextrin: Preparation and characterization; effects on solubility of drugs.* International Journal of Pharmaceutics, 1986. **29**(1): p. 73-82.

242. Kilsdonk, E.P., et al., *Cellular cholesterol efflux mediated by cyclodextrins.* J Biol Chem, 1995. **270**(29): p. 17250-6.

243. Gould, S. and R.C. Scott, *2-Hydroxypropyl-β-cyclodextrin (HP-β-CD): A toxicology review.* Food and Chemical Toxicology, 2005. **43**(10): p. 1451-1459.

244. Atger, V.M., et al., *Cyclodextrins as catalysts for the removal of cholesterol from macrophage foam cells.* Journal of Clinical Investigation, 1997. **99**(4): p. 773-780.

245. Leventis, R. and J.R. Silvius, *Use of cyclodextrins to monitor transbilayer movement and differential lipid affinities of cholesterol.* Biophysical Journal, 2001. **81**(4): p. 2257-2267.

246. Liu, B., et al., *Reversal of defective lysosomal transport in NPC disease ameliorates liver dysfunction and neurodegeneration in the npc1-/- mouse.* Proc Natl Acad Sci U S A, 2009. **106**(7): p. 2377-82.

247. Ramirez, C.M., et al., *Weekly cyclodextrin administration normalizes cholesterol metabolism in nearly every organ of the niemann-pick type C1 mouse and markedly prolongs life.* Pediatric Research, 2010. **68**(4): p. 309-315.

248. Davidson, C.D., et al., *Chronic cyclodextrin treatment of murine Niemann-Pick C disease ameliorates neuronal cholesterol and glycosphingolipid storage and disease progression.* PLoS One, 2009. **4**(9): p. e6951.

249. Abi-Mosleh, L., et al., *Cyclodextrin overcomes deficient lysosome-to-endoplasmic reticulum transport of cholesterol in Niemann-Pick type C cells.* Proc Natl Acad Sci U S A, 2009. **106**(46): p. 19316-21.

250. Rosenbaum, A.I., et al., *Endocytosis of beta-cyclodextrins is responsible for cholesterol reduction in Niemann-Pick type C mutant cells.* Proc Natl Acad Sci U S A, 2010. **107**(12): p. 5477-82.

251. Yanjanin, N.M., et al., *Linear clinical progression, independent of age of onset, in Niemann-Pick disease, type C.* Am J Med Genet B Neuropsychiatr Genet, 2010. **153B**(1): p. 132-40.

252. Liu, B., et al., *Cyclodextrin overcomes the transport defect in nearly every organ of the newborn or mature NPC1 mouse leading to excretion of the sequestered cholesterol as bile acid.* J Lipid Res, 2010. **51**(5): p. 933-944.

253. Gong, J.S., et al., *Apolipoprotein E (ApoE) isoform-dependent lipid release from astrocytes prepared from human ApoE3 and ApoE4 knock-in mice.* Journal of Biological Chemistry, 2002. **277**(33): p. 29919-29926.

254. Saura, J., J.M. Tusell, and J. Serratosa, *High-Yield Isolation of Murine Microglia by Mild Trypsinization.* Glia, 2003. **44**(3): p. 183-189.

255. Giulian, D. and T.J. Baker, *Characterization of ameboid microglia isolated from developing mammalian brain.* Journal of Neuroscience, 1986. **6**(8): p. 2163-2178.

256. Michikawa, M. and K. Yanagisawa, *Apolipoprotein E4 induces neuronal cell death under conditions of suppressed de novo cholesterol synthesis.* J Neurosci Res, 1998. **54**(1): p. 58-67.

257. Hawkes, C. and S. Kar, *Insulin-like growth factor-II/mannose-6-phosphate receptor: Widespread distribution in neurons of the central nervous system including those expressing cholinergic phenotype.* Journal of Comparative Neurology, 2003. **458**(2): p. 113-127.

258. Jafferali, S., et al., *Insulin-like growth factor-I and its receptor in the frontal cortex, hippocampus, and cerebellum of normal human and Alzheimer disease brains.* Synapse, 2000. **38**(4): p. 450-459.

259. Lai, A.Y. and K.G. Todd, *Hypoxia-activated microglial mediators of neuronal survival are differentially regulated by tetracyclines.* Glia, 2006. **53**(8): p. 809-816.

260. Mukherjee, S., et al., *Cholesterol distribution in living cells: Fluorescence imaging using dehydroergosterol as a fluorescent cholesterol analog.* Biophysical Journal, 1998. **75**(4): p. 1915-1925.

261. Sawada, M., et al., *Production of tumor necrosis factor-alpha by microglia and astrocytes in culture.* Brain Res, 1989. **491**(2): p. 394-397.

262. Alderton, W.K., C.E. Cooper, and R.G. Knowles, *Nitric oxide synthases: Structure, function and inhibition.* Biochemical Journal, 2001. **357**(3): p. 593-615.

263. Lambeth, J.D., *NOX enzymes and the biology of reactive oxygen.* Nature Reviews Immunology, 2004. **4**(3): p. 181-189.

264. Takeuchi, H., et al., *Tumor necrosis factor-alpha induces neurotoxicity via glutamate release from hemichannels of activated microglia in an autocrine manner.* Journal of Biological Chemistry, 2006. **281**(30): p. 21362-21368.

265. Mitrasinovic, O.M., et al., *Overexpression of Macrophage Colony-stimulating Factor Receptor on Microglial Cells Induces an Inflammatory Response.* Journal of Biological Chemistry, 2001. **276**(32): p. 30142-30149.

266. D'Mello, C., T. Le, and M.G. Swain, *Cerebral microglia recruit monocytes into the brain in response to tumor necrosis factora signaling during peripheral organ inflammation.* Journal of Neuroscience, 2009. **29**(7): p. 2089-2102.

267. Streit, W.J. and D.L. Sparks, *Activation of microglia in the brains of humans with heart disease and hypercholesterolemic rabbits.* Journal of Molecular Medicine, 1997. **75**(2): p. 130-138.

268. Zatta, P., et al., *Astrocytosis, microgliosis, metallothionein-I-II and amyloid expression in high cholesterol-fed rabbits.* Journal of Alzheimer's Disease, 2002. **4**(1): p. 1-9.

269. Banks, W.A., et al., *Human interleukin (IL) 1α, murine IL-1α and murine IL-1β are transported from blood to brain in the mouse by a shared saturable mechanism.* Journal of Pharmacology and Experimental Therapeutics, 1991. **259**(3): p. 988-996.

270. Gutierrez, E.G., W.A. Banks, and A.J. Kastin, *Murine tumor necrosis factor alpha is transported from blood to brain in the mouse.* Journal of Neuroimmunology, 1993. **47**(2): p. 169-176.

271. De Vries, H.E., et al., *The influence of cytokines on the integrity of the blood-brain barrier in vitro.* Journal of Neuroimmunology, 1996. **64**(1): p. 37-43.

272. Hickey, W.F. and H. Kimura, *Perivascular microglial cells of the CNS are bone marrow-derived and present antigen in vivo.* Science, 1988. **239**(4837): p. 290-292.

273. Kokovay, E. and L.A. Cunningham, *Bone marrow-derived microglia contribute to the neuroinflammatory response and express iNOS in the MPTP mouse model of Parkinson's disease.* Neurobiol Dis, 2005. **19**(3): p. 471-478.

274. Priller, J., et al., *Targeting gene-modified hematopoietic cells to the central nervous system: Use of green fluorescent protein uncovers microglial engraftment.* Nat Med, 2001. **7**(12): p. 1356-1361.

275. Stalder, A.K., et al., *Invasion of hematopoietic cells into the brain of amyloid precursor protein transgenic mice.* Journal of Neuroscience, 2005. **25**(48): p. 11125-11132.

276. Massengale, M., et al., *Hematopoietic cells maintain hematopoietic fates upon entering the brain.* Journal of Experimental Medicine, 2005. **201**(10): p. 1579-1589.

277. Mildner, A., et al., *Microglia in the adult brain arise from Ly-6ChiCCR2+ monocytes only under defined host conditions.* Nature Neuroscience, 2007. **10**(12): p. 1544-1553.

278. Carson, M.J., et al., *Mature microglia resemble immature antigen-presenting cells.* Glia, 1998. **22**(1): p. 72-85.

279. Ford, A.L., et al., *Normal adult ramified microglia separated from other central nervous system macrophages by flow cytometric sorting: Phenotypic differences defined and direct ex vivo antigen presentation to myelin basic protein-reactive CD4+ T cells compared.* Journal of Immunology, 1995. **154**(9): p. 4309-4321.

280. Sedgwick, J.D., et al., *Isolation and direct characterization of resident microglial cells from the normal and inflamed central nervous system.* Proc Natl Acad Sci U S A, 1991. **88**(16): p. 7438-7442.

281. Imai, Y., et al., *A novel gene iba1 in the major histocompatibility complex class III region encoding an EF hand protein expressed in a monocytic lineage.* Biochem Biophys Res Commun, 1996. **224**(3): p. 855-862.

282. Ito, D., et al., *Microglia-specific localisation of a novel calcium binding protein, Iba1.* Molecular Brain Research, 1998. **57**(1): p. 1-9.

283. Cordle, A. and G. Landreth, *3-Hydroxy-3-methylglutaryl-coenzyme A reductase inhibitors attenuate β-amyloid-induced microglial inflammatory responses.* Journal of Neuroscience, 2005. **25**(2): p. 299-307.

284. Townsend, K.P., et al., *Lovastatin modulation of microglial activation via suppression of functional CD40 expression.* J Neurosci Res, 2004. **78**(2): p. 167-176.

285. Pahan, K., et al., *Lovastatin and phenylacetate inhibit the induction of nitric oxide synthase and cytokines in rat primary astrocytes, microglia, and macrophages.* Journal of Clinical Investigation, 1997. **100**(11): p. 2671-2679.

286. Clarke, R.M., et al., *A pivotal role for interleukin-4 in atorvastatin-associated neuroprotection in rat brain.* Journal of Biological Chemistry, 2008. **283**(4): p. 1808-1817.

287. Zhang, F.L. and P.J. Casey, *Protein prenylation: Molecular mechanisms and functional consequences*. Annual Review of Biochemistry, 1996. **65**: p. 241-269.

288. Kuipers, H.F., et al., *Simvastatin affects cell motility and actin cytoskeleton distribution of microglia.* Glia, 2006. **53**(2): p. 115-123.

289. Bi, X., et al., *Inhibition of geranylgeranylation mediates the effects of 3-hydroxy-3-methylglutaryl (HMG)-CoA reductase inhibitors on microglia.* Journal of Biological Chemistry, 2004. **279**(46): p. 48238-48245.

290. Huynh, K.K., E. Gershenzon, and S. Grinstein, *Cholesterol accumulation by macrophages impairs phagosome maturation.* Journal of Biological Chemistry, 2008. **283**(51): p. 35745-35755.

291. Iftakhar-E-Khuda, I., et al., *Novel mechanism of U18666A-induced tumour necrosis factor-α production in RAW 264.7 macrophage cells.* Clinical and Experimental Immunology, 2009. **155**(3): p. 552-558.

292. Rimkunas, V.M., et al., *TNF-α plays a role in hepatocyte apoptosis in Niemann-Pick type C liver disease.* J Lipid Res, 2009. **50**(2): p. 327-333.

293. Kriegler, M., et al., *A novel form of TNF/cachectin is a cell surface cytotoxic transmembrane protein: Ramifications for the complex physiology of TNF.* Cell, 1988. **53**(1): p. 45-53.

294. Hsu, H., et al., *TRADD-TRAF2 and TRADD-FADD interactions define two distinct TNF receptor 1 signal transduction pathways.* Cell, 1996. **84**(2): p. 299-308.

295. Baud, V. and M. Karin, *Signal transduction by tumor necrosis factor and its relatives.* Trends in Cell Biology, 2001. **11**(9): p. 372-377.

296. Aggarwal, B.B., *Signalling pathways of the TNF superfamily: A double-edged sword.* Nature Reviews Immunology, 2003. **3**(9): p. 745-756.

297. Grell, M., et al., *The transmembrane form of tumor necrosis factor is the prime activating ligand of the 80 kDa tumor necrosis factor receptor.* Cell, 1995. **83**(5): p. 793-802.

298. Grell, M., et al., *The type 1 receptor (CD120a) is the high-affinity receptor for soluble tumor necrosis factor.* Proc Natl Acad Sci U S A, 1998. **95**(2): p. 570-575.

299. Tartaglia, L.A., et al., *A novel domain within the 55 kd TNF receptor signals cell death.* Cell, 1993. **74**(5): p. 845-853.

300. Micheau, O. and J. Tschopp, *Induction of TNF receptor I-mediated apoptosis via two sequential signaling complexes.* Cell, 2003. **114**(2): p. 181-190.

301. Schutze, S., V. Tchikov, and W. Schneider-Brachert, *Regulation of TNFR1 and CD95 signalling by receptor compartmentalization.* Nature Reviews Molecular Cell Biology, 2008. **9**(8): p. 655-662.

302. Liu, Z.G., et al., *Dissection of TNF receptor 1 effector functions: JNK activation is not linked to apoptosis while NF-κB activation prevents cell death.* Cell, 1996. **87**(3): p. 565-576.

303. Beg, A.A. and D. Baltimore, *An essential role for NF-κB in preventing TNF-α-induced cell death.* Science, 1996. **274**(5288): p. 782-784.

304. Van Antwerp, D.J., et al., *Suppression of TNF-α-induced apoptosis by NF-κB.* Science, 1996. **274**(5288): p. 787-789.

305. Gordon, J.R. and S.J. Galli, *Mast cells as a source of both preformed and immunologically inducible TNF-α/cachectin.* Nature, 1990. **346**(6281): p. 274-276.

306. Olszewski, M.B., et al., *TNF trafficking to human mast cell granules: Mature chain-dependent endocytosis.* Journal of Immunology, 2007. **178**(9): p. 5701-5709.

307. Black, R.A., et al., *A metalloproteinase disintegrin that releases tumour-necrosis factor-α from cells.* Nature, 1997. **385**(6618): p. 729-733.

308. Murray, R.Z., et al., *Cell biology: A role for the phagosome in cytokine secretion.* Science, 2005. **310**(5753): p. 1492-1495.

309. Solomon, K.A., et al., *The Fate of Pro-TNF-α Following Inhibition of Metalloprotease-Dependent Processing to Soluble TNF-α in Human Monocytes.* Journal of Immunology, 1997. **159**(9): p. 4524-4531.

310. Moss, M.L., et al., *Cloning of a disintegrin metalloproteinase that processes precursor tumour-necrosis factor-α.* Nature, 1997. **385**(6618): p. 733-736.

311. Shurety, W., et al., *Localization and post-Golgi trafficking of tumor necrosis factor-α in macrophages.* Journal of Interferon and Cytokine Research, 2000. **20**(4): p. 427-438.

312. Lahat, N., et al., *Hypoxia enhances lysosomal TNF-α degradation in mouse peritoneal macrophages.* American Journal of Physiology - Cell Physiology, 2008. **295**(1): p. C2-C12.

313. Holt, O.J., F. Gallo, and G.M. Griffiths, *Regulating secretory lysosomes.* Journal of Biochemistry, 2006. **140**(1): p. 7-12.

314. Andrei, C., et al., *The secretory route of the leaderless protein interleukin 1β involves exocytosis of endolysosome-related vesicles.* Mol Biol Cell, 1999. **10**(5): p. 1463-1475.

315. Shurety, W., et al., *Endocytosis of uncleaved tumor necrosis factor-α in macrophages.* Laboratory Investigation, 2001. **81**(1): p. 107-117.

316. Rozenova, K.A., et al., *Studies on the role of acid sphingomyelinase and ceramide in the regulation of tumor necrosis factor α (TNFα)-converting enzyme activity and TNFα secretion in macrophages.* Journal of Biological Chemistry, 2010. **285**(27): p. 21103-21113.

317. Matthews, V., et al., *Cellular cholesterol depletion triggers shedding of the human interleukin-6 receptor by ADAM10 and ADAM17 (TACE).* Journal of Biological Chemistry, 2003. **278**(40): p. 38829-38839.

318. Von Tresckow, B., et al., *Depletion of Cellular Cholesterol and Lipid Rafts Increases Shedding of CD30.* Journal of Immunology, 2004. **172**(7): p. 4324-4331.

319. Gil, C., R. Cubi, and J. Aguilera, *Shedding of the p75NTR neurotrophin receptor is modulated by lipid rafts.* FEBS Lett, 2007. **581**(9): p. 1851-1858.

320. Tellier, E., et al., *The shedding activity of ADAM17 is sequestered in lipid rafts.* Experimental Cell Research, 2006. **312**(20): p. 3969-3980.

321. Ha, S.D., et al., *Cathepsin B is involved in the trafficking of TNF-α-containing vesicles to the plasma membrane in macrophages.* Journal of Immunology, 2008. **181**(1): p. 690-697.

322. Chao, C.C., et al., *Priming effect of morphine on the production of tumor necrosis factor-α by microglia: Implications in respiratory burst activity and human immunodeficiency virus-1 expression.* Journal of Pharmacology and Experimental Therapeutics, 1994. **269**(1): p. 198-203.

323. Dilger, R.N. and R.W. Johnson, *Aging, microglial cell priming, and the discordant central inflammatory response to signals from the peripheral immune system.* Journal of Leukocyte Biology, 2008. **84**(4): p. 932-939.

324. Meda, L., et al., *Priming of monocyte respiratory burst by β-amyloid fragment (25-35).* Neurosci Lett, 1996. **219**(2): p. 91-94.

325. Reddy, P., et al., *Functional analysis of the domain structure of tumor necrosis factor-α converting enzyme.* Journal of Biological Chemistry, 2000. **275**(19): p. 14608-14614.

326. Engelmann, H., D. Novick, and D. Wallach, *Two tumor necrosis factor-binding proteins purified from human urine. Evidence for immunological cross-reactivity with cell surface tumor necrosis factor receptors.* Journal of Biological Chemistry, 1990. **265**(3): p. 1531-1536.

327. Nophar, Y., et al., *Soluble forms of tumor necrosis factor receptors (TNF-Rs). The cDNA for the type I TNF-R, cloned using amino acid sequence data of its soluble form, encodes both the cell surface and a soluble form of the receptor.* EMBO Journal, 1990. **9**(10): p. 3269-3278.

328. Van Zee, K.J., et al., *Tumor necrosis factor soluble receptors circulate during experimental and clinical inflammation and can protect against excessive tumor necrosis factor α in vitro and in vivo.* Proc Natl Acad Sci U S A, 1992. **89**(11): p. 4845-4849.

329. Scalzo, P., et al., *Increased serum levels of soluble tumor necrosis factor-α receptor-1 in patients with Parkinson's disease.* Journal of Neuroimmunology, 2009. **216**(1-2): p. 122-125.

330. Kuno, R., et al., *Autocrine activation of microglia by tumor necrosis factor-α.* Journal of Neuroimmunology, 2005. **162**(1-2): p. 89-96.

331. Bogdan, C., Y. Vodovotz, and C. Nathan, *Macrophage deactivation by interleukin 10.* Journal of Experimental Medicine, 1991. **174**(6): p. 1549-1555.

332. Di Santo, E., et al., *Systemic interleukin 10 administration inhibits brain tumor necrosis factor production in mice.* European Journal of Pharmacology, 1997. **336**(2-3): p. 197-202.

333. Sawada, M., et al., *Interleukin-10 inhibits both production of cytokines and expression of cytokine receptors in microglia.* J Neurochem, 1999. **72**(4): p. 1466-1471.

334. Wang, P., et al., *IL-10 inhibits transcription of cytokine genes in human peripheral blood mononuclear cells.* Journal of Immunology, 1994. **153**(2): p. 811-816.

335. Keun, W.P., et al., *Interleukin-10 endogenously expressed in microglia prevents lipopolysaccharide-induced neurodegeneration in the rat cerebral cortex in vivo.* Experimental and Molecular Medicine, 2007. **39**(6): p. 812-819.

336. Spera, P.A., et al., *IL-10 reduces rat brain injury following focal stroke.* Neurosci Lett, 1998. **251**(3): p. 189-192.

337. Bethea, J.R., et al., *Systemically administered interleukin-10 reduces tumor necrosis factor- alpha production and significantly improves functional recovery following traumatic spinal cord injury in rats.* Journal of Neurotrauma, 1999. **16**(10): p. 851-863.

338. Grilli, M., et al., *Interleukin-10 modulates neuronal threshold of vulnerability to ischaemic damage.* European Journal of Neuroscience, 2000. **12**(7): p. 2265-2272.

339. Bachis, A., et al., *Interleukin-10 prevents glutamate-mediated cerebellar granule cell death by blocking caspase-3-like activity.* Journal of Neuroscience, 2001. **21**(9): p. 3104-3112.

340. de Haas, A.H., H.W.G.M. Boddeke, and K. Biber, *Region-specific expression of immunoregulatory proteins on microglia in the healthy CNS.* Glia, 2008. **56**(8): p. 888-894.

341. Ensinger, E.M., et al., *Regional topographical differences of canine microglial immunophenotype and function in the healthy spinal cord.* Journal of Neuroimmunology, 2010. **227**(1-2): p. 144-152.

342. Tanaka, J., H. Nakamura, and S. Miyawaki, *Cerebellar involvement in murine sphingomyelinosis: A new model of Niemann-Pick disease.* J Neuropathol Exp Neurol, 1988. **47**(3): p. 291-300.

343. Aderem, A. and D.M. Underhill, *Mechanisms of phagocytosis in macrophages*. Annual Review of Immunology, 1999. **17**: p. 593-623.

344. Fraser, D.A., K. Pisalyaput, and A.J. Tenner, *C1q enhances microglial clearance of apoptotic neurons and neuronal blebs, and modulates subsequent inflammatory cytokine production.* J Neurochem, 2010. **112**(3): p. 733-743.

345. Tassiulas, I., et al., *Apoptotic Cells Inhibit LPS-Induced Cytokine and Chemokine Production and IFN Responses in Macrophages.* Human Immunology, 2007. **68**(3): p. 156-164.

346. Underhill, D.M. and A. Ozinsky, *Phagocytosis of microbes: Complexity in action*. Annual Review of Immunology, 2002. **20**: p. 825-852.

347. Erwig, L.P., et al., *Differential regulation of phagosome maturation in macrophages and dendritic cells mediated by Rho GTPases and ezrin-radixin-moesin (ERM) proteins.* Proc Natl Acad Sci U S A, 2006. **103**(34): p. 12825-12830.

348. Albert, M.L., et al., *Immature dendritic cells phagocytose apoptotic cells via αvβ5 and CD36, and cross-present antigens to cytotoxic T lymphocytes.* Journal of Experimental Medicine, 1998. **188**(7): p. 1359-1368.

349. Fadok, V.A., et al., *A receptor for phosphatidylserine-specific clearance of apoptotic cells.* Nature, 2000. **405**(6782): p. 85-90.

350. Fadok, V.A., et al., *Exposure of phosphatidylserine on the surface of apoptotic lymphocytes triggers specific recognition and removal by macrophages.* Journal of Immunology, 1992. **148**(7): p. 2207-2216.

351. Zhang, Z., et al., *Inclusion complex of a Bcl-2 inhibitor with cyclodextrin: Characterization, cellular accumulation, and in vivo antitumor activity.* Molecular Pharmaceutics, 2010. **7**(4): p. 1349-1354.

352. Diaz-Moscoso, A., et al., *Insights in cellular uptake mechanisms of pDNA-polycationic amphiphilic cyclodextrin nanoparticles (CDplexes).* Journal of Controlled Release, 2010. **143**(3): p. 318-325.

353. Turk, B., D. Turk, and V. Turk, *Lysosomal cysteine proteases: More than scavengers.* Biochimica et Biophysica Acta - Protein Structure and Molecular Enzymology, 2000. **1477**(1-2): p. 98-111.

354. Ottico, E., et al., *Dynamics of membrane lipid domains in neuronal cells differentiated in culture.* J Lipid Res, 2003. **44**(11): p. 2142-2151.

355. Maxfield, F.R. and G. van Meer, *Cholesterol, the central lipid of mammalian cells.* Current Opinion in Cell Biology, 2010. **22**(4): p. 422-429.

356. Monnaert, V., et al., *Behavior of α-,β-, and γ-cyclodextrins and their derivatives on an in vitro model of blood-brain barrier.* Journal of Pharmacology and Experimental Therapeutics, 2004. **310**(2): p. 745-751.

357. Camargo, F., et al., *Cyclodextrins in the treatment of a mouse model of Niemann-Pick C disease.* Life Sciences, 2001. **70**(2): p. 131-142.

358. Nonaka, N., et al., *Delivery of galanin-like peptide to the brain: Targeting with intranasal delivery and cyclodextrins.* Journal of Pharmacology and Experimental Therapeutics, 2008. **325**(2): p. 513-519.

359. Jeulin, H., et al., *Effective ribavirin concentration in mice brain using cyclodextrin as a drug carrier: Evaluation in a measles encephalitis model.* Antiviral Research, 2009. **81**(3): p. 261-266.

360. Vorbrodt, A.W., A.S. Lossinsky, and H.M. Wisniewski, *Localization of alkaline phosphatase activity in endothelia of developing and mature mouse blood-brain barrier.* Developmental Neuroscience, 1986. **8**(1): p. 1-13.

361. Vorbrodt, A.W., D.H. Dobrogowska, and M. Tarnawski, *Immunogold study of interendothelial junction-associated and glucose transporter proteins during postnatal maturation of the mouse blood-brain barrier.* Journal of Neurocytology, 2001. **30**(8): p. 705-716.

362. Ward, S., et al., *2-Hydroxypropyl-β-cyclodextrin raises hearing threshold in normal cats and in cats with niemann-pick type C disease.* Pediatric Research, 2010. **68**(1): p. 52-56.

363. Smith, D., et al., *Beneficial effects of anti-inflammatory therapy in a mouse model of Niemann-Pick disease type C1.* Neurobiol Dis, 2009. **36**(2): p. 242-251.